

**Utility of Cardiovascular  
Magnetic Resonance Ischaemia Assessment  
of Chronic Kidney Disease and Post Renal  
Transplant Population**

A thesis submitted for the degree  
**Doctor of Philosophy**

**Susie Fei Cen Parnham**

**MBBS.BMedSci.FRACP**

**(Student number: 2101572)**

**School of Medicine  
Flinders University**

**October 2015**

# **Declaration**

The work of the thesis has never been previously submitted for any degree or diploma at any university or any other institutions. To my best knowledge and belief, the thesis contains no materials that have previously been published, except where due references are made.

Susie Fei Cen Parnham

Date: 22 October 2015

# Table of Contents

<b>Acknowledgements</b>	<b>i</b>
<b>Abstract</b>	<b>iii</b>
<b>Thesis Related Publications</b>	<b>v</b>
<b>Abbreviations</b>	<b>ix</b>
<b>CHAPTER 1 - Background</b>	<b>1</b>
<b>1.1 Clinical Problem</b>	<b>1</b>
<b>1.2 Strategies and Current Evidence</b>	<b>5</b>
1.2.1 Diagnostic Evaluation of Myocardial Ischaemia in Renal Population	5
1.2.1.1 Exercise Stress ECG	6
1.2.1.2 Exercise Stress Echocardiography and Dobutamine Stress	
Echocardiography	7
1.2.1.3 Myocardial Perfusion Scintigraphy (MPS)	9
1.2.1.4 Cardiovascular Magnetic Resonance (CMR)	10
1.2.1.5 Aim of Thesis	11
<b>1.3 Utility of Stress Cardiovascular Magnetic Resonance (CMR) in</b>	
<b>Assessment of Myocardial Ischaemia</b>	<b>12</b>
1.3.1 Stress Perfusion CMR	12
1.3.1.1 Stress CMR Reproducibility	15
1.3.1.2 Stress Perfusion CMR in Assessing Prognosis	15
1.3.1.3 Stressors in Stress CMR and Their Safety	15
1.3.1.4 Stress CMR Image Analysis Techniques	16
1.3.2 Blood Oxygen Level-Dependent (BOLD) CMR	16
1.3.3 CMR Assessment of Myocardial Infarction/Replacement Fibrosis	20
1.3.4 CMR Assessment of Epicardial Coronary Artery Disease	21
1.3.4.1 Magnetic Resonance Coronary Angiography (MRCA)	
Techniques	22
1.3.4.2 Accuracy of MRCA in Detecting Coronary Artery Stenosis	23

1.3.4.3 MRCA Reproducibility	24
1.3.4.4 MRCA in Assessing Prognosis	24
<b>CHAPTER 2 - General Methods</b>	<b>25</b>
<b>2.1 Study Protocol</b>	<b>25</b>
2.1.1 Ethics	25
2.1.2 Preparation	25
<b>2.2 CMR Image Acquisition</b>	<b>27</b>
2.2.1 Multi Plane Localisers	27
2.2.1.1 Two Chamber (Vertical Long Axis or VLA) Localiser	27
2.2.1.2 Four Chamber (Horizontal Long Axis or HLA) Localiser	28
2.2.1.3 Short Axis (SA) Localiser	29
2.2.2 Cine Imaging	30
2.2.2.1 Two Chamber (Vertical Long Axis or VLA) Cine	30
2.2.2.2 Four Chamber (Horizontal Long Axis or HLA) Cine	31
2.2.2.3 Left Ventricular Outflow Tract (LVOT) Cine	32
2.2.2.4 Left Ventricular Outflow Tract (LVOT) Cross Cut Cine	33
2.2.2.5 Short Axis (SA) Cine	34
2.2.3 Blood Oxygen Level Dependent (BOLD) Imaging	36
2.2.4 Stress Perfusion Imaging	37
2.2.5 Late Gadolinium Imaging	38
2.2.6 Magnetic Resonance Coronary Angiography (MRCA)	39
2.2.7 Pulse Wave Velocity Imaging of the Aorta	40
<b>2.3 CMR Image Analysis</b>	<b>40</b>
2.3.1 Ventricular Volumes, Function and Mass	40
2.3.2 BOLD Analysis	41
2.3.3 Stress Perfusion Analysis	42
2.3.4 Late Gadolinium Enhancement Analysis	43
2.3.5 MRCA Analysis	43
2.3.6 Pulse Wave Velocity Analysis	43
2.3.7 Strain Echocardiography Protocol	44

**CHAPTER 3 - Impaired Myocardial Oxygenation Response to Stress in Patients with Chronic Kidney Disease** **45**

<b>3.1</b>	<b>Introduction</b>	<b>45</b>
<b>3.2</b>	<b>Methods</b>	<b>46</b>
3.2.1	Study Population	46
3.2.2	Biochemistry	47
3.2.3	CMR Protocol	47
3.2.4	Strain Echocardiography	48
3.2.5	CMR Image Analysis	49
3.2.6	Statistical Analysis	50
<b>3.3</b>	<b>Results</b>	<b>51</b>
3.3.1	Subject Characteristics	51
3.3.2	Assessment of Left Ventricular Mass, Volumes and Function	52
3.3.3	Assessment of Myocardial Oxygenation	52
3.3.4	Association Between Myocardial Oxygenation and Renal Function	53
3.3.5	Assessment of Myocardial Fibrosis	54
<b>3.4</b>	<b>Discussion</b>	<b>54</b>
3.4.1	BOLD CMR Technique	54
3.4.2	Myocardial Oxygenation, Epicardial and Microvascular Coronary Artery Disease	55
3.4.3	Myocardial Oxygenation Response to Stress and Myocardial Fibrosis	57
3.4.4	Myocardial Oxygenation and Chronic Kidney Disease	57
3.4.5	Clinical Implications	58
3.4.6	Study Limitations	58
<b>3.5</b>	<b>Conclusion</b>	<b>59</b>

**CHAPTER 4 - Dissociation Between Myocardial Oxygenation Response to Stress and Epicardial Coronary Artery Disease in Chronic Kidney Disease Patients** **69**

<b>4.1</b>	<b>Introduction</b>	<b>69</b>
------------	---------------------	-----------

<b>4.2</b>	<b>Methods</b>	<b>70</b>
4.2.1	Study Population	70
4.2.2	CMR Protocol	70
4.2.3	CMR Image Analysis	71
4.2.4	Statistical Analysis	72
<b>4.3</b>	<b>Results</b>	<b>72</b>
4.3.1	Subject Characteristics	72
4.3.2	Assessment of Myocardial Oxygenation Response to Stress	73
4.3.3	Assessment of Epicardial Coronary Artery Disease	73
4.4.4	Association Between Myocardial Oxygenation and Epicardial CAD in Chronic Kidney Disease and Renal Transplant Groups	74
<b>4.4</b>	<b>Discussion</b>	<b>74</b>
<b>4.5</b>	<b>Conclusion</b>	<b>76</b>

## **CHAPTER 5 - Myocardial Perfusion is Impaired in Renal Transplant Recipients** **81**

<b>5.1</b>	<b>Introduction</b>	<b>81</b>
<b>5.2</b>	<b>Methods</b>	<b>82</b>
5.2.1	Study Population	82
5.2.2	CMR Protocol	83
5.2.3	CMR Image Analysis	84
5.2.4	Statistical Analysis	86
<b>5.3</b>	<b>Results</b>	<b>86</b>
5.3.1	Subject Characteristics	86
5.3.2	Assessment of Left Ventricular Mass, Volumes and Function	87
5.3.3	Assessment of Myocardial Perfusion Reserve Index (MPRI)	87
5.3.4	Assessment of Myocardial Fibrosis	88
5.3.5	Assessment of Epicardial Coronary Artery Disease	88
<b>5.4</b>	<b>Discussion</b>	<b>89</b>
<b>5.5</b>	<b>Conclusion</b>	<b>92</b>

**CHAPTER 6 - Relationship Between Myocardial Perfusion and Aortic Stiffness in Asymptomatic Renal Transplant Recipients 101**

<b>6.1</b>	<b>Introduction</b>	<b>101</b>
<b>6.2</b>	<b>Methods</b>	<b>102</b>
6.2.1	Study Population	102
6.2.2	CMR Protocol	102
<b>6.3</b>	<b>Results</b>	<b>103</b>
<b>6.4</b>	<b>Discussion</b>	<b>104</b>
<b>6.5</b>	<b>Conclusion</b>	<b>105</b>

**CHAPTER 7 - Blood Oxygen Level Dependent (BOLD) Cardiovascular Magnetic Resonance (CMR) as Predictor of Cardiac Prognosis in Asymptomatic Chronic Kidney Disease Patients 111**

<b>7.1</b>	<b>Introduction</b>	<b>111</b>
<b>7.2</b>	<b>Methods</b>	<b>112</b>
7.2.1	Study Population	112
7.2.2	CMR Protocol	112
7.2.3	CMR Image Analysis	113
7.2.4	Follow-up	113
7.2.5	Statistical Analysis	114
<b>7.3</b>	<b>Results</b>	<b>114</b>
7.3.1	Subject Characteristics	114
7.3.2	Outcomes	114
7.3.3	Comparison Between CKD Group With and Without Blunted Myocardial Oxygenation Response to Stress	115
7.3.4	Predictors of Major Adverse Cardiac Events	116
<b>7.4</b>	<b>Discussion</b>	<b>117</b>
<b>7.5</b>	<b>Conclusion</b>	<b>119</b>

<b>CHAPTER 8 - Conclusion</b>	<b>126</b>
<b>8.1 Myocardial Oxygenation Response to Stress in Chronic Kidney Disease Patients</b>	<b>126</b>
<b>8.2 Myocardial Perfusion in Renal Transplant Recipients</b>	<b>127</b>
<b>CHAPTER 9 - Future Directions</b>	<b>128</b>
<b>References</b>	<b>130</b>

# Acknowledgements

This thesis is dedicated to God, my husband, the research participants, my research supervisors and team.

First of all, I would like to thank my husband Dr Stuart Parnham and our dogs Goku and Sayang for moving all the way from Melbourne to Adelaide for my PhD and fellowship. To my husband, thank you for everything. Thank you for my family for all the supports.

I thank my supervisors Prof Joseph Selvanayagam, A/Prof Carmine De Pasquale and Prof Jonathan Gleadle. Prof Joseph Selvanayagam has been my mentor, not just in PhD, but also in cardiology and research. A/Prof Carmine De Pasquale has always been available during stressful PhD years. Thank you for Prof Jonathan Gleadle PhD help and supports.

I thank Prof Bill Heddle for all his help and encouragement. I thank my colleagues Dr Tapash Bakshi, Dr Bronte Ayres, Dr Justin Ardill, Dr Richard Hillock and Dr Derek Yiu for all the help and supports. A special mention for Simon Boag and receptionists for the supports.

I thank Prof Richard Woodman for being the most wonderful statistic mentor. Thank you also for Dr Darryl Leong for the initial statistic teaching. I thank Dr John-Paul Tantiongco for helping putting up flyers for normal volunteers. Many thanks to Dr Lora Papa and Christine Edwards for the help with ethics applications. I thank Dr Suchi Grover, Dr Hanim Amin, Dr Srinivasan Govindarajan, Dr Rachael Lloyd, Dr Gareth Crouch, Dr Pey Wen Lou for the supports throughout different steps of PhD process. A special mention to my senior colleague Dr Kuan Leong Yew for encouraging the drive to publish.

I thank Prof Derek Chew and the Flinders Cardiology Department and Dr Jeffrey Barbara and the Renal Team. I thank Craig Bradbrook, Emma Smith, Kylie Hood, Jeremy Cullinan, Angela Walls. Cherie Raven, Charlotte Wigley and Martina Bryant for scanning the MRI. Thank you Jan Roesler for helping with the bookings. Thank you also to Bec Perry, Lynn Brown and Flinders Echo Department for the strain echo. Thank you Nola Grande for your help, supports and friendship. Thank you to Jane McKinnon for your help. Thank you to Dr Andrew Russell for PhD process input and cardiology reference.

Last but not least, everything is possible because God lets it happens. May this work lead to us fulfilling, or at least partly, the purpose of our life helping one another. Thank you for all the research participants and team for wanting to help others.

# Abstract

Cardiovascular disease is the major cause of death in the chronic kidney disease (CKD) population. Coronary artery disease (CAD) in CKD is often asymptomatic, with multi-vessel ischaemia, and carries a poor prognosis. Although the risk of death is reduced with renal transplantation, cardiovascular disease is still one of the major causes of death post transplant with mechanisms not well defined.

Despite the high prevalence of CAD, current functional cardiac investigations to assess inducible myocardial ischaemia in CKD population are suboptimal and may lead to significant adverse effects. Multi-modality cardiovascular magnetic resonance (CMR) imaging has emerged as a non-invasive clinical tool to assess cardiomyopathy, infarction and viability and myocardial perfusion, without risk of radiation. Stress CMR potentially detects inducible myocardial ischaemia from both epicardial and microvascular CAD. The use of gadolinium contrast is, however, contraindicated in CKD population.

The aim of this thesis is to 1) utilise a non-gadolinium contrast blood oxygen level dependent (BOLD) CMR technique to assess myocardial oxygenation response to stress in the CKD population as a measure of ischaemia and 2) characterise cardiac phenotype in post renal transplant population using non-invasive approaches.

BOLD CMR technique is utilised in Chapter 3 and shows impaired myocardial oxygenation response to stress in CKD population. The reduced BOLD signal intensity in the CKD population could be related to the declining renal function.

Chapter 4 examines the association between myocardial oxygenation response to stress and coronary artery anatomy in the CKD and post renal transplant population.

The study in Chapter 5 demonstrates that myocardial perfusion is impaired in renal transplant population, similar to liver transplant recipients without prior CKD, thus most likely post-transplant related rather than secondary to previous CKD. It utilises stress perfusion CMR and magnetic resonance coronary angiography (MRCA) in renal transplant population with reasonable residual renal function. The impaired myocardial perfusion is independent of the degree of left ventricular hypertrophy and is not fully explained by the presence of significant epicardial CAD, implying microvascular disease.

Chapter 6 investigates the association between reduced myocardial perfusion reserve and aortic stiffness in renal transplant recipients. The study does not show any association between myocardial perfusion reserve and central pulse wave velocity.

Chapter 7 examines blunted myocardial oxygenation response to stress in predicting major cardiac events in asymptomatic people with pre-existing CKD.

This thesis explores the role of CMR in assessing myocardial ischaemia in the renal population. It leads to a potential diagnosis of microvascular disease that has been shown to decrease survival, yet often missed by current clinical cardiac stress investigations. Further research is needed for therapeutic and prognostic study in microvascular coronary artery disease in renal population.

# Thesis Related Publications

## Peer Reviewed Journal Publications

### Chapter 1

**Parnham S.F.C.**, Gleadle J.M., De Pasquale, C.G., Selvanayagam, J.B. Myocardial Ischemia Assessment in Chronic Kidney Disease: Challenges and Pitfalls. *Front. Cardiovasc. Med.* 2014; 1:1-5.

**Parnham, S.F.C.**, Selvanayagam, J.B. Myocardial Blood Oxygenation: Ready for Clinical Prime Time? *Current Cardiovascular Imaging Reports.* 2013; 1-3.

### Chapter 3

**Parnham, S.**, Gleadle, J., Bangalore, S., Grover, S., Perry, R., Woodman, R., De Pasquale, C., Selvanayagam, J. Impaired Myocardial Oxygenation Response to Stress in Patients With Chronic Kidney Disease. *Journal of the American Heart Association.* 2015; 4(8): 1-11.

### Chapter 5

**Parnham, S.**, Gleadle, J.M., Leong, D., Grover, S., Bradbrook, C., Woodman, R.J., De Pasquale, C.G., Selvanayagam, J.B. Myocardial Perfusion is Impaired in Asymptomatic Renal and Liver Transplant Recipients: A Cardiovascular Magnetic Resonance Study. *Journal of Cardiovascular Magnetic Resonance.* 2015; 17: 1-9.

## **Chapter 6**

Submitted to Journal as Letter to Editor.

### **Abstracts**

**Parnham, S.**, Gleadle, J., Grover, S., Perry, R., Woodman, R., De Pasquale, C., Selvanayagam, J. Impaired Myocardial Oxygenation Response to Stress in Patients With Chronic Kidney Disease. (Oral). *Cardiac Society of Australia and New Zealand (CSANZ) 63rd Annual Scientific Meeting*, Melbourne, Australia, 13-16 August 2015.

**Parnham, S.**, Gleadle, J., Leong, D., Grover, S., Bradbrook, C., Woodman, R., De Pasquale, C., Selvanayagam, J. Myocardial Perfusion is Impaired in Renal and Liver Transplant Recipients: A Cardiovascular Magnetic Resonance Imaging Study. (Poster). *Cardiac Society of Australia and New Zealand (CSANZ) 63rd Annual Scientific Meeting*, Melbourne, Australia, 13-16 August 2015.

**Parnham, S.**, Grover, S., Bradbrook, C., Leong, D., De Pasquale, C., Woodman, R., Gleadle, J., Selvanayagam, J. Reduced Myocardial Perfusion in Post Renal Transplant Population is Not Associated with Aortic Stiffness. (Poster). *Cardiac Society of Australia and New Zealand (CSANZ) 63rd Annual Scientific Meeting*, Melbourne, Australia, 13-16 August 2015.

**Parnham, S.**, Gleadle, J., Leong, D., Grover, S., Perry, R., Bradbrook, C., Woodman, R., De Pasquale, C., Selvanayagam, J. Myocardial Oxygenation is Impaired in Advanced Chronic Kidney Disease and Renal Transplant Patients. (Poster). *2015 SCMR/EuroCMR Joint Scientific Sessions*, Nice, France, February 4-7, 2015.

**Parnham, S.**, Gleadle, J., Leong, D., Grover, S., Bradbrook, C., Woodman, R., De Pasquale, C., Selvanayagam, J. Myocardial Perfusion is Impaired in Renal

Transplant and Liver Transplant Patients. (Oral). *2015 SCMR/EuroCMR Joint Scientific Sessions*, Nice, France, February 4-7, 2015.

**Parnham, S.**, Grover, S., Bradbrook, C., De Pasquale, C., Leong, D., Gleadle, J., Selvanayagam, J. Myocardial Oxygenation is Reduced in End-Stage Renal Failure: A Novel Blood Oxygen Level Dependant (BOLD)-Cardiac MRI Study. (Poster). *World Congress of Cardiology*, Melbourne, VIC, 4-7 May, 2014.

**Parnham, S.**, Grover, S., Bradbrook, C., De Pasquale, C., Leong, D., Gleadle, J., Selvanayagam, J. Myocardial Oxygenation is Reduced in End-Stage Renal Failure: A Novel Blood Oxygen Level Dependant (BOLD)-Cardiac MRI Study. (Poster). *Society for Cardiovascular Magnetic Resonance (SCMR) 17th Annual Scientific Sessions*, New Orleans, USA, January 16-19, 2014.

**Parnham, S.**, Grover, S., Bradbrook, C., Leong, D., De Pasquale, C., Woodman, R., Gleadle, J., Selvanayagam, J. Reduced Myocardial Perfusion in Post Renal Transplant Population is Not Associated with Aortic Stiffness (Poster). *Society for Cardiovascular Magnetic Resonance (SCMR) 17th Annual Scientific Sessions*, New Orleans, USA, January 16-19, 2014.

**Parnham, S.**, Grover, S., Bradbrook, C., De Pasquale, C., Leong, D., Gleadle, J., Selvanayagam, J. Myocardial Oxygenation is Reduced in End-Stage Renal Failure: A Novel Blood Oxygen Level Dependant (BOLD)-Cardiac MRI Study. *American Heart Association (AHA) Conference*, Dallas, Texas, USA, November 16-20, 2013.

**Parnham, S.**, Grover, S., Bradbrook, C., Leong, D., De Pasquale, C., Woodman, R., Gleadle, J., Selvanayagam, J. Renal Transplant Patients Have Impaired Myocardial Perfusion Independent of the Degree of Left Ventricular Hypertrophy: A CMR Study (oral). *European Society of Cardiology (ESC) Congress 2013*, Amsterdam, Netherlands, 31 August-4 September 2013.

**Parnham, S.**, Grover, S., Bradbrook, C., De Pasquale, C., Woodman, R., Gleadle, J., Selvanayagam, J. Myocardial Perfusion is Impaired in Asymptomatic Patients Post Renal Transplantation (oral). *Cardiac Society of Australia and New Zealand (CSANZ) 61st Annual Scientific Meeting*, Gold Coast, Australia, 8-11 August 2013.

**Parnham, S.**, Grover, S., Bradbrook, C., Srinivasan, G., De Pasquale, C., Woodman, R., Gleadle, J., Selvanayagam, J. Myocardial Perfusion is Impaired in Asymptomatic Patients Post Renal Transplantation (ePoster). *Society for Cardiovascular Magnetic Resonance (SCMR) 16th Annual Scientific Sessions*, San Francisco, USA, January 31-February 03, 2013.

# Abbreviations

BOLD	Blood Oxygen Level Dependent
BSA	Body Surface Area
CAD	Coronary Artery Disease
CKD	Chronic Kidney Disease
CMR	Cardiovascular Magnetic Resonance
CRP	C-Reactive Protein
CT	Computed Tomography
CVD	Cardiovascular Disease
DSE	Dobutamine Stress Echocardiography
ECG	Electrocardiogram
eGFR	estimated Glomerular Filtration Rate
EF	Ejection Fraction
ESE	Exercise Stress Echocardiography
EST	Exercise Stress Test
FA	Flip Angle
FFR	Fractional Flow Reserve
FoV	Field of View
HASTE	Half-Fourier Single Shot Turbo Spin Echo
HLA	Horizontal Long Axis
HT	Hypertensive
IHD	Ischaemic Heart Disease
LA	Left Atrium
LAD	Left Anterior Descending
LCx	Left Circumflex
LGE	Late Gadolinium Enhancement
LT	Liver Transplant
LV	Left Ventricle
LVEF	Left Ventricular Ejection Fraction
LVH	Left Ventricular Hypertrophy

LVOT	Left Ventricular Outflow Tract
MACE	Major Adverse Cardiovascular Events
MRCA	Magnetic Resonance Coronary Angiography
MPRI	Myocardial Perfusion Reserve Index
NT-proBNP	N-terminal pro-Brain Natriuretic Peptide
PET	Positron Emission Tomography
PTDM	Post-Transplant Diabetes Mellitus
RA	Right Atrium
RCA	Right Coronary Artery
RPP	Rate Pressure Product
RT	Renal Transplant
RV	Right Ventricle
SA	Short Axis
SI	Signal Intensity
SNR	Signal to Noise Ratio
SPECT	Single Photon Emission Computed Tomography
SSFP	Steady-State Free Precession
STIR	Short-Tau Inversion Recovery
T	Tesla
TE	Echo Time
TI	Inversion Time
TR	Repetition Time
TTE	Transthoracic Echocardiography
VLA	Vertical Long Axis

# **CHAPTER 1 - Background**

Coronary artery disease is the leading cause of mortality and morbidity in the chronic kidney disease population and often presents with atypical symptoms. Current diagnostic investigations of myocardial ischaemia in chronic kidney disease lack sensitivity and specificity. Chapter 1 explores the challenges of diagnostic myocardial stress investigation in patients with chronic kidney disease.

## **1.1 Clinical Problem**

Cardiovascular disease (CVD) is the number one cause of death worldwide, accounting for 17 million deaths and 30% of all total mortality (World Health Organisation 2008). In Australia, it is also the number one cause of death, causing 45,600 deaths in 2011 and 35% of all total mortality [1]. There were approximately 3.7 million Australian people with CVD [1].

CKD is common in Australia. ANZDATA 2013 reported 2534 new patients who commenced treatment for end-stage renal disease (ESRD) in Australia in 2012 [2]. Type 2 diabetes mellitus, glomerulonephritis, hypertension and polycystic kidney disease accounted for the majority of all new diagnosed cases of ESRD [2].

CVD and CKD often coexist. CVD is the leading cause of mortality and morbidity in people with CKD [3, 4]. The mortality rate of people with CKD worldwide is approximately 20% annually, and CVD accounts for 50% of these deaths [4-6]. Decreasing renal function has been shown to be associated with increased risk of deaths [3, 7] and increased severity of cardiac disease [8-10].

Myocardial ischaemia is a major cause of death in CKD patients. Myocardial ischaemia can be caused by both epicardial or microvascular coronary artery disease (CAD).

Coronary artery disease is highly prevalent in the CKD population [11] being evident even in early renal disease [8, 12] and in young CKD patients [13]. CKD patients have both traditional and non-traditional cardiac risk factors (Table 1.1).

Table 1.1 Cardiovascular Risk Factors in the Chronic Kidney Disease Population

<b>Traditional Cardiovascular Risk Factors</b>	<b>Non-Traditional Cardiovascular Risk Factors</b>
Hypertension	Left ventricular hypertrophy
Diabetes mellitus	Fluid overload
Dyslipidaemia	Uraemia
Smoking	Anaemia
Family history of coronary artery disease	Disorders of vitamin D, calcium and phosphate
Age	Hyperparathyroidism
	Inflammatory state
	Proteinuria
	Nephrotic state

In the CKD population CAD is often multi-vessel and causes silent or asymptomatic myocardial ischaemia [14, 15]. Asymptomatic epicardial CAD has been detected even in people with early stage CKD [16] and is associated with a higher major adverse cardiac event rate compared to those without CAD [15]. While the coronary plaque characteristics in patients with CKD showed no difference in the prevalence of high-risk plaque compared to the group without CKD [17], Kawai et al. showed that patients with mild CKD had higher prevalence of severe epicardial CAD compared to those without CKD [17], thus, suggesting that the problem relates to coronary stenosis rather than plaque stability.

Microvascular CAD is also present in the CKD population. Charytan et al. assessed mild to moderate CKD subjects without diabetes or uncontrolled hypertension using positron emission tomography imaging and found that the CKD cohort had decreased coronary flow reserve (CFR) compared to controls [18]. Chade et al. suggested that microvascular dysfunction occurred in early CKD [19]. They performed coronary flow wire to the left anterior descending artery using adenosine on early CKD subjects with no angiographically significant CAD and found the CKD subjects had lower CFR compared to normal controls [19]. Microvascular CAD has been shown to be associated with reduced survival, although the rate of survival is better than for epicardial CAD [20].

The presence of left ventricular hypertrophy (LVH) may contribute to ischaemia due to microvascular disease. The prevalence of left ventricular hypertrophy (LVH) in CKD population is 75% [21]. LVH increases with progressive decline of renal function [22]. It has been shown to be an independent predictor of survival and cardiovascular events in dialysis patients [23].

Although renal transplantation improves overall survival, CVD is still a major cause of mortality in this population, accounting for 30% post transplant deaths [24, 25]. It is the most frequent cause of death in renal transplant recipients worldwide [26]. The annual risk of CVD event in renal transplant recipients is 3.5 to 5%, which is 50-times higher than the general population [25]. In Australia malignancy has surpassed CVD as the all-cause mortality in the post renal transplant populations [27]. The age of ESRD patients undergoing transplantation is increasing and may partly account for CVD mortality [28].

The mechanism of CVD in renal transplant population is not well defined. Nanmoku et al. studied 64 people in the “Elderly Group” with mean age  $63.2 \pm 3.4$  years and 500 people in the “Young Group” with mean age  $37.4 \pm 13.5$  years and showed that the main cause of graft loss in the “Elderly Group” was sudden death with a functioning graft due to heart failure [28]. The aetiology of heart failure in this study was not specified. We may argue that the older renal transplant cohort might

well have silent ischaemic cardiomyopathy. There is a suggestion that both ischaemic heart disease and congestive heart failure occur in the first few years post renal transplant [29].

Marcassi et al., on the other hand, found ventricular arrhythmia had a high prevalence in the first few months post renal transplant [30]. The presence of coronary artery calcification was shown to be a risk factor for arrhythmia [30].

In addition to the traditional cardiac risk factors, renal transplant recipients have additional risk factors related to the immunosuppressive therapy. Prednisolone is well known to be atherogenic and increases the risk of developing diabetes mellitus, obesity, hypertension and hypercholesterolaemia [31]. Mycophenolate is associated with bone marrow suppression and diarrhoea [32], thus may cause anaemia and electrolytes imbalance, which may contribute to myocardial ischaemia, increased risk of arrhythmia and cardiac failure [33]. Cyclosporine is associated with development of post-transplant hypercholesterolaemia and diabetes mellitus [34]. It also causes nephrotoxicity and vasoconstriction of the renal afferent arteriole [35, 36], which may also cause coronary vasospasm. The administration of calcium channel blocker can prevent the arteriolar vasoconstriction [37]. Post renal transplant LVH in the absence of hypertension was shown to be cyclosporin-related [38]. Although it is preferred to cyclosporine [39-43], tacrolimus is associated with post-transplant hypercholesterolaemia and diabetes mellitus [44], which increases the risk of developing CAD. Marked LVH has been reported in children on tacrolimus [45]. Sirolimus use is associated with lower risk of post-transplant malignancy [46-48] and nephrotoxicity compared to calcineurin inhibitors [49], thus may be associated with less CVD post transplantation. Everolimus is also an mTOR inhibitor [50] with similar side effects to sirolimus [51].

## 1.2 Strategies and Current Evidence

### 1.2.1 Diagnostic Evaluation of Myocardial Ischaemia in Renal Population

Diagnostic evaluation starts with thorough clinical history and examination and a baseline 12-lead ECG. Cardiovascular examination of significant aortic stenosis is important prior to cardiac stress investigation. Cardiac stress investigations in CKD patients and their limitations are outlined in Table 1.2.

Table 1.2 Cardiac Stress Investigations in the Normal Renal Function versus Advanced Chronic Kidney Disease Patients

Cardiac Stress Modalities	Sensitivity (%)		Specificity (%)		Issues
	Normal Renal Function	CKD	Normal Renal Function	CKD	
Exercise Stress ECG [52-55]	68 (52-84)	36 (21-54)	77 (60-94)	91 (83-96)	Reduced exercise capacity (deconditioning) Impaired chronotropic response Abnormal baseline ECG and left ventricular hypertrophy
Exercise Stress Echocardiography [56, 57]	71-97	Possibly similar to DSE	64-90	Possibly similar to DSE	Reduced exercise capacity (deconditioning) Impaired chronotropic response Left ventricular hypertrophy

Cardiac Stress Modalities	Sensitivity (%)		Specificity (%)		Issues
	Normal Renal Function	CKD	Normal Renal Function	CKD	
Pharmacological Stress Echocardiography [59-61]	86 (78-91)	80 (64-90)	86 (75-89)	89 (79-94)	Blunted chronotropic response Left ventricular hypertrophy Microvascular disease potentially can be missed
Myocardial Perfusion Scintigraphy [66-71, 236]	89	69 (48-85)	75	77 (59-89)	False negative results in multi-vessel disease due to balanced ischaemia Radiation increases risk of malignancy post transplantation
Dobutamine Stress Cardiovascular Magnetic Resonance [90]		Research ongoing		Research ongoing	Blunted chronotropic response Left ventricular hypertrophy Microvascular disease potentially can be missed

### 1.2.1.1 Exercise Stress ECG

In patients with normal renal function, exercise stress test (EST) with ECG has a low to moderate sensitivity and specificity,  $68 \pm 16\%$  and  $77 \pm 17\%$  respectively, even when adequate exercise capacity and 85% heart rate is achieved [52]. EST is further limited in the advanced CKD population with poor sensitivity of 36% [53] (especially those undergoing dialysis), as deconditioning leads to reduced exercise capacity [54]. Deconditioning can be due to vascular, neurological or musculoskeletal comorbidities and the catabolic/cachectic metabolic state associated

with CKD. CKD patients have also been shown to have impaired heart rate response to exercise [55], and the frequently abnormal baseline ECG in CKD patients (often secondary to hypertension) hampers the interpretation of standard stress testing. In advanced CKD patients, the ST segment changes at stress were shown to be not significantly different between non-severe CAD and severe CAD group, despite a longer treadmill exercise time in the non-severe group [53].

#### **1.2.1.2 Exercise Stress Echocardiography and Dobutamine Stress Echocardiography**

Exercise stress echocardiography (ESE) is better than the standard stress ECG in ruling in CAD (Positive likelihood ratio ESE 7.94 versus EST 3.57) and ruling out CAD (Negative likelihood ratio ESE 0.19 versus EST 0.38) [56]. Its sensitivity has been reported ranging from 71% to 97% with specificity ranging from 64% to 90% [57]. However, the utility of ESE in CKD population remains limited due to the same physical reasons as EST limitations above.

The addition of echocardiography allows assessment of ventricular size and function, aortic and mitral valvular calcification, left ventricular hypertrophy (LVH), and potentially coronary flow reserve (CFR). CFR measurement by Doppler echocardiography in the left anterior descending artery has been shown to be a determinant of cardiac events in CKD patients in the absence of obstructive epicardial CAD [58], although this is not performed routinely by many echocardiography laboratories due to technical difficulties.

Stress echocardiography technique detects inducible myocardial ischaemia based on detection of wall motion abnormalities, thus would detect significant epicardial CAD, not microvascular disease.

A meta-analysis in 2008 showed that dipyridamole and dobutamine stress echocardiography had a sensitivity of 85% (confidence interval 80-89) and 86%

(confidence interval 78-91), respectively, and a specificity of 89% (confidence interval 82-94) and 86% (confidence interval 75-89), respectively, in detecting myocardial ischaemia in the non-renal population [59]. It is often recommended as a screening test in advanced CKD patients.

A systematic review in 2011 identified 11 DSE studies with 690 potential renal transplant recipients [60]. Overall, DSE had moderate sensitivity of 80% (confidence interval 64-90) in detecting inducible myocardial ischaemia in renal transplant candidates [60]. Several mechanisms may explain the reduced accuracy of DSE in the advanced CKD population. The majority of advanced CKD patients had a blunted chronotropic response, thus did not achieve 85% maximal predicted heart rate despite the use of atropine, significantly reducing the sensitivity of DSE in detecting myocardial ischaemia [61]. The thick myocardium of LVH with small intracavitary volume, commonly found in CKD patients, obscures the detection of wall motion abnormalities at stress, thus significantly reducing the sensitivity of stress echocardiography in detecting inducible myocardial ischaemia in CKD population. Microvascular CAD is difficult to appreciate given the focus on regional wall motion abnormality and likely to be missed.

Abnormal DSE results in CKD patients have been associated with poorer prognosis for cardiac events and overall mortality [53, 62-64]. Bergeron et al. showed that among 485 patients with CKD, the percentage of ischaemic segments during DSE was an independent predictor of mortality [62]. Negative stress echocardiography results, on the other hand, have been shown to be associated with low incidence of major adverse cardiac events [61].

Blunted chronotropic response with exercise in CKD population may relate to poorer overall cardiac prognosis. A 2012 meta-analysis of 11,542 patients showed that submaximal age-predicted heart rate (<85% maximum heart rate) in the setting of normal ESE and DSE had higher cardiovascular risk than those who achieved >85% maximal predicted heart rate [65].

### **1.2.1.3 Myocardial Perfusion Scintigraphy (MPS)**

Exercise and pharmacological MPS have sensitivity of 87% and 89%, and specificity of 73% and 75%, respectively, in detecting >50% coronary artery stenosis in patients without advanced CKD [66]. Exercise Myocardial Perfusion Scintigraphy (MPS) in the advanced CKD population has the same limitation as EST and ESE, i.e. related to the inadequate exercise performance and chronotropic incompetence [67]. MPS radiation may increase the risk of malignancy in the renal transplant population who is already at high risk of cancer.

A systematic review in 2011 showed that MPS has sensitivity of 69% (confidence interval 48-85) and specificity of 77% (confidence interval 59-89) in diagnosing inducible myocardial ischaemia in the pre-renal transplant population [60]. MPS has high false negative result in detecting ischaemia in people with significant triple vessel CAD, as in the CKD population, because of homogeneous tracer uptake due to 'balanced ischaemia' [68, 69].

Normal myocardial perfusion measured by single-photon emission computed tomography (SPECT) may not be associated with excellent prognosis in CKD population unlike the normal population [70, 71], perhaps due to the high false negative result from balanced ischaemia. A recent systematic review in 2015 showed that although functional cardiac stress investigations were as good as coronary angiography in predicting major adverse cardiac events, a substantial number of potential kidney transplant recipients with negative results still experienced adverse cardiac events [72]. Hakeem et al. showed patients with CKD with normal MPS still had a three times higher cardiac death rate than those with normal MPS and no CKD [71]. In addition, concurrent reduced coronary flow reserve and left ventricular hypertrophy may play a role. Fukushima et al. reported CKD patients with normal clinical myocardial perfusion by PET scan had reduced global myocardial flow reserve, which implied an underlying microvascular dysfunction in this population [73] that could explain the poorer prognosis. Increased

baseline myocardial blood flow and peripheral endothelial dysfunction in CKD patients have been suggested by Koivuvuori et al. [74].

Nonetheless, abnormal MPS results in CKD patients have been shown to be associated with higher incidence of cardiac events and mortality [75-81]. A meta-analysis of 12 studies of pre-renal transplant patients showed that the presence of reversible defects of inducible myocardial ischaemia was associated with sixfold increased risk of myocardial infarction and almost fourfold risk of cardiac death [82]. The presence of fixed defects was associated with a nearly fivefold increased risk of cardiac death [82]. Joki et al. suggested that myocardial perfusion abnormalities significantly predicted cardiac events in CKD patients independently of eGFR and left ventricular ejection fraction [75]. Among 2967 patients with CKD, the incidence of major adverse cardiac events at one year was 1.0%, 3.9%, 5.9%, and 7.3% for normal, mild, moderate, and severe summed stress score, respectively [77]. Al-Mallah et al. demonstrated an interaction between renal function and the magnitude of perfusion deficit assessed by stress MPS in patients with moderate and severe CKD in the presence of abnormal MPS [79].

Blunted heart rate response in CKD patients during stress myocardial perfusion imaging has been reported to be associated with mortality [83-85].

#### **1.2.1.4 Cardiovascular Magnetic Resonance (CMR)**

Cardiovascular Magnetic Resonance (CMR) with gadolinium contrast has not been widely utilised clinically in the CKD population due to the concern of nephrogenic systemic fibrosis (NSF) [86-88]. The use of Gadolinium chelates is prohibitive in CKD patients due to the rare but serious side effect of NSF. NSF manifests as a hardening of the skin and internal organs resembling scleroderma, which is irreversible and potentially fatal.

Cardiovascular magnetic resonance spectroscopy has been studied to assess early cardiac dysfunction in paediatric population with advanced CKD [89]. Dobutamine stress CMR was shown to be safe in the pre-renal transplant population [90], however there are issues with blunted chronotropic response, LVH obscuring wall motion interpretation and microvascular disease potentially can be missed.

#### **1.2.1.5 Aim of Thesis**

Further research is needed for better and safer diagnostic testing for myocardial ischaemia in CKD and renal transplant population. Cardiovascular magnetic resonance (CMR) imaging has emerged as a useful clinical and research tool in cardiology. It allows assessment of myocardial function, stress perfusion, oedema and infarction. It has a high temporal resolution and reproducibility, and does not have the risk of radiation. A new non-contrast blood oxygen level dependent (BOLD) CMR technique has been utilised in several human studies to assess myocardial oxygenation as a measure of ischaemia with promising benefits [91-97], namely in syndrome X, hypertensive patients, patients with CAD, hypertrophic cardiomyopathy and aortic stenosis. It detects both epicardial and microvascular CAD without the use of potentially toxic contrast.

The aim of this thesis is to 1) utilise a non-gadolinium contrast blood oxygen level dependent (BOLD) CMR technique to assess myocardial oxygenation response to stress in the CKD population as a measure of ischaemia and 2) characterise cardiac phenotype in post renal transplant population using non-invasive approaches.

## 1.3 Utility of Stress Cardiovascular Magnetic Resonance (CMR) in Assessment of Myocardial Ischaemia

### 1.3.1 Stress Perfusion CMR

Stress perfusion CMR provides comprehensive assessment of inducible myocardial ischaemia with high spatial resolution. During adenosine pharmacological vasodilatation, myocardial areas supplied by normal coronary arteries show a three- to five-fold increase of blood flow, whereas no or minimal change is found downstream of severely diseased arteries because arteriolar beds are already maximally vasodilated [98, 99]. Such areas therefore show lower peak enhancement with delayed uptake of the contrast, and thus appear dark (or hypointense) compared to the adjacent normal myocardium [99]. Stress perfusion CMR has high spatial resolution (< 3 mm) allowing the identification of very small perfusion defects in subendocardium [100]. Because of its high resolution and lack of ionising radiation, it has increasingly become a very attractive noninvasive cardiac imaging modality for people with suspected myocardial ischaemia, especially those with poor echocardiographic windows.

Stress perfusion CMR has high sensitivity and negative predictive value for the detection of myocardial ischaemia (Table 1.3). There is a good body of evidence supporting the diagnostic accuracy of stress CMR.

Table 1.3 Stress Perfusion CMR versus SPECT

	Meta-Analysis	CE-MARC		MR-IMPACT II	
	[101]	[103]		[104]	
%	Stress CMR	Stress CMR	SPECT	Stress CMR	SPECT
Sensitivity	89	86.5	66.5	67	59
Specificity	80	83.4	82.6	61	72

	<b>Meta-Analysis</b>	<b>CE-MARC</b>		<b>MR-IMPACT II</b>	
	<b>[101]</b>	<b>[103]</b>		<b>[104]</b>	
<b>%</b>	<b>Stress CMR</b>	<b>Stress CMR</b>	<b>SPECT</b>	<b>Stress CMR</b>	<b>SPECT</b>
Positive Predictive Value	82	77.2	71.4	70	73
Negative Predictive Value	88	90.5	79.1	65	60

Stress perfusion CMR is highly sensitive for detection of CAD with moderate specificity. Two meta-analyses have analysed the diagnostic performance of stress perfusion CMR. A meta-analysis in 2010 demonstrated a stress CMR sensitivity of 89% (95% CI: 88-91%), and a specificity of 80% (95% CI: 78-83%) [101]. Adenosine stress perfusion CMR had better sensitivity than with dipyridamole (90% (88-92%) versus 86% (80-90%),  $p=0.022$ ), and a tendency to a better specificity (81% (78-84%) versus 77% (71-82%),  $p=0.065$ ) [101]. An earlier meta-analysis in 2007 with 14 datasets (754 patients) using stress-induced wall motion abnormalities imaging and 24 dataset (1,516 patients) using perfusion imaging demonstrated a sensitivity of 83% (95% confidence interval 79-88%) and specificity of 86% (95% confidence interval 0.81 to 0.91) with disease prevalence of 71% and sensitivity of 91% and specificity of 81% with lower disease prevalence of 57% [102]. Thus, stress perfusion CMR is highly sensitive for detection of CAD but its specificity remains moderate.

CE-MARC (Cardiovascular magnetic resonance and single-photon emission computed tomography for diagnosis of coronary heart disease) is the largest prospective controlled trial, comparing adenosine stress CMR and adenosine stress SPECT [103]. They showed that stress perfusion CMR was superior than SPECT with higher sensitivity 86.5% versus 66.5% ( $p<0.0001$ ) and higher negative predictive value 90.5% versus 79.1% ( $p<0.0001$ ) [103], however the specificity and positive predictive value of stress CMR and SPECT are similar 83.4% versus 82.6%

and 77.2% versus 71.4%, respectively [103]. This study is limited by the use of visual perfusion analysis rather than quantitative analysis and also the use of coronary angiography that only diagnose epicardial coronary disease, not microvascular disease. The second largest trial, MR-IMPACT II (Magnetic Resonance Imaging for Myocardial Perfusion Assessment in Coronary Artery Disease), is a multi-centre study of 533 patients enrolled in 33 centres (USA and Europe) [104]. For CMR and SPECT, the sensitivity was 67% and 59% respectively, indicating the superiority of CMR over SPECT [104], however the specificity scores for CMR was lower than SPECT, 61% and 72% respectively [104].

The accuracy of stress perfusion CMR has also been compared with invasive fractional flow reserve (FFR). A meta-analysis in 2013 of 12 studies (761 patients) demonstrated that the sensitivity of stress perfusion CMR was 89.1% (95% confidence interval 84-93%) and specificity 84.9% (95% confidence interval 76.6-91.1%) using FFR as the reference standard for coronary artery stenosis [105]. Quantitative analysis with myocardial perfusion reserve index (MPRI) of 1.58 was shown to have a sensitivity of 0.80, specificity of 0.89 ( $p < 0.0001$ ), and area under the curve of 0.89 ( $p < 0.0001$ ) for FFR  $< 0.75$  [106]. The MPRI cutoff of 2.04 was shown to be 92.9% (95% confidence interval 77.9 to 100.0) sensitive and 56.7% (95% confidence interval 32.8 to 80.6) specific in predicting a coronary segment with FFR  $\leq 0.75$  [107].

Stress CMR also detects microvascular disease, which may explain the high sensitivity and moderate specificity. Panting et al. studied patients with syndrome X and normal control subjects. They found that in the controls, the myocardial perfusion index is increased with adenosine, whereas in patients with syndrome X, the subendocardial perfusion index did not change significantly [108].

Stress CMR is superior than SPECT in detecting myocardial ischaemia in patients with triple-vessel disease [109]. The overall sensitivity for identifying perfusion defects in three vascular territories was higher for stress perfusion CMR than for SPECT (84.6% versus 55.1%,  $p < 0.001$ ) [109].

### **1.3.1.1 Stress CMR Reproducibility**

Stress CMR has been shown to have a good inter-study reproducibility. Chih et al. examined qualitative and semi-qualitative stress CMR in 10 patients with CAD and 10 patients at low risk of CAD [110]. They found that MPRI was lower in patients with CAD compared to those with low risk CAD, with good reproducibility [110].

### **1.3.1.2 Stress Perfusion CMR in Assessing Prognosis**

Stress perfusion CMR has been shown to correlate with cardiac prognosis. Adenosine-induced reversible perfusion defect has been shown to be an independent predictor of cardiac events [111]. Similarly, dobutamine and dipyridamole stress CMR also correlates with prognosis [112-114].

A normal CMR perfusion is associated with a very low cardiac event rate and good prognosis. A negative adenosine stress CMR for ischaemia has high negative predictive value of 96% for significant CAD [115] and high negative predictive value of 99.2% for major adverse cardiac events [116].

### **1.3.1.3 Stressors in Stress CMR and Their Safety**

Adenosine is a purine nucleoside molecule which causes coronary vasodilatation through activation of A<sub>2A</sub> receptors. The safety and tolerance of adenosine 140 µg/kg/min has been studied in patients with significant CAD [117]. There were no deaths, myocardial infarctions, or bronchospasm during the CMR study [117]. Transient second degree atrioventricular block (Mobitz II) or third-degree atrioventricular block occurred in 8% of patients, however there was no sustained atrioventricular block demonstrated [117]. Transient chest pain was the most common side effect, occurred in 57% of patients [117].

#### **1.3.1.4 Stress CMR Image Analysis Techniques**

There are varieties of techniques of stress CMR, namely visual or qualitative, semiquantitative and quantitative methods. Quantitative stress CMR analysis has higher accuracy compared to visual qualitative analysis [118], especially in multi-vessel CAD [118]. Quantitative analysis is, however, not readily available. Huber, et al. compared the diagnostic accuracy of stress perfusion CMR using semiquantitative and quantitative methods and found that the semiquantitative method provides identical diagnostic performance similar to the quantitative method if both stress and rest examinations were used [119].

The addition of magnetic resonance coronary angiography (MRCA) to stress perfusion CMR may increase the accuracy of the result in diagnosing haemodynamically significant coronary artery stenosis. Heer et al. showed that the addition of non-contrast MRCA to stress perfusion CMR increased the specificity of stress perfusion alone [120]. Bettencourt et al. suggested that the MRCA improved the sensitivity of the stress perfusion CMR [121].

#### **1.3.2 Blood Oxygen Level-Dependent (BOLD) CMR**

Coronary artery stenosis initially leads to a mismatch between myocardial oxygen demand and supply, particularly during stress. This in turn leads to post-stenotic capillary recruitment and elevated levels of de-oxyhaemoglobin in these vessels. BOLD CMR differentiates areas containing high levels of de-oxyhaemoglobin from remote normal myocardium, and therefore is able to demonstrate myocardium subtended by coronary artery stenoses. This technique utilises the T2/T2\* effect that is the incoherence in the phase behavior due to local inhomogeneity in the magnetic field, and is similar to the technique used to measure myocardial iron [122]. T2/T2\* signal is lower from tissue with a high de-oxyhaemoglobin content. Furthermore

direct quantification of cardiac tissue de-oxygenation is possible, which may be a superior parameter for myocardial ischaemia.

The myocardial BOLD technique has been validated in human and animal models with promising results [96, 97, 123-131]. BOLD CMR accuracy in detecting significant CAD has been evaluated, overall with moderately good sensitivity and specificity. The first BOLD CMR study in coronary artery disease was by Wacker et al. 1999 [132], at the time using T2\* measurements using a segmented gradient echo pulse sequence with ten echoes under pharmacological stress with dipyridamole. Later, in 2003, they concluded that in regions associated with the stenotic artery, T2\* was significantly lower than in residual myocardium ( $p < 0.01$ ) [93]. Friedrich et al. 2003 studied 25 patients with stress-induced angina using BOLD CMR T2\*-sensitive echo planar imaging sequence before and during adenosine in a single-slice approach, comparing with quantitative angiography and adenosine thallium SPECT [94]. They observed that a mean signal intensity decrease during adenosine was related to coronary stenoses  $>75\%$  [94]. According to this study, the BOLD-CMR signal intensity increase cutoff value of 1.2% had a sensitivity of 88% and a specificity of 47% to correctly classify severe stenoses [94]. However, all these studies were undertaken using 1.5T, which is fundamentally limited by the relatively small difference in T2\* between normal and de-oxygenated myocardial regions ( $43 \pm 21\%$ ).

At 3T, the blood and extra-vascular tissue T2\* is much more sensitive to differences in oxygenation levels, consequently increasing the contrast compared to 1.5T. This boost in contrast is accompanied by an increased SNR at 3T, which makes cardiac BOLD imaging considerably more robust. The first study at 3T validating the BOLD technique against PET in patients with known single or double vessel coronary disease was reported in 2010 [92]. This showed regional myocardial perfusion and oxygenation are dissociated in a significant proportion of patients, indicating that in patients with CAD reduced perfusion does not always lead to deoxygenation.

Manka et al. 2010 studied 46 patients (34 men; age  $65 \pm 9$  years) with suspected or known coronary artery disease underwent adenosine BOLD CMR at 3T prior to clinically indicated invasive coronary angiography [133]. Significant stenosis was defined as coronary artery with  $\geq 50\%$  luminal narrowing. Coronary angiography demonstrated significant CAD in 23 patients [133]. BOLD CMR at rest revealed significantly lower T2\* values for ischaemic segments ( $26.7 \pm 11.6$  ms) compared to normal ( $31.9 \pm 11.9$  ms;  $p < 0.0001$ ) and non-ischaemic segments ( $31.2 \pm 12.2$  ms;  $p = 0.0003$ ) [133]. Under adenosine stress T2\* values increased significantly in normal segments only ( $37.2 \pm 14.7$  ms;  $p < 0.0001$ ) [133]. This study was confirmed by a prospective study by Arnold, et al. 2012 compared quantitative BOLD CMR to coronary angiography, in which a significant CAD was defined as the presence of at least 1 stenosis of  $\geq 50\%$  diameter in any of the main epicardial coronary arteries or their branches with a diameter of  $\geq 2$  mm [134]. BOLD CMR has an accuracy of 84%, a sensitivity of 92% and a specificity of 72% [134]. Their study also suggested that hypertension increased the likelihood of abnormal BOLD response, however not diabetes mellitus, hypercholesterolaemia or myocardial scarring [134]. Walcher et al. 2012 further researched the diagnostic accuracy of BOLD CMR compared to invasive FFR, current gold standard for measuring haemodynamically significant coronary artery lesion [135]. They scanned 36 patients on 1.5T and performed FFR in all patients. An FFR  $\leq 0.8$  was regarded to indicate a significant coronary lesion. They found that relative BOLD signal intensity increase was significantly lower in myocardial segments supplied by coronary arteries with an FFR  $\leq 0.8$  compared with segments with an FFR  $> 0.8$  ( $1.1 \pm 0.2$  versus  $1.5 \pm 0.2$ ;  $p < 0.0001$ ) [135]. The BOLD CMR sensitivity and specificity compared to FFR  $\leq 0.8$  were 88.2% and 89.5%, respectively [135].

It is recognised that the interplay between myocardial ischaemia, perfusion, and oxygenation in the setting of CAD is complex and that myocardial oxygenation and perfusion may become dissociated. McCommis et al. 2010 compared CMR and PET imaging at rest and during dipyridamole vasodilation or dobutamine stress in canines to induce a wide range of changes in cardiac perfusion and oxygenation [126]. CMR

first-pass perfusion imaging was performed to quantify myocardial blood flow and volume and CMR BOLD technique was used to determine the myocardial oxygen extraction fraction during pharmacological hyperaemia.  $^{15}\text{O}$ -water and  $^{11}\text{C}$ -acetate were used to measure myocardial blood flow and myocardial oxygen consumption, respectively, by PET. They found that CMR results correlated with PET values for myocardial blood flow ( $r^2=0.79$ ,  $p<0.001$ ), myocardial oxygen consumption ( $r^2=0.74$ ,  $p<0.001$ ), and oxygen extraction fraction ( $r^2=0.66$ ,  $p<0.01$ ) [126]. The Karamitsos et al. study referred to above found that 40% of myocardial segments with stress myocardial blood flow below the cutoff of 2.45 mL/min/g did not show deoxygenation [92]. It is tempting to speculate that the normal oxygenation measurements seen in these segments with impaired perfusion indicate the absence of true ischaemia in these territories despite reduced regional blood flow. Arnold et al. studied the correlation between adenosine stress perfusion CMR and adenosine BOLD CMR and also confirmed that oxygenation and perfusion were not strongly correlated ( $r= -0.26$ ) [134].

BOLD images have several limitations, namely, low signal to noise ratio (SNR), long acquisition times and off resonance artifacts that may mimic deoxygenation even at 3T [134]. Even higher field strength (7T) magnets with corresponding increases in SNR will overcome these problems but clinical availability is likely to be limited. Novel means of coronary vasodilation, including  $\text{CO}_2$  retention rather than IV Adenosine also offers promise.

In conclusion, BOLD CMR potentially offers an attractive option for non-invasive ischaemia detection, given it does not use exogenous contrast, making it especially useful in cases where Gadolinium chelates are contraindicated (e.g. advanced CKD and ESRD). However, at present, only one (mid-ventricular) slice can be interrogated, limiting its sensitivity. It is hence unlikely to replace first pass perfusion as the preferred CMR method for ischaemia assessment in most patients, unless improvements in signal-noise can be made. BOLD CMR nevertheless adds value in providing new insights into states of myocardial hibernation, hypertrophy, and diseases of the coronary macro- and micro-vasculature. A greater pathophysiological

understanding of the underlying disease processes might enable the development of new therapies aimed at symptom relief and reducing disease progression.

### **1.3.3 CMR Assessment of Myocardial Infarction/Replacement Fibrosis**

Late gadolinium enhancement (LGE) CMR administers relatively inert extracellular gadolinium T1 contrast during gradient-echo inversion recovery imaging [136]. To optimise the contrast between gadolinium-enhanced infarcted myocardium and normal tissue, an inversion-recovery sequence is used [137]. An inversion time is chosen at the zero (null) point for normal myocardium, which appears black due to low signal. The infarcted or fibrotic tissue appears bright (hyperenhanced) because of reduced clearance and increased volume of distribution of gadolinium [138].

LGE CMR is useful in detecting myocardial infarction and viability and to distinguish ischaemic from non-ischaemic cardiomyopathy. LGE is a transmural or a subendocardial pattern in myocardial infarction, due to the course of the coronary arteries from the epicardium to the endocardium [139]. LGE CMR has a high specificity 98% for the detection of myocardial infarction [140]. The infarct size determined on CMR LGE in animal models was highly correlated with histopathology [141].

The presence of myocardial fibrosis detected by late gadolinium hyperenhancement has been shown to correlate with prognosis. A meta-analysis in 2015 showed LGE was associated with all-cause mortality, cardiac death, hospitalisation, sustained ventricular tachycardia or fibrillation in patients with dilated cardiomyopathy [142]. Another 2015 meta-analysis showed LGE was significantly associated with sudden cardiac death and all-cause mortality in patients with hypertrophic cardiomyopathy [143]. The prognostic value of delayed gadolinium CMR has also been shown in patients with ischaemic cardiomyopathy [144, 145].

LGE CMR utility is limited in advanced CKD patients due to potential risk of NSF as outlined above, which manifests as hardening of skin and internal organs resembling scleroderma which is potentially fatal. The incidence of NSF in people with normal renal function is zero and in CKD patients ranging from 0.26% to 8.8% [146, 147]. There has been no proven therapy for NSF. American College of Radiology 2015 recommended gadolinium precautions in patients with eGFR <40 mL/min/1.73 m<sup>2</sup> [148]. An in vitro experiment by Bose, et al. in CKD mice suggested a possible iron chelator deferiprone in preventing NSF [149].

A recently developed non-contrast T1 mapping is potentially useful to detect myocardial fibrosis of ischaemic and non-ischaemic pattern [150], especially in patients in whom gadolinium contrast is contraindicated. Non-contrast T1 mapping is currently a research tool and has not been utilised for clinical purpose. Further research is needed regarding accuracy and reproducibility of T1 mapping in multi-centre trials, multi-vendor application, both in normal individuals and various disease states. Non-contrast T1 mapping was not available in our centre during the thesis study.

### **1.3.4 CMR Assessment of Epicardial Coronary Artery Disease**

The prevalence of coronary artery disease in the CKD and renal transplant population are high and contribute to increased mortality. Therefore, there is a need of non-invasive imaging of the coronary artery anatomy in this population, ones without any risk of contrast induced nephropathy, nephrogenic systemic fibrosis and radiation induced malignancy. Both coronary angiography and CT coronary angiography carried radiation risk that may further increase the risk of malignancy in renal transplant population with already high mortality risk from cancer death. Non-contrast, free-breathing, whole-heart magnetic resonance coronary angiography (MRCA) sounds promising, especially in conjunction with stress CMR. MRCA has been studied in humans with promising results [151-158], namely, coronary

anomaly, Kawasaki disease, congenital heart disease in children, coronary artery stenosis, coronary artery bypass graft and cardiac allograft vasculopathy.

#### **1.3.4.1 Magnetic Resonance Coronary Angiography (MRCA) Techniques**

Two-dimensional gradient-echo fat suppressed breath-hold MRCA was first studied by Manning et al. in 1993 [159]. Three-dimensional navigator-gated with T2-weighted free breathing MRCA technique allows improvement of coronary artery visualisation and better contrast to noise ratio [160]. Then, the use of contrast agent was demonstrated to improve contrast of blood to myocardium [161, 162]. Interleaved spiral sequence was shown to have better image quality compared to segmented k-space fast low-angle short (FLASH) imaging [163]. SSFP sequence further improves the contrast between the myocardium and the coronary arteries [164]. Sakuma et al. performed whole-heart 3D MRCA in less than 30 minutes with good visualisation of all major coronary arteries [151].

Respiratory motion is a potential problem in MRCA. Respiratory gating reduces motion artifacts as compared to the diaphragmatic navigator technique [165]. Correction of heart rate variability with trigger delay may improve image quality in mid RCA and mid LAD [166].

MRCA at 1.5T and 3T has been studied. MRCA at 1.5 T has demonstrated better visualisation of the posterior descending artery with whole-heart approach, however, higher apparent contrast to noise ratio using volume-targeted approach but with longer scanning times without any difference in the length of the visualised coronary arteries [167]. MRCA at 3 T was shown to have sharper images with the targeted-volume approach as compared with the whole-heart approach [168], and with contrast-enhanced [169]. The MRCA performance with 32-channel significantly reduced the scanning time compared with five-channel coils [170].

### **1.3.4.2 Accuracy of MRCA in Detecting Coronary Artery Stenosis**

MRCA currently can detect significant stenosis in the ostial, proximal and mid coronary arteries, but not distally. For this reason, MRCA has been clinically utilised in young people with anomalous origin of coronary artery, coronary aneurysm and Kawasaki disease [171, 172].

MRCA has moderate accuracy for detecting significant coronary artery stenosis. It is currently inferior compared to CTCA in diagnosing coronary artery disease. A meta-analysis in 2010 of 20 MRCA studies and 89 CTCA studies showed that MRCA had a sensitivity of 87.1 and a specificity of 70.3%, whereas CTCA sensitivity was 97.2% and specificity was 87.4% [173]. A previous meta-analysis in 2006 of 51 studies comparing MRCA and CTCA, similarly, showed that MRCA sensitivity was 72% and specificity 87% compared to CTCA sensitivity 85% and specificity 95% [174]. MRCA has high accuracy for diagnosis of left main disease and triple vessel disease with a sensitivity of 100% and a specificity of 85% [175]. A multicentre trial of 138 patients with suspected CAD showed that non-contrast whole-heart MRCA had a high negative predictive value of 88%, thus may be able to exclude significant epicardial CAD [153].

MRCA has been studied for assessing the patency of coronary artery bypass grafts. Wittlinger et al. demonstrated the sensitivity of MRCA in detecting occluded graft was 94% with specificity of 88% [152]. Unfortunately, MRCA use is limited in detecting cardiac allograft vasculopathy in heart transplant recipients with sensitivity of only 60% [156]

Given its current limitations, MRCA can be regarded as an alternative imaging modality to exclude left main disease, triple vessel disease and any proximal epicardial coronary artery stenosis in selected patients, such as the CKD and renal transplant patients, in whom invasive coronary angiography and CTCA radiation and contrast are hazardous.

### **1.4.7.3 MRCA Reproducibility**

Free-breathing non-contrast MRCA has been shown to be reproducible with high-degree of intra-observer, inter-observer and inter-scan agreements [176].

### **1.4.7.4 MRCA in Assessing Prognosis**

Non-contrast MRCA has the potential capacity in assessing cardiac prognosis. Yoon et al. studied 207 patients with a median follow-up of 25 months and showed that the presence of significant stenosis on MRCA was associated with a >20-fold hazard increase for all cardiac events [177].

# **CHAPTER 2 - General Methods**

This chapter elaborates the general methodologies used in all our research participants. Specific methodologies for different study population are described in subsequent chapters.

## **2.1 Study Protocol**

### **2.1.1 Ethics**

The study protocol was approved by the Southern Adelaide Health Service/Flinders University Human Research Ethics Committee (Ethics Number 380.10 and 31.09). All study participants gave written informed consent.

### **2.1.2 Preparation**

All participants were screened for ensuring their MRI safety using a standard Flinders Medical Centre MRI safety form (Figure 2.1).

Four ECG electrodes for 1.5T machine (or three for the 3.0T machine) were placed on the anterior chest wall.



# MRI Safety Form

Patient name: .....

Date of Birth: ..... Height: ..... Weight: .....

When are you next seeing the doctor who sent you for this test?: .....

Where are you seeing your doctor? .....

Have you had a previous MRI scan? .....  YES  NO

In order to complete the examination safely we need to know the following information. Answer by ticking yes or no to each question. If you answer 'yes' to any implants we need to know the model and type of implant that you have before your arrival in the MRI Department.

- Have you ever been a metal worker or welder? .....  YES  NO
- Have you ever had an eye injury caused by metal? .....  YES  NO
- Do you have, or have you ever had a cardiac pacemaker or defibrillator? .....  YES  NO
- Do you have a stent?.....  YES  NO
- Do you have an artificial heart valve or clip? .....  YES  NO
- Do you have an ear or eye implant? .....  YES  NO
- Do you have a Neuro stimulator? .....  YES  NO
- Do you have a brain aneurysm clip? .....  YES  NO
- Do you have any implanted stimulation or drug infusion devices? .....  YES  NO
- Do you have an implanted prosthesis or artificial body part?.....  YES  NO
- Do you have a penile prosthesis? .....  YES  NO
- Do you have an intra uterine device (IUD)? .....  YES  NO
- Is there a possibility you may be pregnant?.....  YES  NO
- Are you breast feeding? .....  YES  NO
- Do you have any surgical clips or wire sutures? .....  YES  NO
- Do you have an embolisation coil? .....  YES  NO
- Do you have an inferior vena cava (IVC) filter? .....  YES  NO
- Do you have a brain shunt tube? .....  YES  NO
- Have you ever had gastric banding surgery?.....  YES  NO
- Do you have metal pins, screws, wires or mesh in your body ? .....  YES  NO
- Do you have any drug patches on your skin? .....  YES  NO
- Do you have any shrapnel, bullets or gun shot in your body? .....  YES  NO
- Do you have any metallic foreign bodies? .....  YES  NO
- Are you claustrophobic? .....  YES  NO
- Have you had an operation in the last 6 weeks? .....  YES  NO
- Do you suffer from hypertension or high blood pressure? .....  YES  NO
- Do you suffer from diabetes? .....  YES  NO
- Do you have a history of renal disease? .....  YES  NO
- Do you have tattoos or body piercing? .....  YES  NO

If you have answered 'yes' to any of the above questions it is very important that you advise us on 8204 5750 at your earliest opportunity at least several days prior to your scan. Failure to do so may result in your appointment being rebooked until a time after the relevant medical information has been obtained.

I ..... (Person completing this form)

(if not the patient, please state your relationship to the patient) .....

Acknowledge that to the best of my understanding the above answers are true.

I do/do not consent to contrast if required. (To be discussed at Appointment)

Signature ..... Date .....

Radiographer ..... Date .....

Phase 3 complete  Safe at 1.5T  Safe at 3T

Figure 2.1 Flinders Medical Centre MRI Safety Form.

All metals and metallic objects were removed prior MRI scan. Intravenous cannulation was established beforehand. An explanation of breath-holding commands was given at the start of the examination. Participants who are

claustrophobic or have implantable metals, pacemakers, defibrillators, cerebral aneurysm clips were excluded. All participants were explained the effects of stress adenosine. Coil configuration included a spine array coil embedded in the scan table and a flex array coil placed over the patient's anterior chest wall. A foam wedge was placed under the patient's knees for comfort. A baseline ECG, heart rate and blood pressure were performed before the stress imaging.

## **2.2 CMR Image Acquisition**

### **2.2.1 Multi Plane Localisers**

The localisers and cine methods are employed at Flinders Medical Centre [178]. Firstly, a set of multi-slice, multi-planar images were acquired. These comprised axial, coronal and sagittal images acquired in a single breath-hold, on every heartbeat, captured cycle for diastolic gating. The field of view (FOV) was adjusted in the antero-posterior direction.

Single shot Half-Fourier Single Shot Turbo Spin Echo (HASTE) with T2-weighted black-blood technique was acquired with free breathing. Fast Imaging with Steady Precession (TrueFISP or TRUFI) with white blood technique was acquired with free breathing.

#### **2.2.1.1 Two Chamber (Vertical Long Axis or VLA) Localiser**

One slice was planned from the axial view parallel to the interventricular septum, bisecting the left ventricle through the mitral valve and the apex (Figure 2.2). It was acquired with a single breath hold and captured cycle for diastolic gating. An example of image acquisitions from a research participant was shown below.

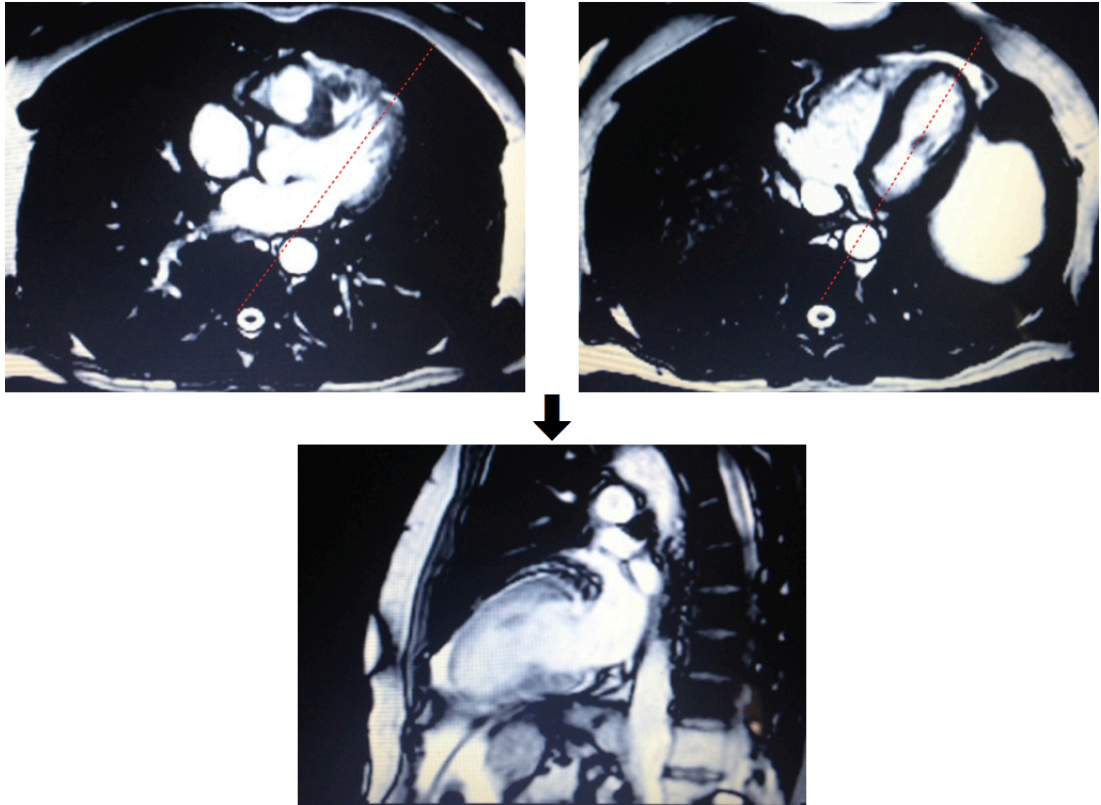


Figure 2.2 VLA Localiser.

#### **2.2.1.2 Four Chamber (Horizontal Long Axis or HLA) Localiser**

One slice was planned from the VLA view, bisecting the left ventricle through the mitral valve and the apex on a single breath hold, captured cycle for diastolic gating (Figure 2.3).

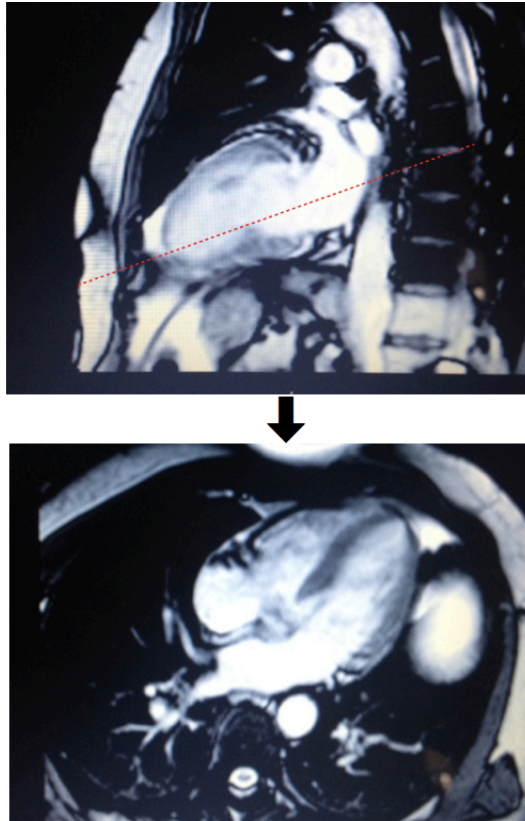


Figure 2.3 HLA Localiser.

### **2.2.1.3 Short Axis (SA) Localiser**

Three short axis slices were acquired using the VLA and HLA views with the most basal slice parallel to the atrio-ventricular groove in both planes, perpendicular to the long axis of the left ventricle, single breath hold with captured cycle (Figure 2.4).

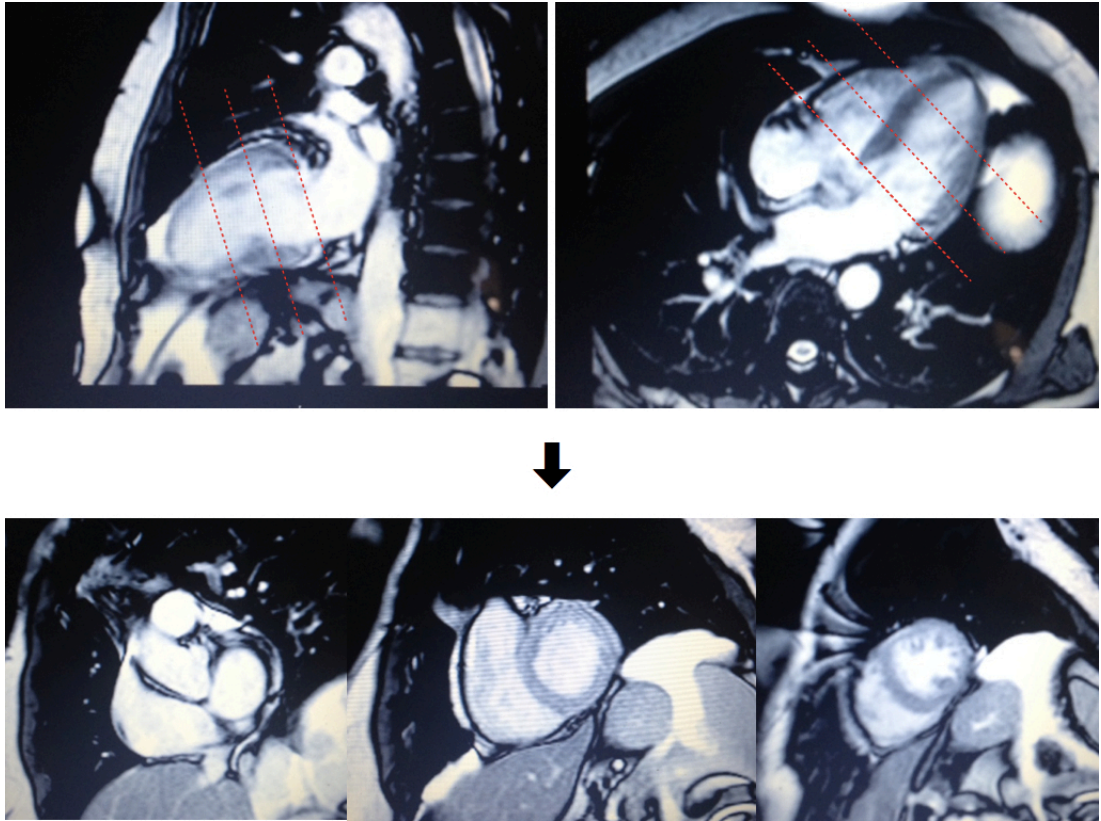


Figure 2.4 SA Localiser.

## 2.2.2 Cine Imaging

Cine images were acquired in VLA, HLA and ten SA images covering the entire left ventricle, using a retrospective ECG gating steady-state free precession (SSFP) sequence (repetition time (TR) 3 ms, echo time (TE) 1.5 ms, flip angle (FA) 55°, 18 phases) [179]. All research participants underwent ventricular function imaging.

### 2.2.2.1 Two Chamber (Vertical Long Axis or VLA) Cine

One slice was planned parallel to the ventricular septum on a short axis view, bisecting the left ventricle through the mitral valve and the apex on the HLA view (Figure 2.5).

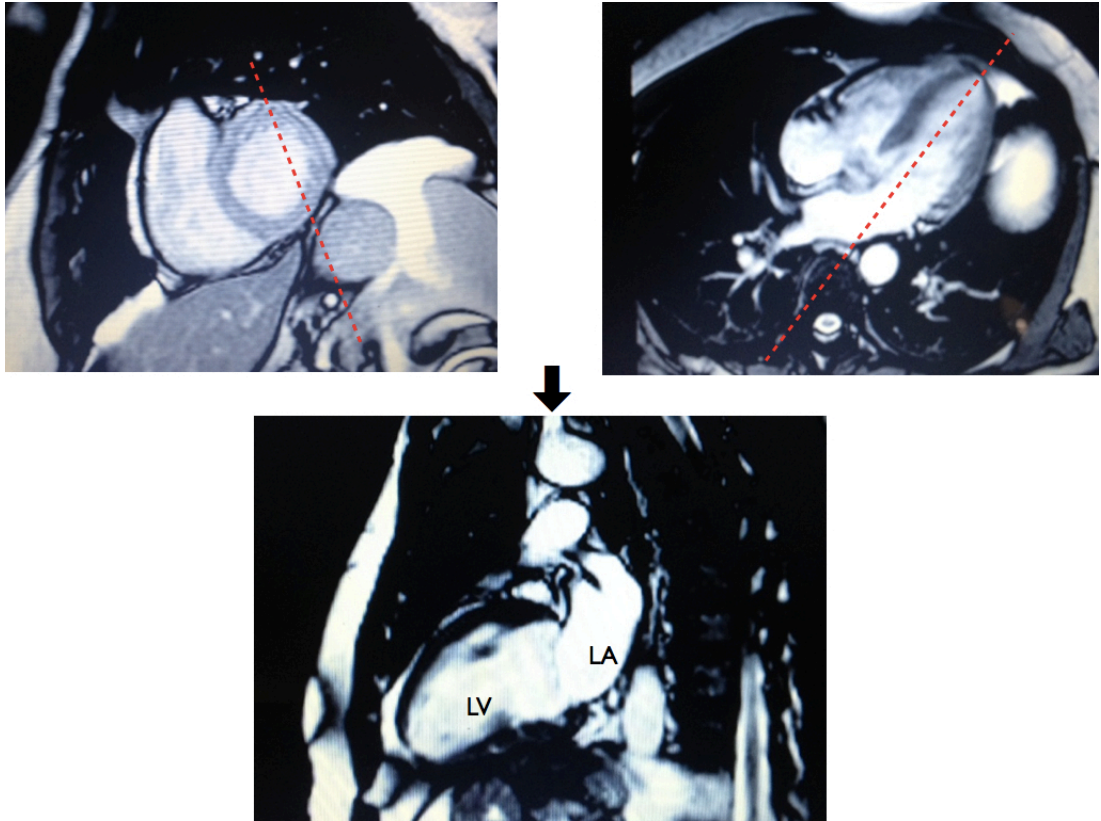


Figure 2.5 VLA Cine. LA indicates left atrium; LV, left ventricle.

#### **2.2.2.2 Four Chamber (Horizontal Long Axis or HLA) Cine**

One slice was planned bisecting the left ventricle through the mitral valve and the apex on a VLA, bisecting the left and right ventricles on an SA view and rotated through the apex (Figure 2.6). It was acquired on a single breath hold with retrospective gating.

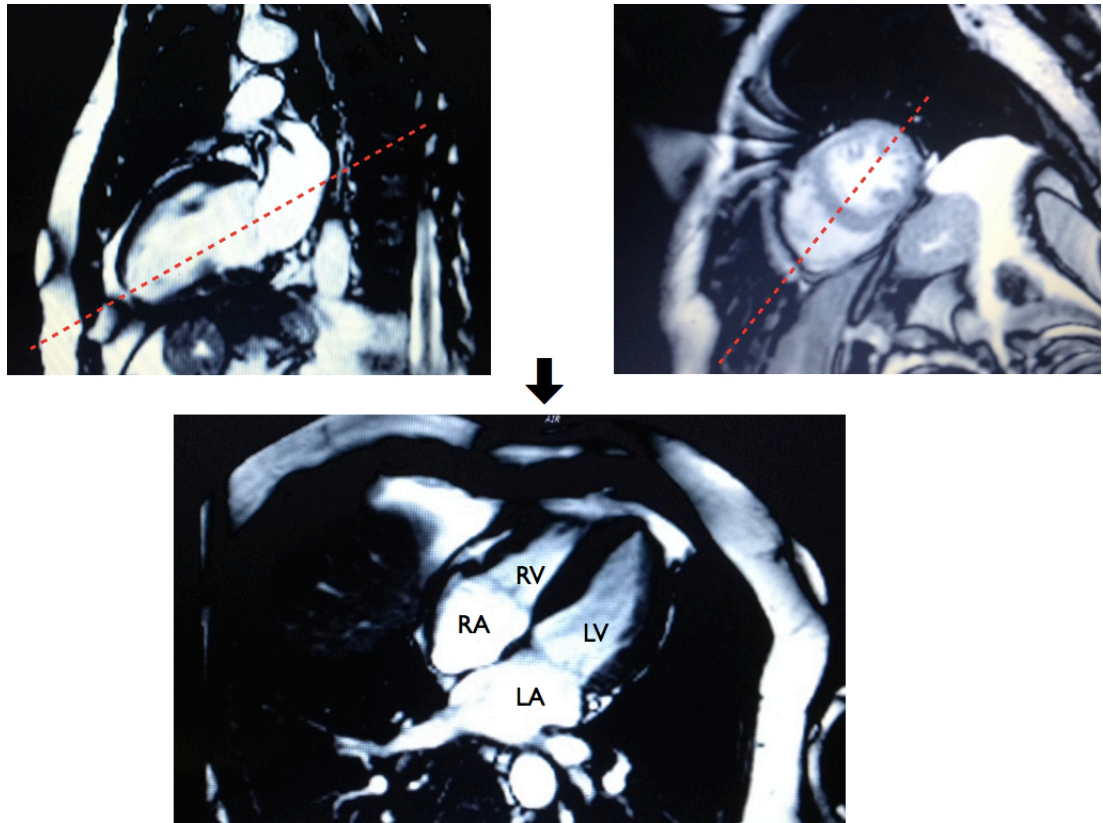


Figure 2.6 HLA Cine. LA indicates left atrium; LV, left ventricle; RA, right atrium; RV, right ventricle.

### 2.2.2.3 Left Ventricular Outflow Tract (LVOT) Cine

One slice was planned bisecting the LVOT and posterolateral left ventricular wall on the most basal short axis view, rotating the slice on the VLA view through the apex of the heart (Figure 2.7). It was acquired on a single breath hold with retrospective gating.

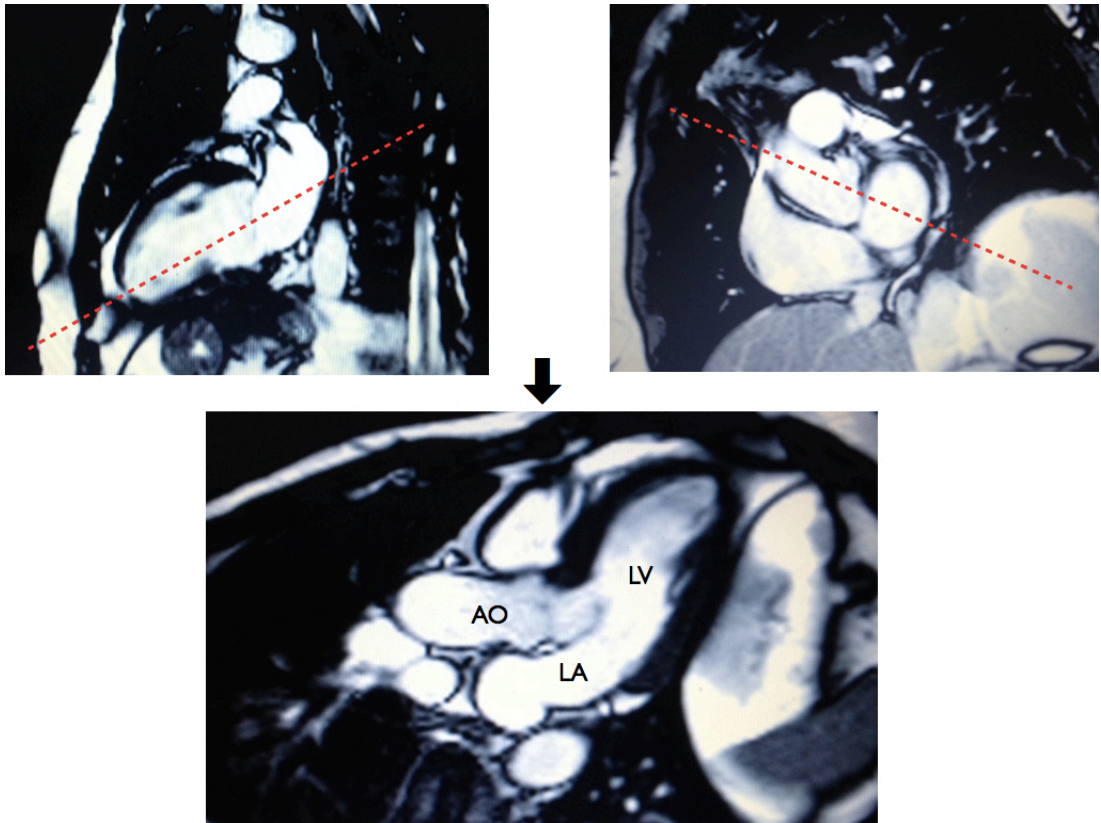


Figure 2.7 LVOT cine. LA indicates left atrium; LV, left ventricle; AO, aorta.

#### 2.2.2.4 Left Ventricular Outflow Tract (LVOT) Cross Cut Cine

The slice was positioned perpendicular to the LVOT cine through the aortic valve and into the proximal ascending aorta (Figure 2.8).

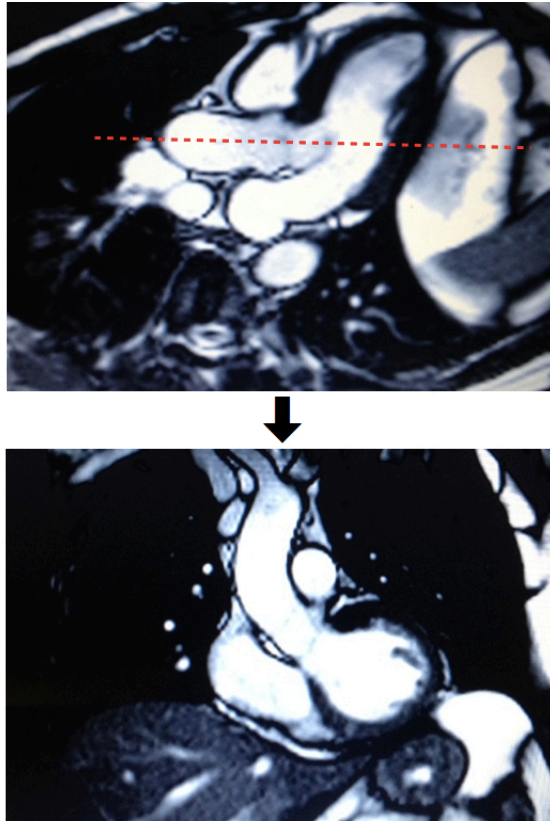


Figure 2.8 LVOT Cross Cut Cine.

#### **2.2.2.5 Short Axis (SA) Cine**

Ten slices were planned from the VLA and HLA cines in end diastole perpendicular to the long axis of the left ventricle in line with the atrioventricular groove, covering from the mitral valve to the apex (Figure 2.9). Slice thickness was 8 mm with 2 mm inter-slice gap.

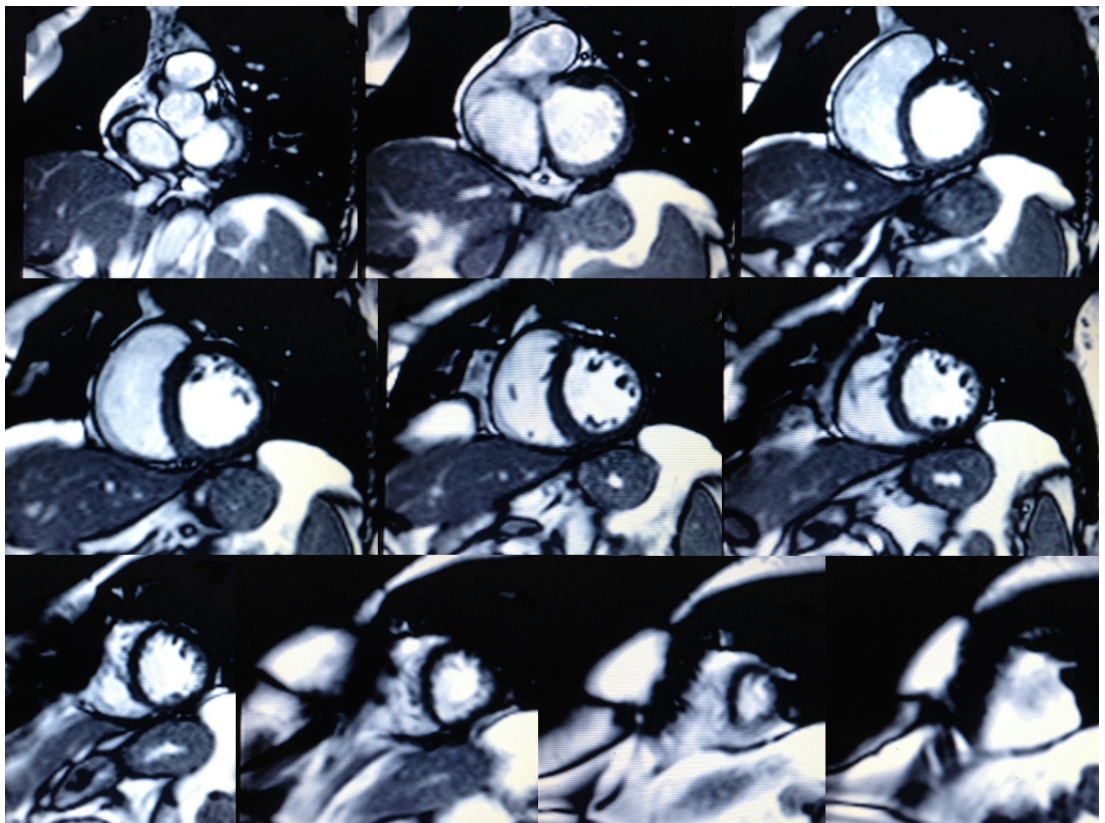
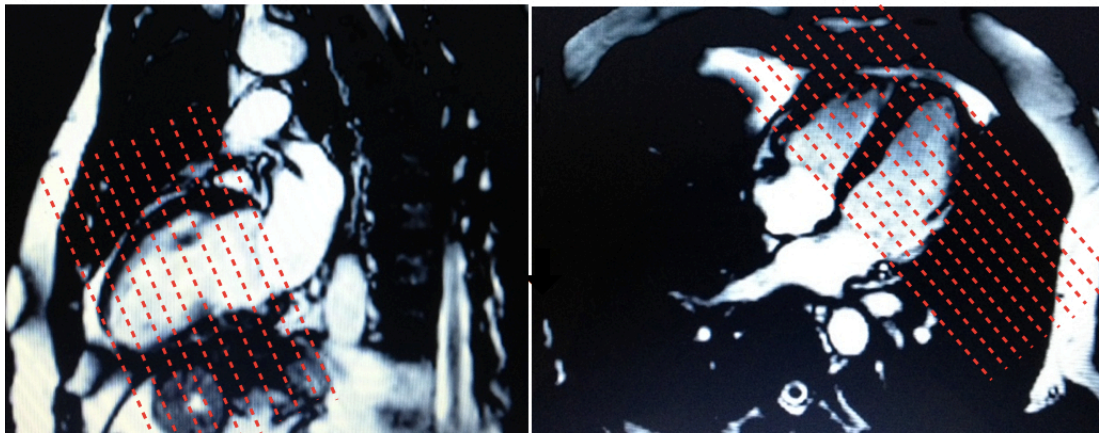


Figure 2.9 Ten SA Stack Cine.

### 2.2.3 Blood Oxygen Level Dependent (BOLD) Imaging

BOLD imaging was acquired in a 3 Tesla MRI scanner (Siemens, 3T Trio, 4 channel Body Flex coil). The participants were instructed to refrain from caffeine 24 hours prior to the scan. A single midventricular slice was acquired at mid-diastole using a T2-prepared ECG-gated SSFP sequence (TR 2.86 ms, TE 1.43 ms, T2 preparation time 40 ms, matrix 168 x 192, FoV 340 x 340 mm, slice thickness 8 mm, FA 44°) [92]. If required, frequency scout and shim adjustments were performed to minimise off-resonance artifacts. A set of six BOLD images were acquired at rest during a single breath-hold over six heart beats. Six stress BOLD images identical to the ones acquired at rest were acquired at peak adenosine stress (140 µg/kg per minute) 90 seconds after initiation for at least 3 minutes. Stress heart rate and blood pressure were obtained every minute of adenosine infusion. Each participant was questioned about the occurrence of adenosine effects: chest pain or tightness, shortness of breath, flushing, headache, and nausea. Figure 2.10 shows an example of a resting and stress BOLD imaging in a CKD participant.

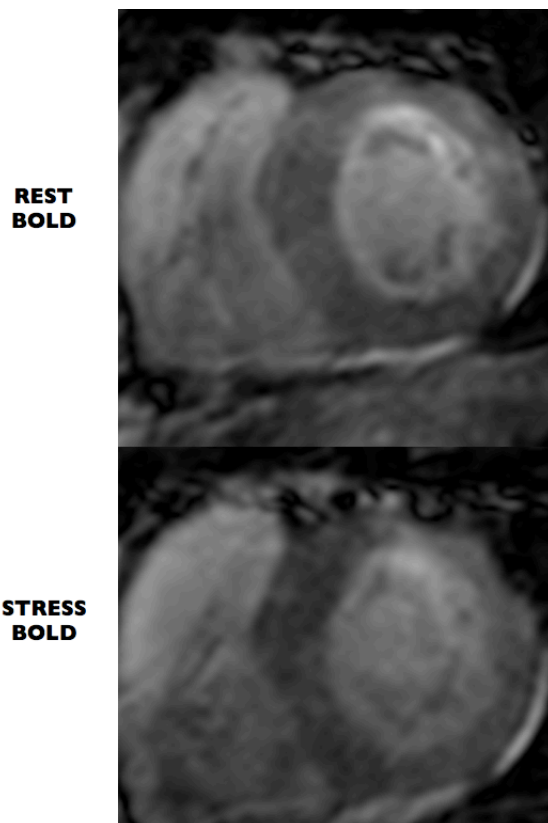


Figure 2.10 BOLD Imaging at Rest and at Stress in a CKD Participant.

### 2.2.4 Stress Perfusion Imaging

Stress perfusion imaging was not performed in the CKD participants with estimated glomerular filtration rate  $<45$  mL/min/1.73 m<sup>2</sup>. The participants were instructed to refrain from caffeine 24 hours prior to the scan. Stress perfusion imaging with adenosine infusion 140 µg/kg/min for 3-4 minutes was performed in the basal, mid, and apical myocardial segments, using an ECG-gated T1-weighted fast gradient echo sequence (TE 1.04 ms; TR 2 ms; voxel size 29x2.3x8 mm, FA 17°), and a peripheral bolus injection of a gadolinium-based agent (0.1 mmol/kg; gadolinium-based contrast agent, Gadovist, Bayer, Australia), followed by a 15-ml bolus of normal saline (rate 5ml/s) [92, 180]. All slices were imaged during each heartbeat, for a total of 50 heart beats. Blood pressure and heart rate were recorded by an automated recording machine at baseline and at 1 minute intervals during adenosine infusion. Each participant was questioned about the occurrence of adenosine effects: chest pain or tightness, shortness of breath, flushing, headache, and nausea. After discontinuing adenosine for 15 minutes, the same sequence was repeated without intravenous adenosine to obtain resting perfusion images. Figure 2.11 shows an example of rest and stress perfusion imaging of a post-transplant participant.

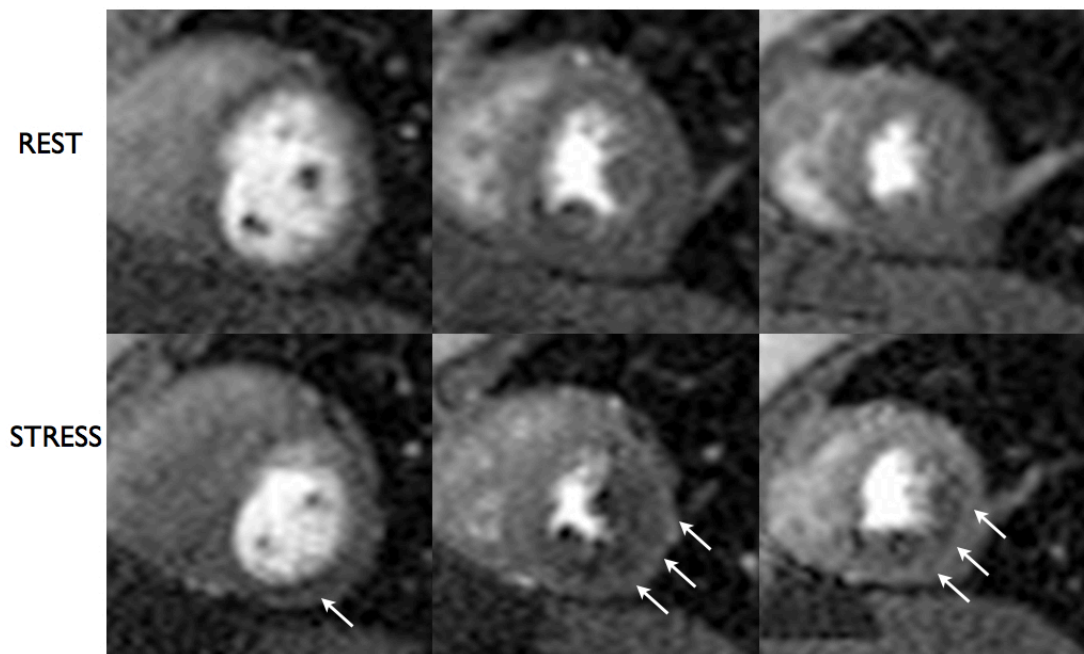


Figure 2.11 Rest and Stress Perfusion Imaging in a Post-Transplant Participant. Arrows indicate visual perfusion defect.

### 2.2.5 Late Gadolinium Imaging

Late gadolinium imaging protocol was not performed in the CKD participants with estimated glomerular filtration rate  $<45$  mL/min/1.73 m<sup>2</sup>. For late enhancement imaging, an additional bolus of Gadovist (0.05 mmol/kg) was injected, and after 6 minutes, images were acquired in the 3 long axes and in the short axis plane to obtain coverage of the entire left ventricle using a gated T1-weighted segmented inversion recovery turbo fast low-angle shot sequence (TE 4.8 ms; voxel size 1.4x2.4x8 mm; FA 20°) [181]. Figure 2.12 shows an example of late gadolinium imaging of a post-transplant participant.



Figure 2.12 Late Gadolinium Imaging in a Post-Transplant Participant.

### **2.2.6 Magnetic Resonance Coronary Angiography (MRCA)**

MRCA images were obtained using an 18-channel flex coil 1.5T clinical MR scanner (Siemens Sonata, Erlangen, Germany). A four-lead ECG was obtained for cardiac gating. Glyceryl trinitrate 400 micrograms/metered dose was administered prior to MRCA. The navigator-gated, free-breathing, non-contrast whole-heart MRCA was acquired using a 3D segmented SSFP sequence [151, 177]. A transaxial cine was used to monitor the minimum motion of right coronary artery with free breathing (TE 1.16 ms, TR 2.6 ms, FA 60°, FoV 320x320x120 mm, matrix 128x128, cardiac phase 50, sensitivity encoding 3.0). Epicardial fat was suppressed using spectral pre-saturation inversion recovery. Myocardial and venous blood signal was suppressed with T2 preparation. Figure 2.13 shows an example of MRCA imaging of a post-transplant participant.

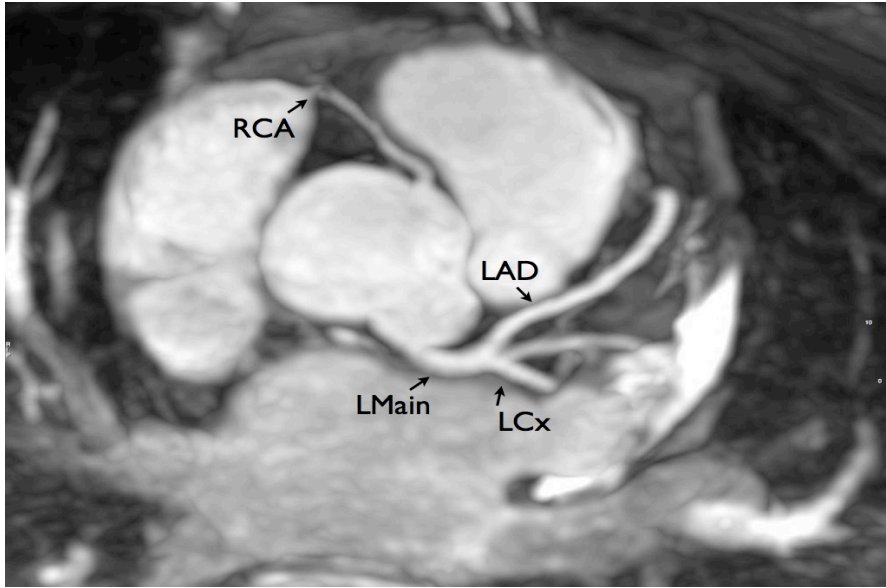


Figure 2.13 shows an example of MRCA imaging of a post-transplant participant. LMain indicates left main; LAD, left anterior descending; LCx, left circumflex; RCA, right coronary artery.

### **2.2.7 Pulse Wave Velocity Imaging of the Aorta**

Using the sagittal and transverse HASTE images, we acquired cine imaging in oblique sagittal view to generate hockey stick aortic view. Pulse wave velocity was assessed simultaneously in the ascending and proximal descending aorta using velocity-encoded imaging 150 cm/sec with a cross-sectional plane at the level of the main pulmonary artery.

## **2.3 CMR IMAGE ANALYSIS**

### **2.3.1 Ventricular Volumes, Function and Mass**

Ventricular volumes and function were analysed using CMR<sup>42</sup> software on a cine SA stack. The most basal slice was defined as the one with at least 50% of myocardium.

The end-diastolic phase was first identified. Using a mid-ventricular slice, the phases were advanced until the end-systolic phase when the smallest cavity was reached [179]. The CMR<sup>42</sup> software automatically calculated the volumes and mass (Figure 2.15). The ventricular volumes and mass were indexed to body surface area (BSA). The septal and lateral wall diameters were measured in end-diastole at mid-ventricular level from short-axis view.

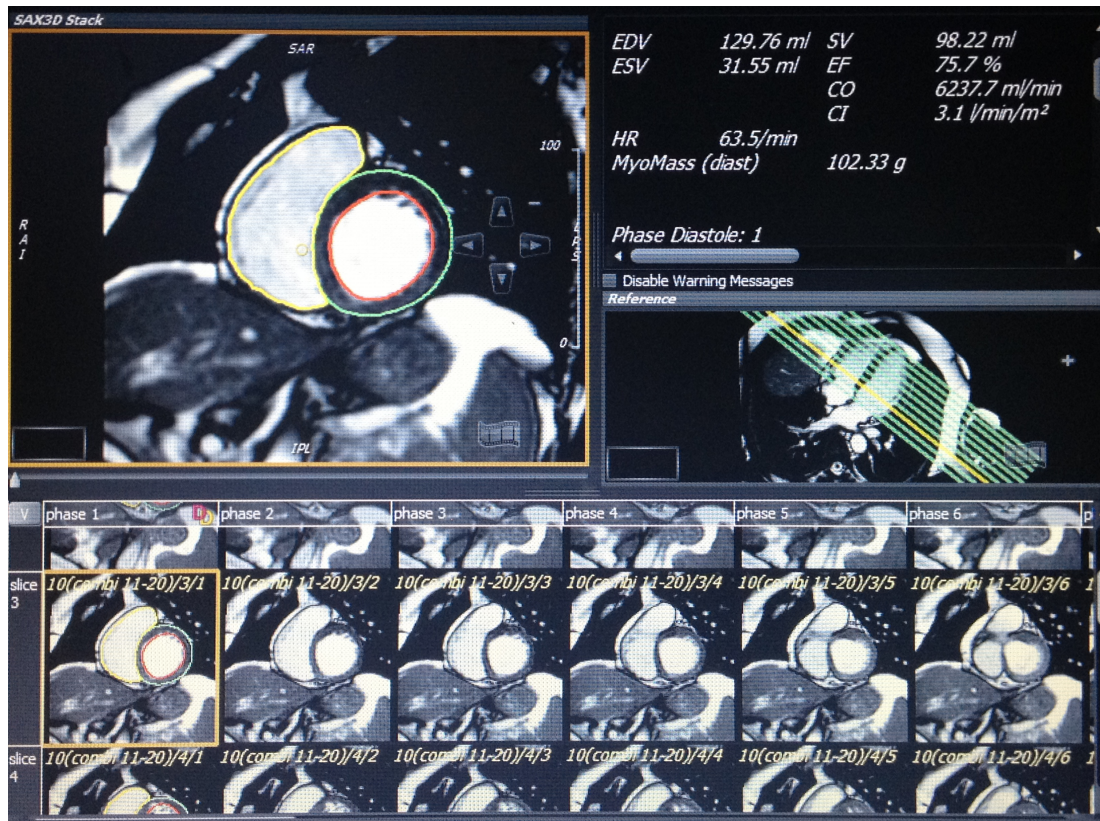


Figure 2.15 CMR<sup>42</sup> Analysis of Ventricular Function, Volumes and Mass.

### 2.3.2 BOLD Analysis

BOLD images were analysed after manually tracing the endocardial and epicardial contours using CMR<sup>42</sup> software, Version 4.0, Circle Cardiovascular Imaging Inc. (Calgary, Canada). Each midventricular short axis BOLD image was divided into six segments (anterior, anterolateral, inferolateral, inferior, inferoseptal, anteroseptal) according to the American Heart Association 17-segment model [182]. The mean

myocardial SI within each segment was obtained, both at rest and stress, and corrected to heart rate variations [92]:

$$SI = SI_0 / (1 - \beta e^{-TR/T1})$$

with  $T1 = 1220$  ms and  $\beta = 0.59$  (determined empirically for this sequence),  $SI_0$  = the measured Signal Intensity,  $SI$  = Signal Intensity corrected to heart rate, and  $TR$  is the image-dependent time between acquisition of sections of k-space, governed by the heart rate (replaced by the RR interval) [92].

The SI Change was calculated as:

$$\Delta SI(\%) = (SI_{\text{stress}} - SI_{\text{rest}}) / SI_{\text{rest}} \times 100\%$$

### **2.3.3 Stress Perfusion Analysis**

For perfusion analysis, semiquantitative analysis using CMR<sup>42</sup> software was used. Transmural, subendocardial and subepicardial contours were traced and manually corrected for breathing displacements. Blood pool contour was manually drawn. Each basal, mid and apical myocardial slice were divided into 6 segments with the right ventricular insertion as the reference point [183]. Since basal myocardial blood flow is closely related to the rate-pressure product (RPP), and index of left ventricular oxygen consumption, values for rest flow in each patient were also corrected for rate-pressure product [184]: Corrected Rest perfusion = (Rest perfusion / RPP)  $\times 10^4$ . Myocardial Perfusion Reserve Index (MPRI) was the relative difference between upslopes of the time-intensity curves at stress and rest and was calculated as the ratio of perfusion during adenosine stress to perfusion at rest corrected for rate pressure product [185].

### **2.3.4 Late Gadolinium Enhancement Analysis**

Areas of late gadolinium hyperenhancement was assessed visually as present or absent. Hyperenhanced pixels were defined as those with image intensities more than 5 standard deviations above the mean intensity in an remote myocardial region in the same image slide [186]. The fibrosis was quantified using CMR<sup>42</sup> software as a percentage of myocardial mass.

### **2.3.5 MRCA Analysis**

MRCA images were analysed using a 4D image reconstruction of CMR<sup>42</sup> software. Three-dimensional volume-rendered images were generated by the software. The left main, left anterior descending artery (LAD), left circumflex (LCx) and right coronary artery (RCA) were manually traced and followed for their course in axial, coronal, sagittal, cranial left anterior oblique, lateral, caudal right anterior oblique and caudal left anterior oblique views, using sliding thin-slab maximum intensity projection.

### **2.3.6 Pulse Wave Velocity Analysis**

The aortic path lengths between the ascending and descending aorta were manually measured along the centre line of the CMR “scout image” of the oblique sagittal (“hockey stick”) view of the aorta. The quantification of flow was achieved by CMR<sup>42</sup> Version 4.1, Circle Cardiovascular Imaging Inc. processing of the through-plane coronary artery phase velocity map in the ascending and descending aorta. Pulse wave velocity was calculated by dividing the distance between the ascending and descending aorta path length and the transit time of the flow wave [187, 188]. The transit time represents the difference in time between onset of flow upstroke.

## **2.4 Strain Echocardiography Protocol**

Participants were imaged in the left lateral decubitus position with a 3.5-Mhz transducer (Vivid E9 Ultrasound and M5S-D probe, General Electric Vingmed, Horten, Norway). Routine, 3 beat grey-scale images of the left ventricle were acquired from the apical 4 chamber, 2 chamber and long axis views. Frame rates in excess of 50 fps were maintained, and care taken to ensure non-foreshortening of the left ventricle. Echocardiographic data were stored in digital format for offline analysis, which was performed using commercially available software (EchoPac BT-11, GE-Vingmed, Horten, Norway). Left ventricular speckle-tracking strain was measured by manually demarcating the myocardial border with the region of interest optimised to ensure accurate tracking. Strain versus time curves were obtained for 18 segments from 3 apical views. Global longitudinal strain was measured from the average of 18 segments.

# **CHAPTER 3 - Impaired Myocardial Oxygenation Response to Stress in Patients with Chronic Kidney Disease**

## **3.1 Introduction**

Cardiovascular disease is the leading cause of mortality in patients with chronic kidney disease (CKD) [3]. CKD patients have a 10-20 times higher risk of cardiac death than the normal population, although the mechanism is uncertain [189]. Furthermore, despite cardiovascular mortality being significantly reduced by renal transplantation [190], cardiovascular disease remains a major cause of mortality in post-renal transplant recipients [25]. The majority of coronary artery disease (CAD) in CKD patients is asymptomatic and due to multi-vessel epicardial disease [14, 191]. These patients have significant cardiovascular risk factors ranging from atherosclerotic (hypercholesterolaemia, diabetes, hypertension), myocardial (fluid overload) and metabolic (hyperphosphataemia, anaemia, chronic inflammation). Left ventricular hypertrophy (LVH) is also a frequent finding in the CKD population with a prevalence of 75% [21].

Current functional cardiac investigations are neither sensitive nor specific for ischaemia in CKD patients [60, 192]. Blood Oxygen Level Dependent (BOLD) CMR assesses myocardial tissue oxygenation, thus is potentially able to measure mismatches in myocardial oxygen demand and supply and indicate ischaemia [193]. It exploits the paramagnetic properties of deoxyhaemoglobin as an endogenous contrast agent with increased deoxyhaemoglobin content leading to signal reduction on T2-weighted images [133]. The transition from diamagnetic oxyhaemoglobin to paramagnetic deoxyhaemoglobin induces a change in magnetic resonance signal intensity and thereby generating oxygen-dependent contrast [134]. The BOLD

technique has been validated in animal models [123-131] and utilised in human studies in patients with angina, CAD, syndrome X and hypertension [91-95].

We utilised BOLD CMR to measure myocardial oxygenation response to stress in the CKD population as a measure of myocardial ischaemia and searched for associations with renal function. We hypothesised that myocardial oxygenation would be impaired in the (1) CKD population and (2) in renal transplant recipients without known CAD, irrespective of the presence of diabetes mellitus and/or hypertension.

## **3.2 Methods**

### **3.2.1 Study Population**

CKD patients with an estimated glomerular filtration rate (eGFR) $<30$  ml/min/1.73m<sup>2</sup> or receiving regular dialysis were invited to participate to have CMR imaging at Flinders Medical Centre, a tertiary teaching hospital in South Australia, in 2012-2014. Ten renal transplant (RT) recipients with reasonable renal function eGFR $>45$  mL/min/1.73 m<sup>2</sup> were prospectively recruited from our hospital transplant clinic. CKD and RT patients had the following inclusion criteria: no symptoms of cardiac disease, no established CAD (no history of myocardial infarction, angina, coronary artery stent or bypass surgery or angiographically documented significant CAD $>70\%$ , and no significant inducible myocardial ischaemia on functional testing pre-transplant), and no previous systolic heart failure. Ten people with a clinical diagnosis of hypertension (HT) and who were asymptomatic with no known CAD were prospectively recruited from the hospital's Hypertension Clinic. Ten healthy volunteers without cardiovascular risk factors or symptoms served as normal controls.

The exclusion criteria for each group were severe standard contraindications to CMR (e.g. claustrophobia, metallic implants), and contraindications to adenosine (second or third degree atrioventricular block, obstructive pulmonary disease and dipyridamole use).

All participants gave written informed consent, and the study was approved by Southern Adelaide Clinical Human Research Ethics Committee (SAC HREC number 380.10).

### **3.2.2 Biochemistry**

eGFR was calculated from serum creatinine using the CKD-Epidemiology Collaboration (EPI) formula [194].

### **3.2.3 CMR Protocol**

All participants underwent scanning in a 3 Tesla clinical MR scanner (Siemens, 3T Trio, 4 channel Body Flex coil) and were instructed to refrain from caffeine 24 hours prior to the scan. All scans started with Half-Fourier single shot turbo spin echo (HASTE) and Fast imaging with steady precession (TrueFISP) localisers. Cine images were acquired in vertical and horizontal long-axis, and ten short-axis images covering the entire left ventricle, using a retrospective ECG gating steady-state free precession (SSFP) sequence (repetition time (TR) 3 ms, echo time (TE) 1.5 ms, flip angle 55°, 18 phases) [179]. For BOLD imaging, a single midventricular slice was acquired at mid-diastole using a T2-prepared ECG-gated SSFP sequence (TR 2.86 ms, TE 1.43 ms, T2 preparation time 40 ms, matrix 168 x 192, field of view 340 x 340 mm, slice thickness 8 mm, flip angle 44°), as previously described [92]. Shimming and centre frequency adjustments were performed as required before the oxygenation imaging to minimise off-resonance artifacts. A set of six BOLD images

were acquired at rest during a single breath-hold over six heart beats. Six stress BOLD images identical to the ones acquired at rest were acquired at peak adenosine stress (140 µg/kg per minute) 90 seconds after initiation for at least 3 minutes. Stress heart rate and blood pressure were obtained every minute of adenosine infusion. Each participant was questioned about the occurrence of adenosine effects: chest pain or tightness, shortness of breath, flushing, headache, and nausea.

All RT and HT subjects (eGFR>45 ml/min/1.73m<sup>2</sup>) underwent additional late enhancement imaging. Gadovist (Bayer Healthcare, Australia) 0.05 mmol/kg was injected, and after 6 minutes, images were acquired in the 3 long axes and in the short axis plane to obtain coverage of the entire left ventricle using a gated T1-weighted segmented inversion recovery turbo fast low-angle shot sequence (echo time, 4.8 ms; voxel size, 1.4x2.4x8 mm; flip angle, 20°). The inversion time was adjusted to achieve optimal nulling of noninfarcted myocardium [181].

### **3.2.4 Strain Echocardiography**

Due to the risk of nephrogenic systemic fibrosis with gadolinium contrast in patients with severe renal dysfunction [86-88], gadolinium studies were not undertaken in the CKD cohort who instead underwent a speckle tracking strain echocardiography study as a measure of myocardial fibrosis. Patients were imaged in the left lateral decubitus position with a 3.5-Mhz transducer (Vivid E9 Ultrasound and M5S-D probe, General Electric Vingmed, Horten, Norway). Routine, 3 beat grey-scale images of the left ventricle were acquired from the apical 4 chamber, 2 chamber and long axis views. Frame rates in excess of 50 fps were maintained, and care taken to ensure non-foreshortening of the left ventricle. Echocardiographic data were stored in digital format for offline analysis, which was performed using commercially available software (EchoPac BT-11, GE-Vingmed, Horten, Norway). Left ventricular speckle-tracking strain was measured by manually demarcating the myocardial border with the region of interest optimised to ensure accurate tracking. All echocardiographic images were analysed by a single observer who was independent

and blinded to patients' clinical and CMR data. Strain versus time curves were obtained for 18 segments from 3 apical views. Global longitudinal strain was measured from the average of 18 segments.

### 3.2.5 CMR Image Analysis

CMR analysis was performed with CMR<sup>42</sup> Version 4.0, Circle Cardiovascular Imaging Inc. (Calgary, Canada), as described in Chapter 2. In brief, left ventricular mass, left and right ventricular volumes and functions were calculated using the 3D short axis stack by tracing the endocardial and epicardial contours in end-diastole and end-systole, as previously described [179]. Left ventricular mass, left and right ventricular end-diastolic volumes and end-systolic volumes were indexed to body surface area (BSA). The septal and lateral wall diameters were measured in end-diastole at mid-ventricular level from short-axis view.

BOLD analysis was performed as previously described [92]. Myocardial Signal Intensity (SI) was measured by the CMR software, after manually tracing the endocardial and epicardial contours. Each midventricular short axis BOLD image was divided into six segments (anterior, anterolateral, inferolateral, inferior, inferoseptal, anteroseptal) according to the American Heart Association 17-segment model [182]. The mean myocardial SI within each segment was obtained, both at rest and stress, and corrected to variations in heart rate with the following equation previously described [92]:

$$SI = SI_0 / (1 - \beta e^{-TR/T1})$$

with  $T1 = 1220$  ms and  $\beta = 0.59$  (determined empirically for this sequence),  $SI_0$  = the measured Signal Intensity,  $SI$  = Signal Intensity corrected to heart rate, and  $TR$  is the image-dependent time between acquisition of sections of k-space, governed by the heart rate (replaced by the RR interval) [92].

The SI Change was calculated as:

$$\Delta SI(\%) = (SI \text{ stress} - SI \text{ rest}) / SI \text{ rest} \times 100\%$$

A second operator blinded to the clinical data analysed a subset of BOLD CMR scans to assess inter-observer reproducibility.

### **3.2.6 Statistical Analysis**

Statistical analysis was performed with STATA version 13.0. Normally distributed data is expressed as mean  $\pm$  SD and non-normally distributed data as median (inter-quartile range). Either t-test, ANOVA or a Kruskal-Wallis test was used to compare clinical characteristics between the study groups as appropriate. Chi-squared tests or Fisher's exact tests were used for comparison of categorical variables. BOLD SI evaluation of coronary artery level data and association with eGFR was analysed using linear mixed modeling (LMM) with a random intercept used for each subject to account for the within-subject correlation present from measuring at three different artery sites [180]. All analyses were adjusted for age and gender *a priori*, and also for other potential confounders where appropriate. Both unadjusted and adjusted LMM was performed with adjustment for medication use (where significant in univariate analysis) and left ventricular mass *a priori*. Inter-observer reproducibility of BOLD SI Change was assessed by coefficient of variance. Statistical tests were 2-tailed and a p-value  $<0.05$  was considered statistically significant.

## 3.3 Results

### 3.3.1 Subject Characteristics

Fifty-three subjects participated in the study: twenty-three advanced CKD (11 (48%) dialysis and 12 (52%) pre-dialysis), ten RT, ten HT controls and ten normal controls. Clinical characteristics are presented in Table 3.1. Age was similar between the CKD, RT, and HT groups ( $p=0.65$ ). The presence of diabetes mellitus ( $p= 0.47$ ) and hypertension ( $p= 0.57$ ) were similar between the CKD, RT, and HT groups. After adjustment for multiple group comparisons using Bonferroni correction, the eGFR was lower in the CKD group compared to HT control ( $p< 0.0001$ ), lower in the RT group compared to HT control ( $p= 0.001$ ), lower in the CKD group compared to RT group ( $p< 0.0001$ ), and similar between the HT and the normal controls ( $p= 1.00$ ). The level of haemoglobin was lower in the CKD group compared to the HT control ( $p< 0.0001$ ) and lower in the CKD group compared to the RT group ( $p< 0.0001$ ), but similar between the RT and HT control ( $p= 1.00$ ). The HT control had higher level of low-density lipoprotein compared to the CKD group ( $p= 0.004$ ) and compared to the RT group ( $p= 0.007$ ). The use of aspirin, angiotensin-converting enzyme inhibitor, beta-blocker, and statin between the four groups were not statistically different. The use of angiotensin receptor blocker was lower in the CKD group compared to HT group ( $p= 0.017$ ) but similar between the RT and HT group ( $p= 0.36$ ).

The aetiology of renal diseases in the CKD and RT groups were: polycystic kidney disease (seven (30%) CKD, six (60%) RT), glomerulonephritis (three (13%) CKD, three (30%) RT), diabetic nephropathy (four (17%) CKD), medication related (two (9%) CKD, one (10%) RT), Alport's syndrome (one (5%) CKD), previous nephrectomy (two (9%) CKD), and unknown (four (17%) CKD).

### 3.3.2 Assessment of Left Ventricular Mass, Volumes and Function

The CMR results are summarised in Table 3.2. Left ventricular mass index was higher in the dialysis group, but similar between the pre dialysis, RT, and HT groups ( $p= 0.40$ ). Left ventricular septal ( $p= 0.64$ ) and lateral wall diameter ( $p= 0.64$ ) were similar between the CKD, RT, and HT groups.

### 3.3.3 Assessment of Myocardial Oxygenation

A total of 2898 myocardial segments [1200 segments of CKD (648 segments of dialysis and 552 segments of pre-dialysis), 552 segments of RT, 480 segments of HT, and 666 segments of normal controls] were compared using linear mixed modeling.

Global BOLD signal intensity (BOLD SI) change of the CKD (dialysis and pre-dialysis), RT, HT, and normal controls is outlined in Figure 3.1. The mean global BOLD SI change was significantly lower in the CKD and RT groups compared to HT and normal controls [ $-0.89 \pm 10.63\%$  in CKD ( $-3.46 \pm 12.83\%$  in dialysis versus  $1.44 \pm 7.62\%$  in pre-dialysis) versus  $5.66 \pm 7.87\%$  in RT versus  $15.54 \pm 9.58\%$  in HT controls, versus  $16.19 \pm 11.11\%$  in normal controls,  $p < 0.0001$ ). Mean BOLD SI change was significantly lower in CKD compared to HT controls ( $p < 0.0001$ ). Mean BOLD SI change was significantly lower in RT compared to HT controls ( $p = 0.013$ ). There was a trend of mean BOLD SI change to be lower in CKD compared to RT ( $p = 0.068$ ). The mean BOLD SI change was similar between HT and normal controls ( $p = 0.89$ ).

Regional BOLD SI change in the Left Anterior Descending (LAD), Left Circumflex (LCx), and Right Coronary Artery (RCA) territories were significantly lower in CKD and RT compared to HT and normal controls (Figure 3.2) [BOLD SI Change in LAD territory:  $-1.70 \pm 14.00\%$  in CKD ( $-3.95 \pm 14.48\%$  in dialysis versus  $0.34 \pm 13.85\%$  in pre-dialysis) versus  $6.40 \pm 7.90\%$  in RT versus  $16.67 \pm 7.60\%$  in HT

controls, versus  $17.40 \pm 11.54\%$  in normal controls,  $p < 0.001$ ; BOLD SI Change in LCx territory:  $2.19 \pm 14.41\%$  in CKD ( $-3.60 \pm 14.69\%$  in dialysis versus  $7.45 \pm 12.54\%$  in pre-dialysis) versus  $4.86 \pm 8.59\%$  in RT versus  $13.26 \pm 15.49\%$  in HT controls, versus  $16.52 \pm 14.76\%$  in normal controls,  $p = 0.018$ ; BOLD SI Change in RCA territory:  $-3.17 \pm 10.66\%$  in CKD ( $-2.83 \pm 12.77\%$  in dialysis versus  $-3.48 \pm 8.97\%$  in pre-dialysis) versus  $5.73 \pm 12.95\%$  in RT versus  $16.71 \pm 12.09\%$  in HT controls, versus  $14.64 \pm 12.30\%$  in normal controls,  $p < 0.001$ ).

The reproducibility of BOLD SI measurements was good, with a coefficient of variation of 1.2% for rest, 2.4% for stress images, and 3.0% for BOLD SI Change measurements.

Multivariate analysis revealed that only the patient group remained an independent predictor of BOLD SI Change.

Figure 3.3 shows examples of rest and stress BOLD images of each group representative.

### **3.3.4 Association Between Myocardial Oxygenation and Renal Function**

BOLD SI Change was associated with eGFR ( $\beta = 0.16$ , 95%CI= 0.10 to 0.22,  $p < 0.0001$ ) in all groups combined (Figure 3.4). There was a significant positive correlation between BOLD SI Change and eGFR in the CKD group alone ( $r = 0.27$ ,  $p = 0.03$ ) (Figure 3.5). In the RT group alone, however, there was no significant correlation between BOLD SI Change and eGFR ( $r = -0.09$ ,  $p = 0.65$ ).

In the CKD and RT groups, there was no significant correlation between BOLD SI Change and the level of haemoglobin ( $r = 0.19$ ,  $p = 0.13$ ) and ( $r = 0.05$ ,  $p = 0.83$ ), respectively.

### **3.3.5 Assessment of Myocardial Fibrosis**

Global longitudinal strain in the CKD group was  $-18.10 \pm 1.74$  versus in the normal volunteers  $-18.3 \pm 2.16$ ,  $p= 0.82$ , which was within normal limits.

None of the RT subjects had late-gadolinium hyperenhancement. Two HT subjects had mid-wall hyperenhancement typical of hypertensive heart disease.

## **3.4 Discussion**

The principal result from this study is that myocardial oxygenation response to stress is impaired in the CKD patients without known CAD, independent of the presence of diabetes mellitus, LVH, and myocardial scar. Further, the impairment in the stress BOLD signal is associated with the degree of renal dysfunction. To the best of our knowledge, this is the first study to utilise BOLD CMR in CKD and RT patients.

### **3.4.1 BOLD CMR Technique**

A major strength of this study is that we directly quantified and assessed the imbalance between myocardial oxygen demand and supply characteristic of ischaemia non-invasively using non-gadolinium contrast BOLD CMR technique at 3 T. BOLD CMR utilises the fact that deoxygenated haemoglobin in blood can act as an intrinsic contrast agent, changing proton signals in a fashion that can be imaged to reflect the level of blood oxygenation. Increases in  $O_2$  saturation increase the BOLD imaging signal ( $T_2$ ), whereas decreases diminish it. As recently reviewed, the BOLD CMR technique has been extensively validated in pre-clinical and clinical studies at both 1.5T and 3T using a variety of sequences [195]. The SSFP sequence used in this study was initially validated in the canine heart at 1.5T by Fieno et al. [130]. We

used the higher field strength (3 Tesla) given the limited signal to noise ratio between normal and deoxygenated myocardial regions at 1.5 Tesla [131]. The BOLD measurement reproducibility in this study compares favourably with the BOLD SI measurement reproducibility demonstrated by Karamitsos et al. who used the same SSFP sequence at 3T [92].

### **3.4.2 Myocardial Oxygenation, Epicardial and Microvascular Coronary Artery Disease**

BOLD CMR technique can identify not only epicardial coronary artery stenosis, but also potentially coronary microvascular dysfunction. BOLD CMR has moderate accuracy in detecting significant coronary artery disease [93, 132]. Myocardial oxygenation response to stress has been shown to be impaired in patients with significant epicardial coronary artery disease [92, 93]. The normal BOLD Signal Intensity index threshold is defined in recent CAD versus normal control studies (using the same SSFP T2 prep sequence as the current study) as 2.64% (sensitivity 92% and specificity 72% for coronary stenosis >50%) by Arnold et al. [134], 3.74% (sensitivity 67% and specificity 88% for coronary stenosis >50%) by Karamitsos et al. [92], 1.2% (sensitivity 88% and specificity 47% for coronary stenosis >75%) by Friedrich et al. [94]. Walcher et al. using T2-prepared SSFP evaluated the diagnostic accuracy of BOLD CMR compared to invasive fractional flow reserve (FFR), for measuring haemodynamically significant coronary artery lesion [135]. They found that relative BOLD signal intensity increase was significantly lower in myocardial segments supplied by coronary arteries with an FFR  $\leq 0.8$  compared with segments with an FFR  $> 0.8$  ( $1.1 \pm 0.2$  versus  $1.5 \pm 0.2$ ;  $p < 0.0001$ ) [135]. The BOLD CMR sensitivity and specificity compared to FFR  $\leq 0.8$  were 88.2% and 89.5%, respectively [135].

We demonstrated significant blunted myocardial oxygenation response to stress in the CKD patients with negative mean BOLD SI Change values, which could imply significant coronary artery stenosis, either epicardial or microvascular, or both. Luu et al. demonstrated coronary territories with  $FFR < 0.80$  had negative value mean BOLD SI Change, and  $FFR < 0.54$  predicted a complete lack of vasodilator-induced oxygenation increase with sensitivity of 71% and specificity of 75% [196]. Karamitsos et al. also demonstrated negative BOLD SI Change values in patients with significant coronary artery stenoses [92]. Coronary steal phenomenon following vasodilatation has been described in patients with multi-vessel CAD [197]. A possible mechanism is due to vasodilatory depressurisation of the microcirculation reducing the collateral blood supply to the stenosed arteries.

Microvascular CAD can be present in the presence or absence of co-existent epicardial CAD. Karamitsos et al. have previously demonstrated an intermediate BOLD SI Change in the myocardial segments subtended by non-stenosed coronary arteries, compared to segments subtended by stenosed coronary arteries and coronary arteries of normal volunteers [92]. Microvascular disease could also be present in our population in the absence of significant CAD. CKD patients have high prevalence of LVH [21]. Microvascular disease is well known in LVH [198], which explains myocardial ischaemia in the absence of obstructive coronary disease. In addition, Mahmood et al. showed reduced mean BOLD Signal Intensity Change during stress in patients with aortic stenosis without significant epicardial coronary artery stenosis, suggestive of microvascular disease [97]. Blunted myocardial oxygenation response to stress was also demonstrated in patients with hypertrophic cardiomyopathy [96]. Given our CKD cohort were asymptomatic, with no known significant epicardial coronary disease, severe microvascular disease might well explain the impaired myocardial oxygenation response in all coronary artery territories.

### **3.4.3 Myocardial Oxygenation Response to Stress and Myocardial Fibrosis**

Detection of scarred and viable myocardium using BOLD CMR was studied by Egred et al. [199]. They showed reduced BOLD SI Change in scarred myocardial segments [199]. Late gadolinium enhancement to assess myocardial scarring and fibrosis was not performed in the CKD cohort due to the risk of nephrogenic systemic fibrosis. Echocardiographic strain imaging enables a comprehensive assessment of myocardial function with the ability to differentiate between active and passive movement of myocardial segments, longitudinal myocardial shortening and dyssynchrony that are not visually assessable [200]. The accuracy of 2-dimensional speckle tracking echocardiography has been compared with delayed enhancement cardiac MRI where strain value of -15% identified myocardial fibrosis with sensitivity of 83% and specificity of 93% [201]. Our CKD subjects did not exhibit impaired global longitudinal strain assessed by 2-dimensional speckle tracking echocardiography and none of the RT subjects had late gadolinium hyperenhancement, suggesting the impaired BOLD SI Change in our cohort was not related to replacement myocardial fibrosis or scar.

### **3.4.4 Myocardial Oxygenation and Chronic Kidney Disease**

Our study suggests that impaired myocardial oxygenation response to stress may be associated with declining renal function. The severity of renal dysfunction has been shown to have a strong association with the incidence of cardiovascular events [202]. Further analysis of our CKD patients showed that the degree of renal impairment (i.e. lower eGFR) was correlated with more impaired myocardial oxygenation response to stress. The impaired myocardial oxygenation in renal transplant recipients, however, was not associated with the residual renal function, perhaps suggesting that there may be other mechanism(s), such as immunosuppression induced microvascular dysfunction or a legacy effect of previous CKD (prior

transplantation), that may cause the impaired BOLD signal. The impaired oxygen supply and demand in our CKD and renal transplant cohort was not significantly associated with the degree of anaemia.

### **3.4.5 Clinical Implications**

CAD in the CKD patients is often multi-vessel and causes silent or asymptomatic myocardial ischaemia [14, 15]. Asymptomatic epicardial CAD has been detected even in people with early stage CKD [16]. Myocardial ischaemia can be caused by both epicardial and microvascular CAD. Our CKD and RT cohorts demonstrate impaired myocardial oxygenation in all coronary artery territories, suggesting multi-vessel microvascular CAD, which has been shown to be present in the CKD population [18]. It may explain the reduced accuracy of stress echocardiography in detecting ischaemia in CKD patients [60]. Stress echocardiography technique detects inducible myocardial ischaemia based on detection of wall motion abnormalities, thus, would detect significant epicardial CAD, not microvascular disease [192]. Microvascular CAD has been shown to be associated with reduced survival [20]. Thus, our study may lead to better management of multi-vessel/microvascular CAD and cardiac risk factors in the CKD population.

### **3.4.6 Study Limitations**

Our study has some limitations. The sample size was small, therefore, the findings need to be confirmed in a larger patient population. However, we applied strict inclusion and exclusion criteria and made every possible effort to include CKD patients who were reasonably well clinically and without previous coronary artery disease, systolic heart failure, significant valvular stenosis, or significant conduction disorder. The dialysis group was older. It is very difficult to find young patients who are dialysis dependent since the median age of dialysis patients at our institution is

75. However, the pre-dialysis CKD group with impaired myocardial oxygenation had a similar mean age to the controls. Secondly, the CKD patients are unable to have gadolinium contrast due to the risk of nephrogenic systemic fibrosis, therefore absolute quantification of stress perfusion CMR and late gadolinium enhancement cannot be performed. Non-contrast T1 mapping would have been useful for assessing diffuse fibrosis, unfortunately, was not available in our centre at time of the study. Co-registration of images was not performed, but there was careful alignment between the rest and stress images using well recognised landmarks in the heart (e.g. anterior and posterior insertion point of the right ventricle into the intra-ventricular septum). Whilst elastic changes related to stress may not be completely accounted for by this method, we feel that this is unlikely to have resulted in major errors. Recently, myocardial oxygenation response to breathing manoeuvres [203] and controlled vasodilatory carbon dioxide delivery through hypercapnia [204] have been described, and may be able to offer more comfortable option of BOLD CMR in CKD patients, however, further research is indicated. BOLD techniques are constantly evolving. The new approach of cardiac phase-resolved BOLD (CP-BOLD) potentially may enable assessment of myocardial ischaemia completely at rest [205].

### **3.5 Conclusion**

Our study suggests that the myocardial oxygenation response to stress is impaired in chronic kidney disease patients and renal transplant recipients, and is unlikely to be accounted for by the presence of diabetes mellitus, left ventricular hypertrophy or myocardial scarring. These patients did not have known epicardial coronary artery disease, and therefore it is likely microvascular disease. The impaired myocardial oxygenation response to stress may be associated with the degree of renal function. There was no significant correlation between BOLD SI Change and the level of haemoglobin. This study demonstrates a new technique for examining myocardial oxygenation response to stress in patients with chronic kidney disease or who have

received a renal transplant. Furthermore, it suggests that multi-vessel microvascular coronary disease may be highly prevalent in this population which has a high prevalence of cardiac mortality and morbidity.

Table 3.1 Clinical characteristics

	CKD <sup>4</sup> Subjects (n= 23)		Renal Transplant Subjects (n= 10)	Hypertensive Controls (n= 10)	Normal Controls (n= 10)	p value <sup>5</sup>
	Dialysis (n= 11)	Pre- dialysis (n= 12)				
Age, years (mean ± SD)	65 ± 12	54 ± 14	59 ± 7	55 ± 11	45 ± 10	0.02
Male sex, n (%)	6 (55)	5 (42)	6 (60)	5 (50)	4 (40)	0.91
BMI <sup>1</sup> , kg/m <sup>2</sup> (mean ± SD)	27 ± 4	26 ± 6	27 ± 3	33 ± 3	22 ± 2	<0.001
eGFR <sup>2</sup> , mL/min/1.73 m <sup>2</sup> (median) (range)		14 (8-18)	72 (57-114)	108 (57-144)	110 (79-146)	<0.0001
<b>Cardiovascular Risk Factors, n (%)</b>						
Hypertension	8 (73)	8 (67)	9 (90)	10 (100)	0 (0)	<0.001
Diabetes Mellitus	5 (45)	4 (33)	1 (10)	2 (20)	0 (0)	0.20
Total cholesterol (mmol/L)	3.9 ± 1.1	5.4 ± 1.5	4.8 ± 1.3	5.7 ± 1.0	-	0.20
Low-density lipoprotein (mmol/L)	2.0 ± 0.7	2.7 ± 0.6	2.1 ± 1.2	3.6 ± 0.9	-	0.002
Triglyceride (mmol/L)	1.3 ± 0.3	2.6 ± 2.6	2.6 ± 1.7	1.5 ± 0.7	-	0.33
Smoking History	4 (36)	4 (33)	3 (30)	3 (30)	0 (0)	0.20
<b>Cardiac Medications, n (%)</b>						
Aspirin	1 (9)	0 (0)	0 (0)	2 (20)	0 (0)	0.21
Beta blocker	5 (45)	2 (17)	5 (50)	2 (20)	0 (0)	0.05
ACE <sup>3</sup> inhibitor	1 (9)	2 (17)	3 (30)	2 (20)	0 (0)	0.45
Angiotensin Receptor Blocker	0 (0)	2 (17)	2 (10)	5 (50)	0 (0)	0.01
Calcium channel blocker	3 (27)	2 (17)	3 (30)	5 (50)	0 (0)	0.11

	<b>CKD<sup>4</sup> Subjects (n= 23)</b>		<b>Renal Transplant Subjects (n= 10)</b>	<b>Hypertensive Controls (n= 10)</b>	<b>Normal Controls (n= 10)</b>	<b>p value<sup>5</sup></b>
	<b>Dialysis (n= 11)</b>	<b>Pre- dialysis (n= 12)</b>				
Statin	5 (45)	2 (17)	2 (20)	2 (20)	0 (0)	0.16

Data are presented as n (%) or mean  $\pm$  SD. <sup>1</sup>BMI indicates body mass index; <sup>2</sup>eGFR, estimated Glomerular Filtration Rate; <sup>3</sup>ACE, angiotensin-converting enzyme; <sup>4</sup>CKD, Chronic Kidney Disease. <sup>5</sup>Assessed using ANOVA or Fisher's exact as appropriate.

Table 3.2 Left ventricular mass, septal and lateral wall thickness, ventricular volumes and ejection fractions

	CKD <sup>3</sup> Subjects (n= 23)		Renal Transplant Subjects (n= 10)	Hypertensive Controls (n= 10)	Normal Controls (n= 10)	p value <sup>4</sup>
	Dialysis (n= 11)	Pre- dialysis (n= 12)				
LV <sup>1</sup> Mass index, g/m <sup>2</sup>	87 ± 20	69 ± 21	65 ± 10	60 ± 10	67 ± 13	0.053
LV Septal Wall diameter, cm	1.2 ± 0.3	1.1 ± 0.3	1.2 ± 0.2	1.1 ± 0.3	1.1 ± 0.3	<0.001
LV Lateral Wall diameter, cm	1.0 ± 0.2	0.9 ± 0.3	0.9 ± 0.2	0.9 ± 0.2	0.9 ± 0.2	0.30
LV End Diastolic Volume index, ml/m <sup>2</sup>	74 ± 17	71 ± 26	71 ± 19	70 ± 13	67 ± 13	0.91
LV End Systolic Volume index, ml/m <sup>2</sup>	27 ± 10	23 ± 16	19 ± 10	22 ± 9	22 ± 5	0.58
LV Stroke Volume index, ml/m <sup>2</sup>	47 ± 12	48 ± 17	51 ± 13	46 ± 10	46 ± 10	0.79
LV Ejection Fraction, %	64 ± 9	68 ± 13	73 ± 9	69 ± 8	68 ± 6	0.29
RV <sup>2</sup> End Diastolic Volume index, ml/m <sup>2</sup>	69 ± 13	73 ± 31	71 ± 8	71 ± 18	70 ± 14	0.99
RV End Systolic Volume index, ml/m <sup>2</sup>	26 ± 6	27 ± 16	29 ± 8	26 ± 9	26 ± 8	0.91
RV Stroke Volume index, ml/m <sup>2</sup>	43 ± 12	46 ± 20	43 ± 9	46 ± 12	44 ± 9	0.96
RV Ejection Fraction, %	61 ± 11	63 ± 11	61 ± 13	63 ± 6	64 ± 7	0.94

All data are presented as mean ± SD.

<sup>1</sup> LV indicates Left Ventricle, <sup>2</sup> RV, Right Ventricle; <sup>3</sup> CKD, Chronic Kidney Disease.

<sup>4</sup> Assessed using ANOVA.

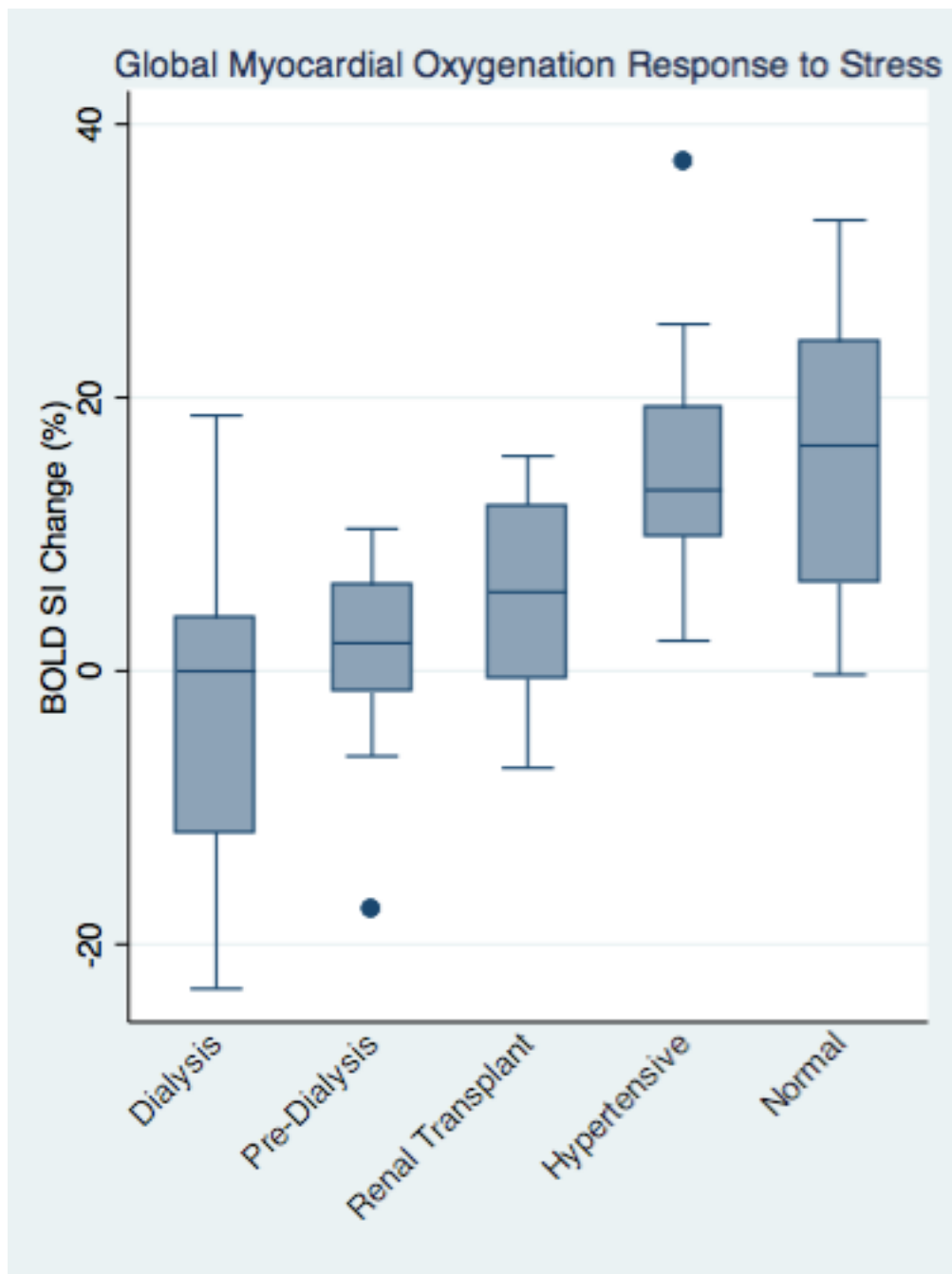


Figure 3.1 Distribution of Myocardial Oxygenation BOLD Signal Intensity (SI) Change of the Chronic Kidney Disease (Dialysis, Pre-Dialysis), Renal Transplant (RT), Hypertensive (HT), and Normal controls groups ( $-3.46 \pm 12.83\%$  in Dialysis versus  $1.44 \pm 7.62\%$  in Pre-Dialysis versus  $5.66 \pm 7.87\%$  in RT versus  $15.54 \pm 9.58\%$  in HT versus  $16.19 \pm 11.11\%$  in Normal controls,  $p < 0.0001$ ).

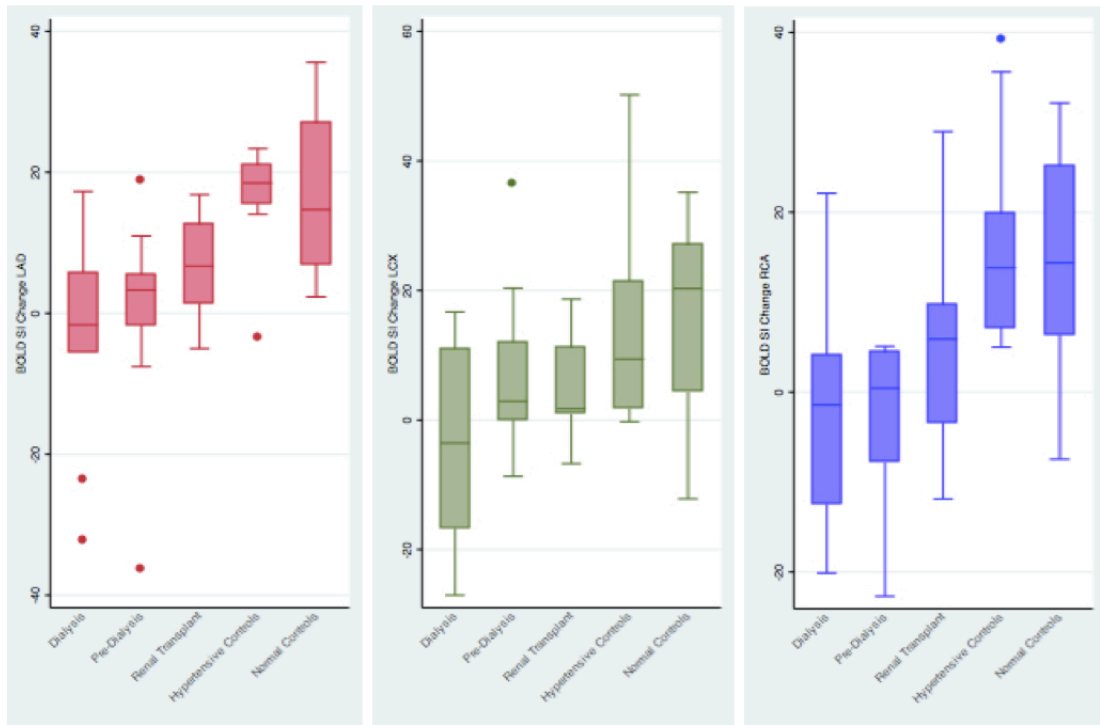


Figure 3.2 Myocardial Oxygenation BOLD Signal Intensity (SI) Change of the Chronic Kidney Disease (CKD) (Dialysis, Pre-Dialysis), Renal Transplant (RT), Hypertensive (HT), and Normal controls groups within each of the three coronary artery territories.

LAD indicates Left Anterior Descending; LCx, Left Circumflex; RCA, Right Coronary Artery.

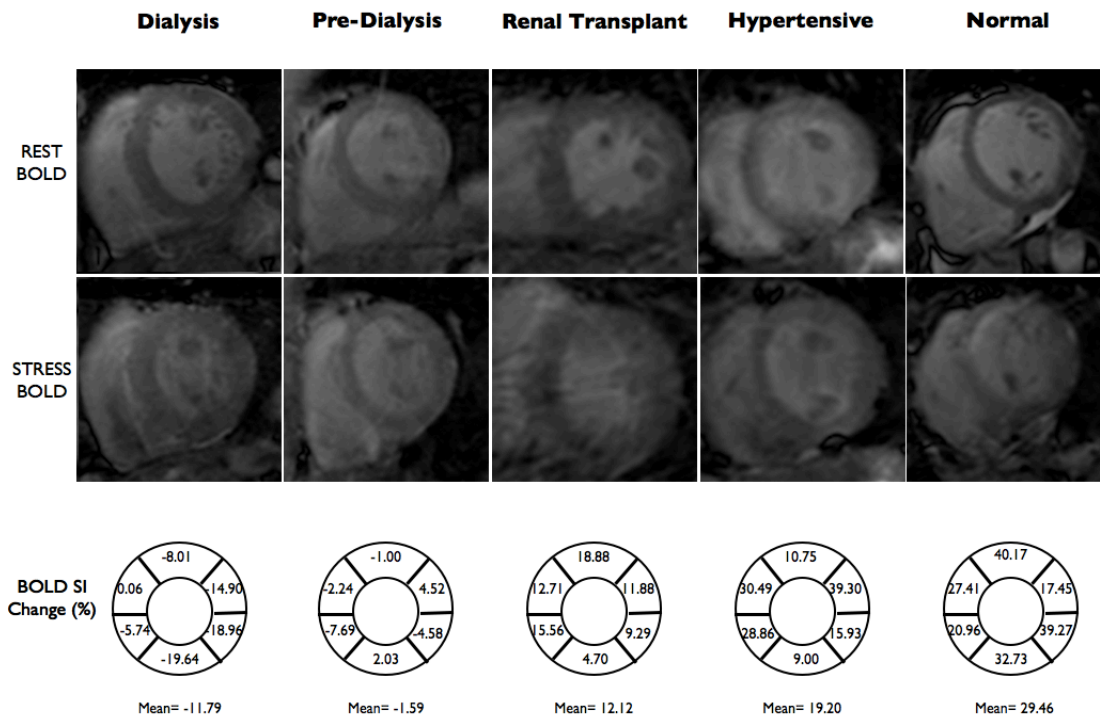


Figure 3.3 Examples of myocardial oxygenation (BOLD) images at rest and during stress of the Chronic Kidney Disease (CKD) (Dialysis, Pre-Dialysis), Renal Transplant (RT), Hypertensive (HT), and Normal controls groups. BOLD Signal Intensity (SI) Change (%) =  $(SI_{\text{stress}} - SI_{\text{rest}}) / SI_{\text{rest}} \times 100\%$ . SI rest and SI stress were automatically calculated by CMR software, and corrected to RR interval.

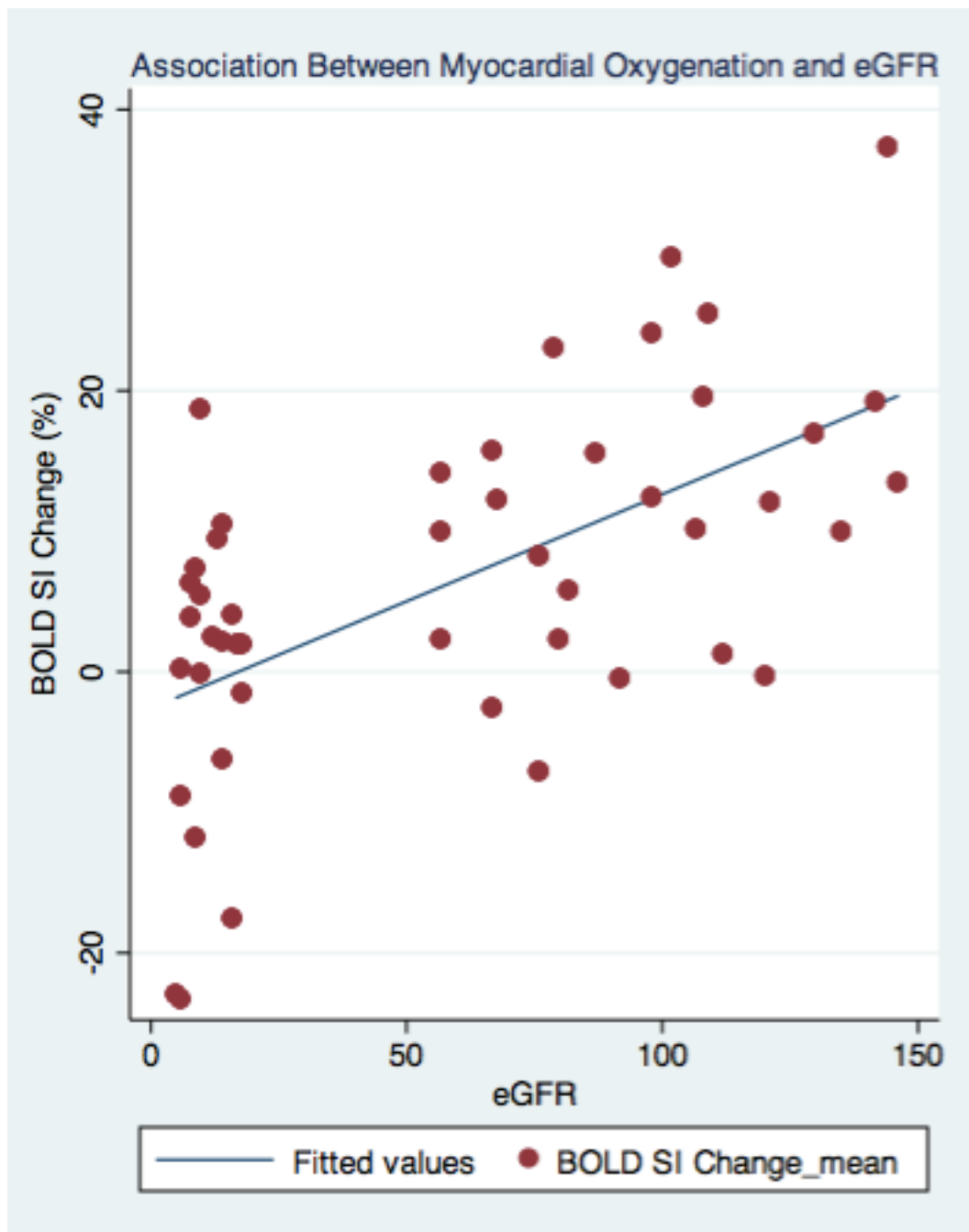


Figure 3.4 Association of Myocardial Oxygenation BOLD Signal Intensity (SI) Change and Renal Function of the Chronic Kidney Disease, Renal Transplant, Hypertensive, and Normal controls groups ( $\beta = 0.16$ , 95%CI= 0.10 to 0.22,  $p < 0.0001$ ).

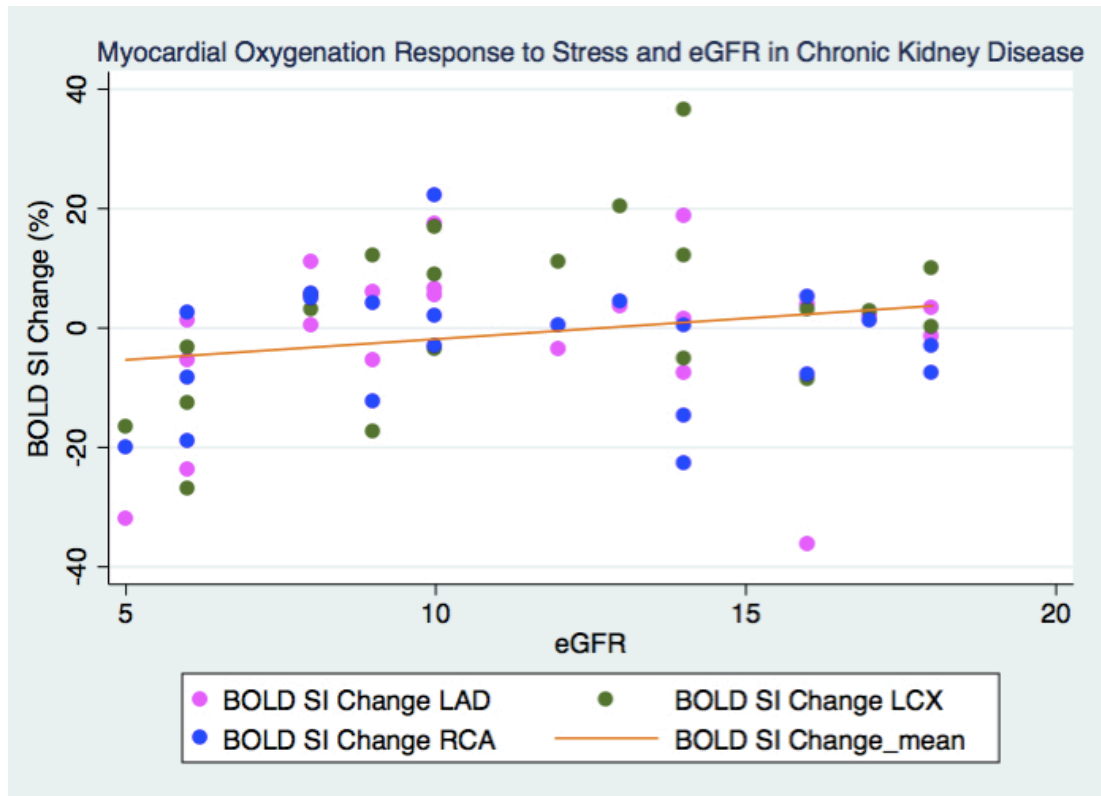


Figure 3.5 Correlation of Myocardial Oxygenation BOLD Signal Intensity (SI) Change and Renal Function of the Chronic Kidney Disease ( $r= 0.27$ ,  $p= 0.03$ ).

# **CHAPTER 4 - Dissociation Between Myocardial Oxygenation Response to Stress and Epicardial Coronary Artery Disease in Chronic Kidney Disease Patients**

## **4.1 Introduction**

Chronic kidney disease (CKD) patients often have multi-vessel coronary artery disease (CAD) and silent or asymptomatic myocardial ischaemia [14, 15], which has been shown to be associated with mortality [206]. Chapter 3 demonstrated impaired myocardial oxygenation response to stress in CKD and renal transplant population in all coronary artery territories [207], and posed a question whether impaired myocardial oxygenation in the CKD and renal transplant patients is due to multi-vessel epicardial CAD, microvascular disease or both.

Oxygenation-sensitive cardiovascular magnetic resonance (CMR) by Blood Oxygen Level Dependent (BOLD) technique detects inducible myocardial ischaemia from both epicardial and microvascular CAD, which are both present in CKD patients [16-19]. Magnetic resonance coronary angiography (MRCA) enables non-invasive detection of significant coronary artery stenoses in the ostial, proximal and mid coronary arteries. Although there are current limitations [173], MRCA can be an alternative imaging modality to exclude left main disease, triple vessel disease and any proximal epicardial coronary artery stenosis in the CKD and renal transplant patients, in whom invasive coronary angiography and CT coronary angiography radiation and contrast are hazardous.

We aim to assess the association between myocardial oxygenation response to stress and epicardial proximal to mid coronary anatomy in CKD and renal transplant population.

## **4.2 Methods**

### **4.2.1 Study Population**

Twenty-five CKD patients, ten renal transplant (RT) recipients and ten controls with normal renal function were recruited into the study. The CKD and RT patients had the following inclusion criteria: no symptoms of cardiac disease, no established CAD (no history of myocardial infarction, angina, coronary artery stent or bypass surgery or angiographically documented significant CAD>70%, and no significant inducible myocardial ischaemia on functional testing pre-transplant), and no previous systolic heart failure. Ten people with clinical diagnosis of hypertension with normal renal function and no previous history of CKD served as controls.

The exclusion criteria for each group were severe standard contraindications to CMR (e.g. claustrophobia, metallic implants), and contraindications to adenosine (second or third degree atrioventricular block, obstructive pulmonary disease and dipyridamole use).

All participants gave written informed consent, and the study was approved by Southern Adelaide Clinical Human Research Ethics Committee (SAC HREC).

### **4.2.2 CMR Protocol**

Cine images were acquired in vertical and horizontal long-axis, and ten short-axis images covering the entire left ventricle, using a retrospective ECG gating steady-state free precession (SSFP) sequence (repetition time (TR) 3 ms, echo time (TE) 1.5 ms, flip angle 55°, 18 phases) [179].

BOLD imaging was acquired in a 3 Tesla MRI scanner (Siemens, 3T Trio, 4 channel Body Flex coil), as described in Chapter 2. In brief, a set of six rest and six stress

BOLD images with adenosine 140 µg/kg per minute were acquired at mid-diastole using a T2-prepared ECG-gated steady-state free precession sequence (TR 2.86 ms, TE 1.43 ms, T2 preparation time 40 ms, matrix 168 x 192, field of view 340 x 340 mm, slice thickness 8 mm, flip angle 44°), as previously described [92].

MRCA images were obtained using an 18-channel flex coil 1.5T clinical MR scanner (Siemens Sonata, Erlangen, Germany). A four-lead ECG was obtained for cardiac gating. Glyceryl trinitrate 400 micrograms/metered dose was administered prior to MRCA. The navigator-gated, free-breathing, non-contrast whole-heart MRCA was acquired using a 3D segmented SSFP sequence [151, 177]. A transaxial cine was used to monitor the minimum motion of right coronary artery with free breathing. Epicardial fat and venous blood signal were suppressed.

### **4.2.3 CMR Image Analysis**

Ventricular volumes and function were analysed using CMR<sup>42</sup> software on a cine SA stack, as described in Chapter 2. The ventricular volumes were indexed to body surface area (BSA).

BOLD images were analysed after manually tracing the endocardial and epicardial contours using CMR<sup>42</sup> software, Version 4.0, Circle Cardiovascular Imaging Inc. (Calgary, Canada), as previously described in Chapter 2. The mean myocardial BOLD Signal Intensity (SI) within each segment was obtained, both at rest and stress, and corrected to heart rate variations, as previously described [92, 207].

MRCA images were analysed using a 4D image reconstruction of CMR<sup>42</sup> software. Three-dimensional volume-rendered images were generated by the software. The left main, left anterior descending artery (LAD), left circumflex (LCx) and right coronary artery (RCA) were manually traced and followed for their course in axial, coronal, sagittal, cranial left anterior oblique, lateral, caudal right anterior oblique

and caudal left anterior oblique views, using sliding thin-slab maximum intensity projection. The coronary arteries were analysed and segmented according to the American College of Cardiology/American Heart Association classification [208]. Significant coronary artery stenosis was defined as luminal narrowing greater than 50% [177]. Minor coronary artery disease was defined as luminal narrowing of less than 50%. The coronary artery was classified normal if it was smooth without any plaque occupying lumen.

#### **4.2.4 Statistical Analysis**

Statistical analysis was performed with STATA version 13.0. Parametric data is expressed as mean  $\pm$  SD and non-parametric data as median (inter-quartile range). ANOVA and independent t-test were used to compare parametric data between the study groups as appropriate. Fisher's exact tests were used for comparison of categorical variables. BOLD SI evaluation of coronary artery level data and association with epicardial CAD of MRCA was analysed using linear mixed modeling (LMM) with a random intercept used for each subject to account for the within-subject correlation present from measuring at three different artery sites [180]. Statistical tests were 2-tailed and a p-value  $<0.05$  was considered statistically significant.

### **4.3 Results**

#### **4.3.1 Subject Characteristics**

Forty-five subjects participated in the study: twenty-five CKD, ten RT, and ten controls. Clinical characteristics are presented in Table 4.1. Age was similar between the groups. The control group had higher body mass index and higher low-density lipoprotein levels. Blood pressure and heart rate were similar between the groups.

The presence of hypertension and diabetes mellitus was similar between the groups. Cardiac medication use was similar between the groups. Left ventricular volumes and function were similar between the groups (Table 4.2).

The aetiology of renal diseases in the CKD and RT groups were: polycystic kidney disease (six (24%) CKD, six (60%) RT), glomerulonephritis (three (12%) CKD, three (30%) RT), diabetic nephropathy (six (24%) CKD), medication related (three (12%) CKD, one (10%) RT), renovascular (one (4%) CKD), previous nephrectomy (two (8%) CKD), and unknown (four (16%) CKD).

### **4.3.2 Assessment of Myocardial Oxygenation Response to Stress**

A total of 2424 analysable myocardial segments [1392 segments of CKD, 552 segments of RT, and 480 segments of controls] were compared using linear mixed modeling. The mean BOLD SI Change was significantly lower in the CKD and RT groups compared to controls ( $-1.54 \pm 9.79\%$  in CKD versus  $5.66 \pm 7.87\%$  in RT versus  $15.54 \pm 9.58\%$  in Controls,  $p < 0.0001$ ). Mean BOLD SI Change was lower in the CKD compared to RT,  $p = 0.045$ . Twelve out of 25 (48%) CKD, three out of 10 (30%) RT, and 0 out of 10 (0%) controls had negative BOLD SI Change value,  $p = 0.015$ .

### **4.3.3 Assessment of Epicardial Coronary Artery Disease**

Ten out of 25 (40%) CKD, four out of 10 (40%) RT, and 0 out of 10 (0%) controls had coronary artery stenosis  $>50\%$  in at least one coronary artery territory,  $p = 0.037$ . Figure 4.1 shows examples of MRCA images and stress BOLD images in CKD subjects. In the CKD and RT subgroups, the mean BOLD SI Change was  $-3.11 \pm 11\%$  in those with significant CAD  $>50\%$  versus  $7.76 \pm 11\%$  in those without,  $p < 0.0001$ .

#### **4.3.4 Association Between Myocardial Oxygenation and Epicardial CAD in Chronic Kidney Disease and Renal Transplant Groups**

There was no significant relationship between epicardial CAD and BOLD Signal Intensity Change as per coronary artery territories in the CKD and RT subgroups ( $\beta = -0.04$ , 95% CI -0.12 to 0.36,  $p=0.30$ ).

#### **4.4 Discussion**

The main finding of this study is that there is a mismatch between myocardial oxygenation response to stress and epicardial CAD in the CKD and renal transplant recipients, suggestive of coronary microvascular disease involvement. To our knowledge, this is the first study to investigate the association between myocardial oxygenation and epicardial CAD in asymptomatic CKD and renal transplant patients using non-contrast BOLD CMR and MRCA.

BOLD CMR technique can identify not only epicardial coronary artery stenosis, but also potentially coronary microvascular dysfunction. BOLD CMR has moderate accuracy in detecting significant epicardial CAD [93, 132]. A dissociation between myocardial perfusion and oxygenation has been demonstrated by Karamitsos et al. [92], possibly reflecting a complex interplay between perfusion, oxygenation and the degree of CAD, either epicardial or microvascular, or both. Previous studies have indicated that myocardial signal intensity changes reflect changes of myocardial oxygenation rather than blood flow [124, 209].

CKD patients can have both epicardial and microvascular CAD. Occult epicardial CAD has been shown among asymptomatic CKD patients at the start of renal replacement therapy [14]. Microvascular disease is well known in the presence of left ventricular hypertrophy [198]. Bozbas et al. showed that CKD patients without epicardial CAD had significantly lower coronary flow reserve suggestive of

microvascular dysfunction [210]. This is consistent with our finding that myocardial oxygenation response to stress is significantly lower in the CKD group compared to the renal transplant group, suggesting more a severe microvascular dysfunction pre-transplantation. The CKD and renal transplant groups in our cohort population had similar degree of epicardial CAD, which was 40% in each group.

Our study interestingly demonstrated negative BOLD SI Change values in the CKD patients. Blunted myocardial oxygenation response to stress with negative BOLD SI Change values has been shown to be associated with significant CAD [92, 196]. Luu et al. demonstrated that a complete lack of increase in oxygenation was associated with a fractional flow reserve of  $<0.54$  [196]. In our cohort study, a negative mean BOLD Signal Intensity Change was found in 40% of the CKD group, 30% renal transplant group and none of controls. It will be interesting to see whether blunted myocardial oxygenation response to stress in asymptomatic patients with CKD correlates with cardiac prognosis. Although there was no significant association between BOLD Signal Intensity Change and CAD as per coronary artery territories, the BOLD Signal Intensity Change was significantly lower in the CKD and renal transplant groups with significant epicardial CAD.

Our study has some limitations. The sample size was small, therefore, the findings need to be confirmed in a larger patient population. Secondly, coronary calcifications are common in the CKD population, which may create artifacts with MRCA. MRCA has lower diagnostic accuracy in the distal vessels compared with CT coronary angiography, thus the possibility of distal epicardial CAD is not excluded. Nevertheless, non-contrast MRCA is safe and non-invasive in advanced CKD patients, and BOLD CMR and MRCA research techniques keep evolving for the needs of better signal to noise ratio and less artifacts.

## **4.5 Conclusion**

Our study suggests dissociation between myocardial oxygenation response to stress and epicardial coronary disease in the CKD patients and renal transplant recipients, suggesting microvascular dysfunction involvement.

Table 4.1 Clinical characteristics

	<b>CKD<sup>4</sup> Subjects (n= 25)</b>	<b>Renal Transplant Subjects (n= 10)</b>	<b>Controls (n= 10)</b>	<b>p value<sup>5</sup></b>
Age, years (mean ± SD)	59 ± 14	59 ± 7	55 ± 11	0.69
Male sex, n (%)	15 (60)	6 (60)	5 (50)	0.92
BMI <sup>1</sup> , kg/m <sup>2</sup> (mean ± SD)	26 ± 5	27 ± 3	33 ± 3	0.001
eGFR <sup>2</sup> , mL/min/1.73 m <sup>2</sup> (median) (range)	13 ± 7	77 ± 18	108 ± 30	<0.0001
Systolic Blood Pressure (mmHg)	137 ± 19	133 ± 19	140 ± 11	0.66
Diastolic Blood Pressure (mmHg)	78 ± 18	80 ± 16	80 ± 11	0.94
Heart Rate (beats per minute)	72 ± 10	71 ± 7	77 ± 15	0.37
<b>Cardiovascular Risk Factors, n (%)</b>				
Hypertension	19 (76)	9 (90)	10 (100)	0.38
Diabetes Mellitus	12 (48)	1 (10)	2 (20)	0.26
Total cholesterol (mmol/L)	4.6 ± 1.4	4.8 ± 1.3	5.7 ± 1.0	0.15
Low-density lipoprotein (mmol/L)	2.2 ± 0.7	2.1 ± 1.2	3.6 ± 0.9	0.001
Triglyceride (mmol/L)	2.1 ± 1.7	2.6 ± 1.7	1.5 ± 0.7	0.32
Smoking History	12 (48)	3 (30)	3 (30)	0.65
<b>Cardiac Medications, n (%)</b>				
Aspirin	2 (8)	0 (0)	2 (20)	0.49
Beta blocker	7 (28)	5 (50)	2 (20)	0.42
ACE <sup>3</sup> inhibitor	5 (20)	3 (30)	2 (20)	0.89
Angiotensin Receptor Blocker	3 (12)	2 (10)	5 (50)	0.06
Calcium channel blocker	7 (28)	3 (30)	5 (50)	0.48
Statin	8 (32)	2 (20)	2 (20)	0.73

Data are presented as n (%) or mean ± SD.

<sup>1</sup>BMI indicates body mass index; <sup>2</sup>eGFR, estimated Glomerular Filtration Rate;

<sup>3</sup>ACE, angiotensin-converting enzyme; <sup>4</sup>CKD, Chronic Kidney Disease. <sup>5</sup> Assessed using ANOVA or Fisher's exact as appropriate.

Table 4.2 Ventricular volumes and ejection fractions

	<b>CKD<sup>3</sup> Subjects (n= 25)</b>	<b>Renal Transplant Subjects (n= 10)</b>	<b>Controls (n= 10)</b>	<b>p value<sup>4</sup></b>
LV End Diastolic Volume index, ml/m <sup>2</sup>	71 ± 23	71 ± 19	70 ± 13	1.00
LV End Systolic Volume index, ml/m <sup>2</sup>	24 ± 14	19 ± 10	22 ± 9	0.66
LV Stroke Volume index, ml/m <sup>2</sup>	47 ± 15	51 ± 13	46 ± 10	0.68
LV Ejection Fraction, %	68 ± 11	73 ± 9	69 ± 8	0.39
BOLD Signal Intensity Change (%)	-1.54 ± 9.79	5.66 ± 7.87	15.54 ± 9.58	< 0.0001
Significant CAD>50% by MRCA, n (%)	10 (40)	4 (40)	0 (0)	0.037
Negative BOLD Signal Intensity Change value (%)	12 (48)	10 (30)	0 (0)	0.015

All data are presented as mean ± SD.

<sup>1</sup> LV indicates Left Ventricle, <sup>2</sup> RV, Right Ventricle; <sup>3</sup> CKD, Chronic Kidney Disease.

<sup>4</sup> Assessed using ANOVA.

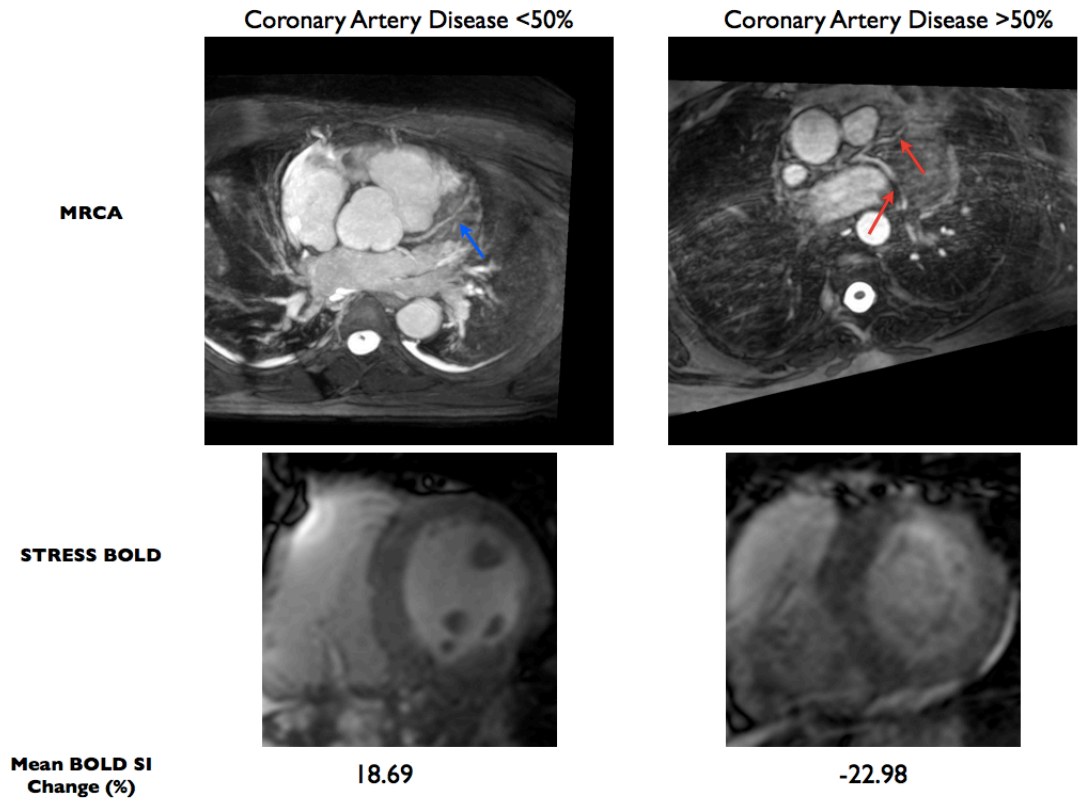


Figure 4.1 Examples of whole-heart magnetic resonance angiography (MRCA) and Stress BOLD Imaging in (left) CKD patient with coronary artery disease <50% (blue arrow) and positive value of mean BOLD Signal Intensity Change, and (right) CKD patient with coronary artery disease >50% stenosis in RCA (red arrows) and negative value of mean BOLD Signal Intensity Change. There was no significant relationship between epicardial CAD and BOLD Signal Intensity Change as per coronary artery territories in the CKD and RT groups ( $\beta = -0.04$ , 95% CI -0.12 to 0.36,  $p=0.30$ ).

# **CHAPTER 5 - Myocardial Perfusion is Impaired in Renal Transplant Recipients**

## **5.1 Introduction**

Cardiovascular disease is the leading cause of mortality and morbidity in the chronic kidney disease (CKD) population, accounting for 50% of all deaths [189]. CKD patients have a 10 to 20 fold risk of cardiac death than normal population, although the mechanism is uncertain [189]. Furthermore, despite the risk of cardiovascular mortality is significantly reduced by renal transplantation [190], cardiovascular disease remains a major cause of mortality in post-renal transplant recipients with an annual event risk of 3.5 to 5% [25]. Renal transplant recipients carry a multitude of threatening risk factors ranging from traditional atherosclerotic (dyslipidaemia, hypertension, diabetes), myocardial (hypertension and fluid overload pre transplant), microvascular (diabetes, renal failure), and immunosuppression.

Current diagnostic investigations of myocardial ischaemia in renal population lack sensitivity and specificity or may have adverse effects [192]. Multi-parametric Cardiac Magnetic Resonance (CMR) imaging enables concurrent assessment of myocardial function, perfusion and irreversible injury with high spatial resolution [99]. In particular, stress perfusion CMR has high sensitivity and negative predictive value for detecting myocardial ischaemia with a sensitivity of 89% and a specificity of 80% [101]. In addition, two large prospective controlled trials,-CE-MARC and MR-IMPACT II- demonstrated higher diagnostic accuracy of stress perfusion CMR compared to SPECT [103, 104]. Huber et al. found that semi-quantitative evaluation provides identical diagnostic performance for CAD similar to quantitative evaluation if both stress and rest examinations were used [119]. Recently, non-contrast magnetic resonance coronary angiography (MRCA) has emerged as an imaging alternative for coronary artery anatomy, especially for the proximal and mid coronary segments [174]. Finally, CMR allows accurate quantification of ventricular function and mass

as well as tissue characterisation, thereby uniquely positioning it as a powerful modality to explore the high cardiovascular event rate in renal transplant patients.

We sought to investigate the mechanism of cardiovascular morbidity and mortality in otherwise well post renal transplant recipients using multi-parametric CMR. Our primary aim was to assess the presence and degree of myocardial ischaemia utilising stress perfusion CMR and the presence of significant epicardial disease using non-contrast whole-heart MRCA. Majority (50-90%) of renal transplant recipients have hypertension [211] and the high (75%) prevalence of left ventricular hypertrophy (LVH) in CKD population [21] likely persists post transplantation [212]. In contrast to the advanced CKD pre-renal transplant population, the prevalence of CAD in the end-stage liver disease patients is similar or only slightly greater than the normal population, ranging from 2.5% to 27%, however, cardiovascular disease is a major cause of mortality post liver transplantation [213]. We used 2 control groups- an aged matched population of hypertensive controls (to control for LVH commonly seen in the renal transplant recipients) and a post-liver transplant group (to allow differentiation of transplant milieu effects from prior renal failure effects).

## **5.2 Methods**

### **5.2.1 Study Population**

Renal transplant (RT) recipients who were well and with stable renal function between three months and five years post transplantation were invited to participate to have CMR imaging at Flinders Medical Centre, a tertiary teaching hospital in South Australia, in 2012-2014. RT subjects had the following inclusion criteria: no established CAD (no history of myocardial infarction, angina, coronary artery stent or bypass surgery or angiographically documented significant CAD>70%, and no significant inducible myocardial ischaemia pre-transplant), and no previous systolic heart failure. Liver transplant (LT) recipients with the same inclusion criteria were

recruited. Ten people with a clinical diagnosis of hypertension (HT) and who were asymptomatic with no known CAD were prospectively recruited from the hospital's Hypertension Clinic.

Exclusion criteria for each group were severe claustrophobia, metallic implants, contraindications to adenosine (second or third degree atrioventricular block, obstructive pulmonary disease, dipyridamole use), and contraindications to gadolinium chelate (anaphylaxis, estimated glomerular filtration rate < 45 ml/min/1.73m<sup>2</sup>).

We identified a total of 171 RT patients from the hospital's renal database within the calendar year 2012. Exclusions were: >60 months post renal transplantation (102), ischaemic heart disease or known CAD (11), CMR contraindication (20), <3 months post renal transplantation (2), declined participation (13), language barrier (2) and pregnancy (1). Following exclusion, a total of 20 RT patients were enrolled into the study.

All participants gave written informed consent, and the study was approved by Southern Adelaide Clinical Human Research Ethics Committee (SAC HREC).

### **5.2.2 CMR Protocol**

All participants were instructed to refrain from caffeine 24 hours prior to the scan. Subjects on beta blockers continued with their medications.

Cine imaging was acquired using standard method [179]. Stress imaging with adenosine infusion 140 µg/kg/min for 3-4 minutes was performed in the basal, mid, and apical myocardial segments, using an ECG-gated T1-weighted fast gradient echo sequence (echo time, 1.04 ms; repetition time, 2 ms; voxel size, 29x2.3x8 mm, flip angle 17°), and a peripheral bolus injection of a gadolinium-based agent (0.1

mmol/kg; gadolinium-based contrast agent, Gadovist, Bayer, Australia), followed by a 15-ml bolus of normal saline (rate 5ml/s), as previously described [92, 180]. All slices were imaged during each heart beat, for a total of 50 heart beats. Blood pressure and heart rate were recorded by an automated recording machine at baseline and at 1 minute intervals during adenosine infusion. After discontinuing adenosine for 15 minutes, the same sequence was repeated without intravenous adenosine to obtain resting perfusion images. For late enhancement imaging, an additional bolus of Gadovist (0.05 mmol/kg) was injected, and after 6 minutes, images were acquired in the 3 long axes and in the short axis plane to obtain coverage of the entire left ventricle using a gated T1-weighted segmented inversion recovery turbo fast low-angle shot sequence (echo time, 4.8 ms; voxel size, 1.4x2.4x8 mm; flip angle, 20°). The inversion time adjusted to achieve optimal nulling of noninfarcted myocardium, as previously described [181].

MRCA images were obtained as a separate exam by using an 18-channel flex coil 1.5T clinical MR scanner (Siemens Sonata, Erlangen, Germany). A four-lead ECG was obtained for cardiac gating. Glyceryl trinitrate 400 micrograms/metered dose was administered prior to MRCA. The navigator-gated, free-breathing, non-contrast whole-heart MRCA was acquired using a 3D segmented Steady-State Free Precession sequence protocol as previously described [151, 177].

### **5.2.3 CMR Image Analysis**

CMR analysis was performed with CMR<sup>42</sup> Version 4.1, Circle Cardiovascular Imaging Inc, as presented in Chapter 2. Left ventricular mass, left and right ventricular volumes and functions were calculated using 3D short axis stack by tracing of the endocardial and epicardial contours in end-diastole and end-systole, as previously described [179]. Each parameter was indexed to body surface area (BSA). The septal and lateral wall diameters were measured in end-diastole at mid-ventricular level from short-axis view.

For perfusion analysis, semiquantitative analysis using CMR<sup>42</sup> software was used. Transmural, subendocardial and subepicardial contours were traced and manually corrected for breathing displacements (Figure 5.1). Each basal, mid and apical myocardial slice were divided into 6 segments with the right ventricular insertion as the reference point [183]. Since basal myocardial blood flow is closely related to the rate-pressure product (RPP), and index of left ventricular oxygen consumption, values for rest flow in each patient were also corrected for rate-pressure product [184]: Corrected Rest perfusion= (Rest perfusion/RPP) x 10<sup>4</sup>. Myocardial Perfusion Reserve Index (MPRI) was calculated as the ratio of perfusion during adenosine-induced hyperaemia to perfusion at rest corrected for RPP [185].

For late enhancement analysis, areas of subendocardial hyperenhancement were assessed visually as present or absent. The fibrosis was quantified using CMR<sup>42</sup> software as a percentage of myocardial mass [214, 215].

MRCA images were transferred to a 4D viewer image reconstruction CMR<sup>42</sup> software. Three-dimensional volume-rendered images were generated by the software. The left main, left anterior descending artery (LAD), left circumflex (LCx) and right coronary artery (RCA) were manually traced and followed for their course in axial, coronal, sagittal, cranial left anterior oblique, lateral, caudal right anterior oblique and caudal left anterior oblique views. The coronary arteries were analysed and segmented according to the American College of Cardiology/American Heart Association classification [208].

One CMR experienced cardiologist blinded to the clinical information and stress perfusion results, evaluated the left main, LAD, LCx and RCA arteries using sliding thin-slab maximum intensity projection. Significant coronary artery stenoses were defined as luminal narrowing greater than 50% [177]. Minor coronary artery disease was defined as luminal narrowing of less than 50%. The coronary artery was classified normal if it was smooth without any plaque occupying lumen.

## 5.2.4 Statistical Analysis

Statistical analysis was performed with STATA version 13.0. Parametric data is expressed as mean  $\pm$  SD and non-parametric values as median (inter-quartile range). Independent t-tests and ANOVA was used to compare the clinical characteristics of the study groups. Fisher's exact test was used for comparison of categorical variables. MPRI evaluation of coronary artery level data was analysed using linear mixed modeling (LMM) with a random intercept used for each subject to account for the within-subject correlation present from measuring at 3 different artery sites. Both unadjusted and adjusted LMM was performed with adjustment for medication use (where significant in univariate analysis) and left ventricular mass *a priori*. Statistical tests were 2-tailed and a p value  $<0.05$  was considered statistically significant.

## 5.3 Results

### 5.3.1 Subject Characteristics

Forty-five subjects participated in the study: twenty RT, fifteen LT controls, and ten HT controls. Clinical characteristics are presented in Table 5.1. After adjustment for multiple group comparisons using Bonferroni correction, the eGFR was lower in the renal transplant group compared to hypertensive control (p= 0.012), similar between the liver transplant and hypertensive control (p= 0.21), and similar compared to liver transplant group (p= 0.67). The presence of hypertension was similar between the renal transplant and hypertensive groups, similar between renal transplant and liver transplant groups (p= 0.06), and lower in the liver transplant group compared to the hypertensive group (p= 0.027). The use of statin between the renal transplant and hypertensive groups was similar (p= 0.95).

The aetiology of renal diseases in the RT group were: polycystic kidney disease (n= 7), glomerulonephritis (n= 9), diabetic nephropathy (n= 1), medication related (n= 1), Alport's syndrome (n= 1), and unknown (n= 1). The aetiology of liver diseases in the LT group were: alcoholic liver disease (n= 7), hepatitis C (n= 5, 1 of which was combined hepatitis C and B), primary sclerosing cholangitis (n= 1), non-alcoholic steatohepatitis (n=1), and unknown (n=1). The mean post transplant duration between the RT and LT groups were similar ( $33 \pm 17$  versus  $36 \pm 18$  months,  $p= 0.63$ ). The immunosuppressant medications received by the RT and LT groups are outlined in Table 5.2. Their exposures were similar apart from LT patients only receiving prednisolone in the first three months post transplantation and the use of mycophenolate, which was more prevalent in RT patients.

### **5.3.2 Assessment of Left Ventricular Mass, Volumes and Function**

The CMR results are summarised in Table 5.3. Left ventricular mass index, septal and lateral wall diameter were similar between the groups.

### **5.3.3 Assessment of Myocardial Perfusion Reserve Index (MPRI)**

A total of 1308 out of 1452 (90%) myocardial segments were analysable. A total of 576 myocardial segments of RT, 468 myocardial segments of LT, and 264 myocardial segments of HT were analysed and compared using mixed linear modeling. Figure 5.2 - 5.4 shows the distribution of the MPRI across the three groups and within each of the three coronary artery sites. Across all three artery sites combined, the mean transmural MPRI was significantly reduced in RT subjects compared to HT controls, but was similar between RT and LT subjects ( $1.19 \pm 0.50$  in RT versus  $1.23 \pm 0.36$  in LT versus  $2.04 \pm 0.32$  in HT controls,  $p < 0.0001$ ). The subepicardial MPRI was  $1.33 \pm 0.57$  in RT versus  $1.30 \pm 0.33$  in LT versus  $2.01 \pm 0.30$  in HT controls,  $p < 0.001$ . The subendocardial MPRI was  $1.19 \pm 0.54$  in RT

versus  $1.11 \pm 0.31$  in LT versus  $1.85 \pm 0.30$  in HT controls,  $p < 0.0001$ . In the renal transplant and liver transplant subgroups, the transmural MPRI was  $0.97 \pm 0.54$  in those with significant CAD  $>50\%$  versus  $1.05 \pm 0.00$  in those without,  $p = 0.02$ . Fifteen out of 20 (75%) RT versus eleven out of 15 (73%) LT versus one out of 10 (10%) HT had transmural MPRI  $< 1.5$  in at least one coronary artery territory,  $p < 0.0001$ .

Results remained similar in mixed model regression analysis after adjustment for statin use, aspirin use and left ventricular mass index with MPRI lower in RT subjects compared to HT controls ( $\beta = 0.85$ ,  $p < 0.0001$ ) but similar to LT subjects ( $\beta = 0.04$ ,  $p = 0.79$ ).

Significantly, in the RT group, the mean MPRI was associated with eGFR ( $\beta = 0.014$ , 95%CI = 0.0023 to 0.026,  $p = 0.0019$ ).

### **5.3.4 Assessment of Myocardial Fibrosis**

One RT subject had late gadolinium enhancement indicating sub-endocardial infarction in the inferoseptal wall (1.7 g of infarct mass (0.8% of LV mass)), while one LT subject had late gadolinium enhancement indicating sub-endocardial infarction in the lateral wall (2.9 g of infarct mass (2.1% of LV mass)).

### **5.3.5 Assessment of Epicardial Coronary Artery Disease**

Seven out of 20 (35%) RT, five out of 15 (33%) LT, and 0 out of 10 (0%) HT controls had coronary artery stenosis  $>50\%$  in at least one coronary artery territory,  $p = 0.12$ . There was no significant relationship between epicardial CAD and transmural MPRI as per coronary artery territories ( $\beta = -0.14$ , 95% CI -0.30 to 0.23,  $p = 0.09$ ). Figure 5.5 shows representative MRCA images of the transplant recipients.

## 5.4 Discussion

Stress perfusion CMR and MRCA provide valuable insight into the cardiac phenotype. To our knowledge, this is the first study to investigate myocardial perfusion in asymptomatic post renal transplantation patients using stress perfusion CMR and MRCA. We have demonstrated that myocardial perfusion is significantly reduced in asymptomatic post renal transplant recipients independently of the degree of left ventricular hypertrophy and diabetes mellitus. Furthermore, MRCA abnormalities do not seem to explain the perfusion abnormalities. Our findings suggest that myocardial perfusion abnormalities in renal transplant patients are predominantly due to coronary microvascular dysfunction possibly secondary to post-transplant milieu rather than significant epicardial disease. Our study findings may assist in understanding the contributors to cardiac mortality and morbidity in the post-renal transplant population, and lead to better management of coronary microvascular disease in this population.

CMR stress perfusion has been well validated in the assessment of epicardial coronary disease and/or coronary microvascular dysfunction. A recent meta-analysis showed stress perfusion CMR to have a high sensitivity of 89% and a specificity of 80% for diagnosis of significant obstructive coronary artery disease [101]. The sensitivity and specificity of stress CMR performed with a semiquantitative measure of myocardial perfusion reserve index (MPRI) with a cutoff value of 1.5 for the detection of functionally significant (by Fractional Flow Reserve) coronary heart disease were 91% and 94%, respectively, with positive and negative predictive values of 91% and 94% [216]. Impaired coronary flow reserve suggestive of microvascular dysfunction has been reported in pre-transplant end-stage renal disease patients without coronary artery disease [210]. Impaired coronary flow reserve, similarly, has been observed in post renal transplant patients, even at a young age [217-219]. Given the association between LVH and reduced MPRI [220], it was important that we controlled for the degree of LVH when assessing myocardial perfusion in the renal cohort. Our HT, RT and LT groups were well

matched in respect of degree of LVH, LV mass, and diabetes mellitus. Hence, our finding of reduced MPRI in the RT group is unlikely to solely reflect LVH or the degree of diabetes, and likely reflects additional abnormalities in coronary microvascular function and/or asymptomatic ('occult') epicardial coronary artery disease.

In order to further identify the mechanisms of MPRI reduction we compared the RT group with a second control group of liver transplant patients. Pre-renal transplant CKD patients have high prevalence of cardiovascular disease, in contrast, pre-liver transplant chronic liver disease (CLD) patients have low prevalence of cardiovascular disease [221]. Whilst most CKD patients have hypertension, CLD patients have portal hypertension, which causes vasodilatation and decreased arterial blood pressure. An et al. studied 1045 liver cirrhosis patients matched with 6283 controls showed that asymptomatic cirrhotic patients had similar prevalence of obstructive CAD compared to controls with healthy livers [221]. However, cardiovascular disease is one of the leading cause of death in post liver transplant patients [222]. A retrospective study of 455 liver transplant recipients by Fussner et al. showed that cardiovascular disease developed in 10.6%, 20.7% and 30.3% of liver transplant recipients within one, five and eight years respectively [223]. In our study, the LT and RT groups were well matched in terms of post-transplant duration, age, and importantly exposure to immunosuppressive medications (except for corticosteroids and mycophenolate). Intriguingly, we found that myocardial perfusion reserve was reduced in asymptomatic post renal transplant patients similar to post liver transplant patients, despite the relatively low prevalence of CAD in chronic liver disease compared to CKD patients, and despite early discontinuation of steroid use in the latter. This finding tends to absolve corticosteroid exposure as responsible for the myocardial perfusion abnormality. In our renal transplant cohort 75% had an MPRI<1.5 in any coronary artery territory, similar to 73% of the liver transplant cohort. Although our numbers are small, there is a strong biologic plausibility to this finding, given the well recognised effect of immunosuppressants in potentiating an increased prevalence of traditional cardiovascular risk factors in this population. Tacrolimus may cause vasoconstriction of the afferent and efferent

glomerular arterioles, similar to cyclosporine [224]. The same mechanism may also induce coronary vasoconstriction or “spasm”.

In order to investigate the presence of asymptomatic epicardial CAD, we further assessed both the RT and LT groups with MRCA. This showed that 31% of patients post transplant (both liver and renal) had significant coronary artery disease in at least one territory. We do not routinely perform invasive coronary angiography before renal or liver transplantation in our centre. Thirty-one out of thirty-five renal transplant recipients had negative stress imaging pre-transplantation. The remaining four transplant recipients had inconclusive stress imaging and underwent coronary angiography greater than five years previously that showed only minor coronary artery disease (less than 50% in major epicardial vessel). There was no significant difference between the presence of significant CAD between RT and LT patients. Furthermore, there was no significant relationship between the presence of significant epicardial coronary artery disease and impaired myocardial perfusion reserve, implying that the mechanism of MPRI reduction is most likely small vessel related (“coronary microvascular”) rather than epicardial disease. Microvascular CAD has been shown to be associated with reduced survival, although the rate of survival is better than for epicardial CAD [20].

Our study has several limitations. Firstly, the sample size for each group of patients was relatively small, consistent with being a pilot study. Secondly, the MRCA has lower diagnostic accuracy in the distal vessels compared with CT coronary angiography and the possibility of the distal CAD is not excluded but is a safer option for post-transplant recipients who have increased risk of malignancy even with small dose of radiation. Thirdly, a semiquantitative method was used to analyse myocardial perfusion reserve since we do not have quantitative method in our centre. Quantitative perfusion using CMR [180] would have permitted distinction between impaired MPRI from reduced stress myocardial blood flow (MBF) versus increased resting MBF in post-transplant population. Non-contrast T1 mapping was also not available at the time of the study. Our study demonstrates the utility of multi-

parametric CMR in renal transplant recipients, and confirmation in larger scale studies is warranted.

## **5.5 Conclusion**

Asymptomatic renal transplant recipients have a global reduction in myocardial perfusion, independent of the degree of LVH and the presence of diabetes mellitus. Myocardial perfusion is also impaired in liver transplant recipients, thus unlikely due to previous CKD. In our transplant cohort, the impaired myocardial perfusion is incompletely accounted for by epicardial coronary artery disease suggesting a pathophysiologic role for coronary microvascular dysfunction in this clinical setting.

Table 5.1 Clinical characteristics

	Renal Transplant Subjects (n= 20)	Liver Transplant Subjects (n= 15)	Hypertensive Controls (n= 10)	p value <sup>4</sup>
Age, years (mean ± SD)	55 ± 11	61 ± 6	55 ± 11	0.17
Male sex, n (%)	11 (55)	12 (80)	5 (50)	0.18
BMI <sup>1</sup> , kg/m <sup>2</sup> (mean ± SD)	29 ± 5	30 ± 4	33 ± 3	0.26
eGFR <sup>2</sup> , mL/min/1.73 m <sup>2</sup> (mean±SD)	78 ± 19	89 ± 29	108 ± 30	0.009
Systolic Blood Pressure (mmHg)	131 ± 19	130 ± 14	140 ± 11	0.26
Diastolic Blood Pressure (mmHg)	77 ± 14	80 ± 9	80 ± 11	0.74
Heart Rate (beats per minute)	71 ± 11	64 ± 9	77 ± 15	0.02
<b>Cardiovascular Risk Factors, n (%)</b>				
Hypertension	18 (90)	9 (60)	10 (100)	0.03
Diabetes Mellitus	3 (15)	4 (27)	2 (20)	0.62
Total cholesterol (mmol/L)	4.8 ± 1.2	4.5 ± 1.1	5.7 ± 1.0	0.06
Low-density lipoprotein (mmol/L)	2.1 ± 1.1	2.6 ± 1.0	3.6 ± 0.9	0.005
Triglyceride (mmol/L)	2.3 ± 1.4	1.5 ± 0.6	1.5 ± 0.7	0.08
Smoking History	7 (35)	6 (40)	3 (30)	1.00
<b>Cardiac Medications, n (%)</b>				
Aspirin	1 (5)	0 (0)	2 (20)	0.14
Beta blocker	9 (45)	3 (20)	2 (20)	0.29
ACE <sup>3</sup> inhibitor	5 (25)	1 (7)	2 (20)	0.41
Angiotensin Receptor Blocker	3 (15)	1 (7)	5 (50)	0.07
Calcium channel blocker	5 (25)	5 (33)	5 (50)	0.54
Statin	7 (35)	0 (0)	2 (20)	0.03

Data are presented as n (%) or mean ± SD.

<sup>1</sup>BMI indicates body mass index; <sup>2</sup>eGFR, estimated Glomerular Filtration Rate;

<sup>3</sup>ACE, angiotensin-converting enzyme. <sup>4</sup> Assessed using ANOVA or Fisher's exact as appropriate.

Table 5.2 Prescribed immunosuppressant medications in the renal and liver transplant groups

<b>Immunosuppressants, n (%)</b>	<b>Renal Transplant Subjects (n= 20)</b>	<b>Liver Transplant Subjects (n=15)</b>	<b>p value<sup>1</sup></b>
Azathioprine	2 (10)	4 (27)	0.37
Mycophenolate	16 (80)	4 (27)	0.002
Prednisolone	18 (90)	0 (0)	< 0.0001
Cyclosporine	1 (5)	1 (7)	0.68
Tacrolimus	16 (80)	14 (93)	0.37
Everolimus	1 (5)	0 (0)	0.57
Sirolimus	1 (5)	0 (0)	0.57

<sup>1</sup> Assessed using Fisher's exact.

Table 5.3 Left ventricular mass, septal and lateral wall thickness, ventricular volumes and ejection fractions

	<b>Renal Transplant Subjects (n= 20)</b>	<b>Liver Transplant Subjects (n= 15)</b>	<b>Hypertensive Controls (n= 10)</b>	<b>p value<sup>3</sup></b>
LV <sup>1</sup> Mass index, g/m <sup>2</sup>	64 ± 13	65 ± 11	60 ± 10	0.60
LV Septal Wall diameter, cm	1.2 ± 0.3	1.2 ± 0.2	1.1 ± 0.3	0.22
LV Lateral Wall diameter, cm	0.9 ± 0.3	0.9 ± 0.2	0.9 ± 0.2	0.81
LV End Diastolic Volume index, ml/m <sup>2</sup>	68 ± 12	62 ± 13	70 ± 13	0.43
LV End Systolic Volume index, ml/m <sup>2</sup>	18 ± 8	19 ± 8	22 ± 9	0.75
LV Stroke Volume index, ml/m <sup>2</sup>	50 ± 12	45 ± 9	46 ± 10	0.26
LV Ejection Fraction, %	74 ± 9	71 ± 8	69 ± 8	0.45
RV <sup>2</sup> End Diastolic Volume index, ml/m <sup>2</sup>	70 ± 11	67 ± 14	71 ± 18	0.73
RV End Systolic Volume index, ml/m <sup>2</sup>	27 ± 8	24 ± 6	26 ± 9	0.47
RV Stroke Volume index, ml/m <sup>2</sup>	43 ± 8	41 ± 11	46 ± 12	0.77
RV Ejection Fraction, %	62 ± 10	63 ± 7	63 ± 6	0.92

All data are presented as mean ± SD.

<sup>1</sup>LV indicates LeftVentricle; <sup>2</sup>RV, Right Ventricle. <sup>3</sup> Assessed using ANOVA.

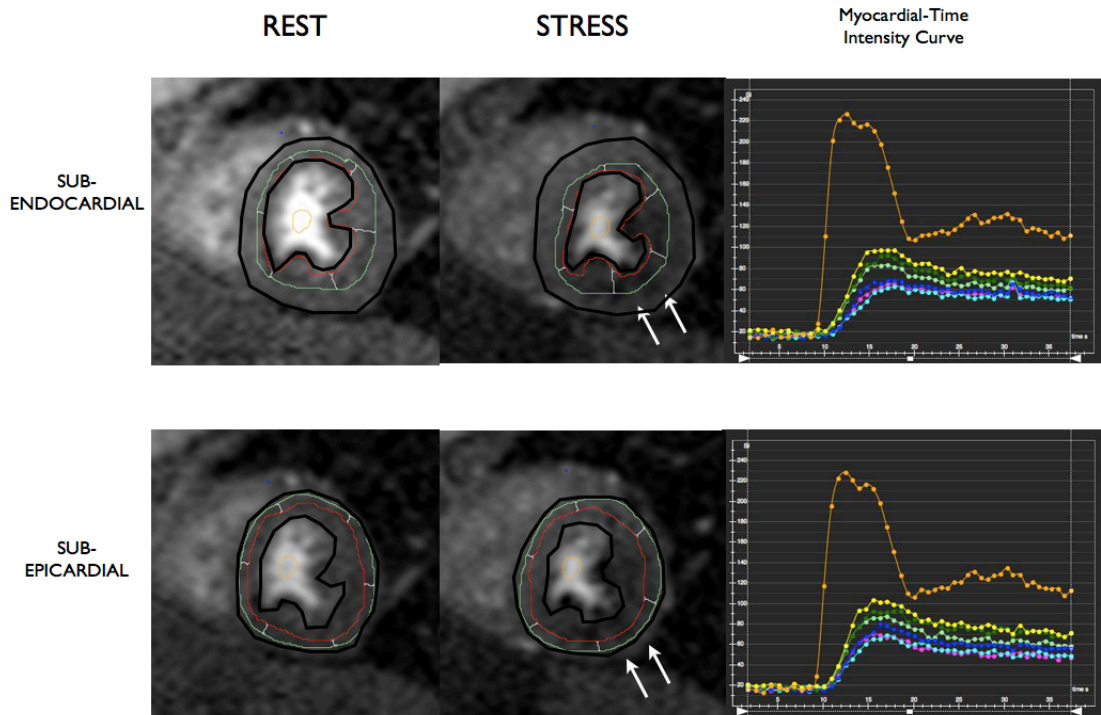


Figure 5.1. Example of Subendocardial and Subepicardial Segmentation. Rest and stress perfusion images of a transplant recipient showing inferior and anterolateral perfusion defect (white arrows). Basal, mid, and apical short axis slices were acquired (a mid short axis slice was shown as representative). Transmural, subepicardial (bottom) and subendocardial (top) contours were traced. The left ventricular myocardium was segmented into six segments (anterior, anterolateral, inferolateral, inferior, inferoseptal, anteroseptal) with right ventricular insertion point as a reference. Segmental myocardial-time intensity curves at stress (shown on the right) and at rest were measured by the CMR<sup>42</sup> software.

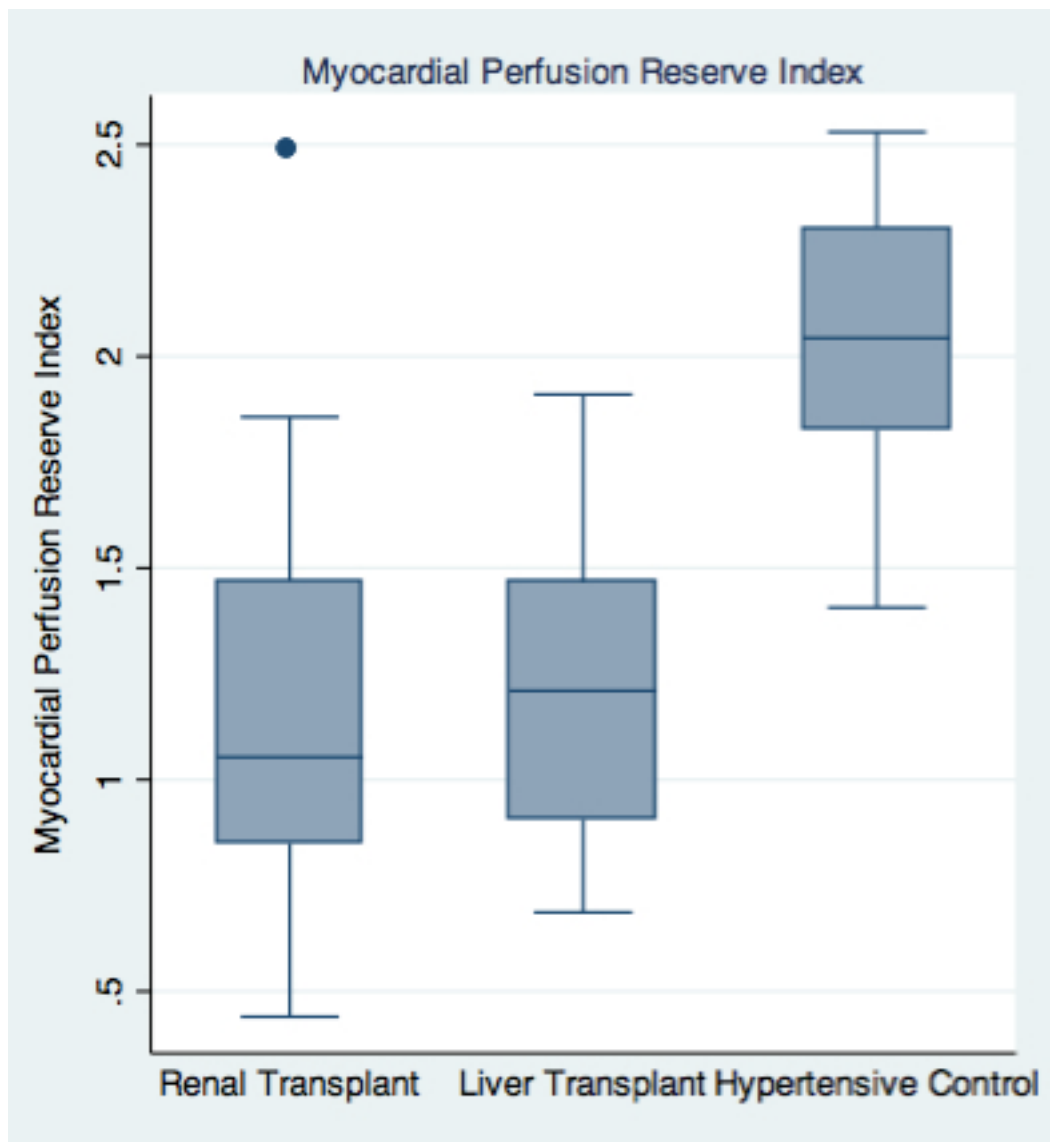


Figure 5.2 Mean Myocardial Perfusion Reserve Index (MPRI) of the Renal Transplant, Liver Transplant, and Hypertensive Controls ( $1.19 \pm 0.50$  in RT versus  $1.23 \pm 0.36$  in LT versus  $2.04 \pm 0.32$  in HT controls,  $p < 0.0001$ ).

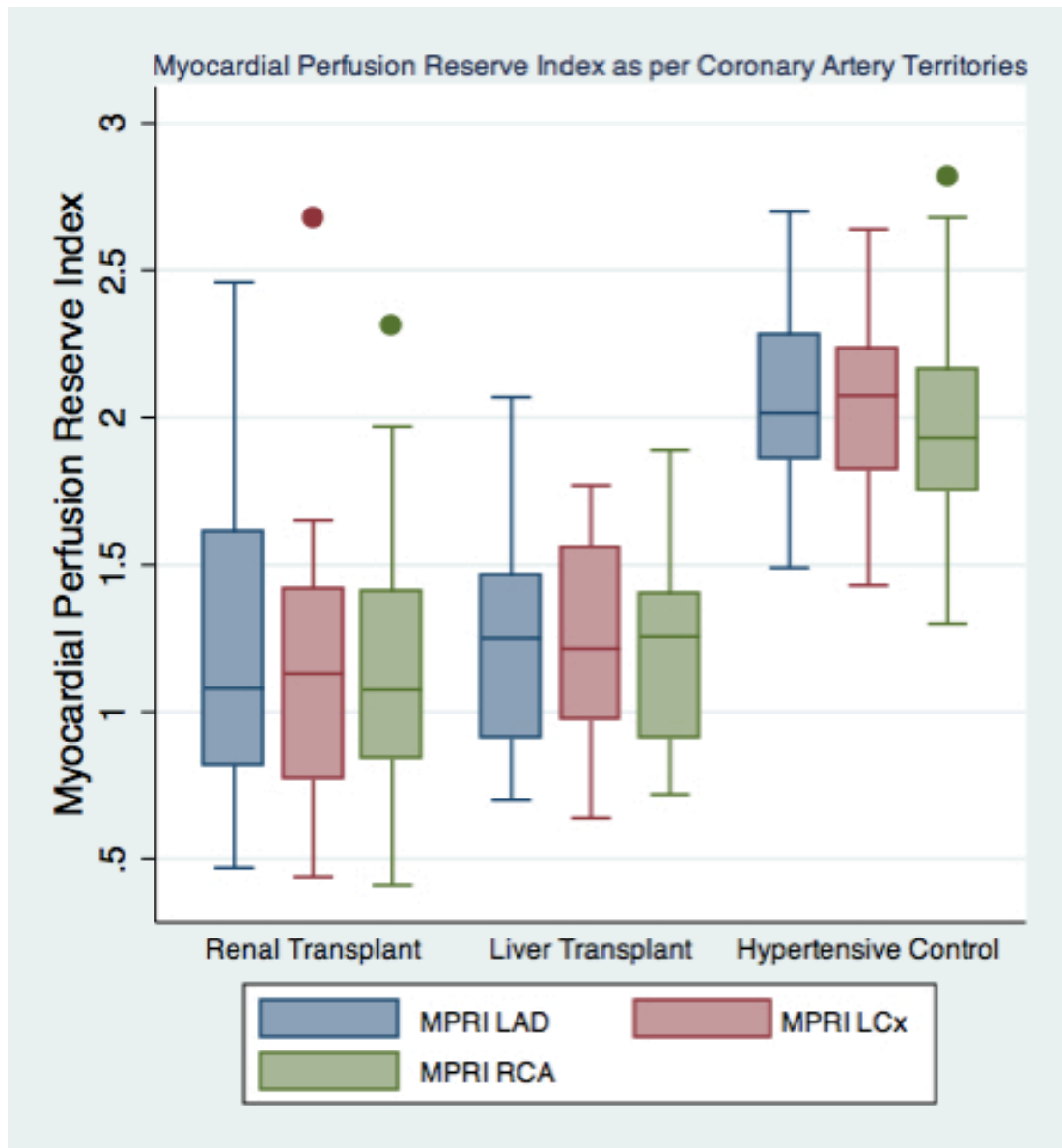


Figure 5.3 Myocardial Perfusion Reserve Index (MPRI) of the Renal Transplant, Liver Transplant, and Hypertensive Controls within each of the three coronary artery territories.

LAD indicates Left Anterior Descending; LCx, Left Circumflex; RCA, Right Coronary Artery.

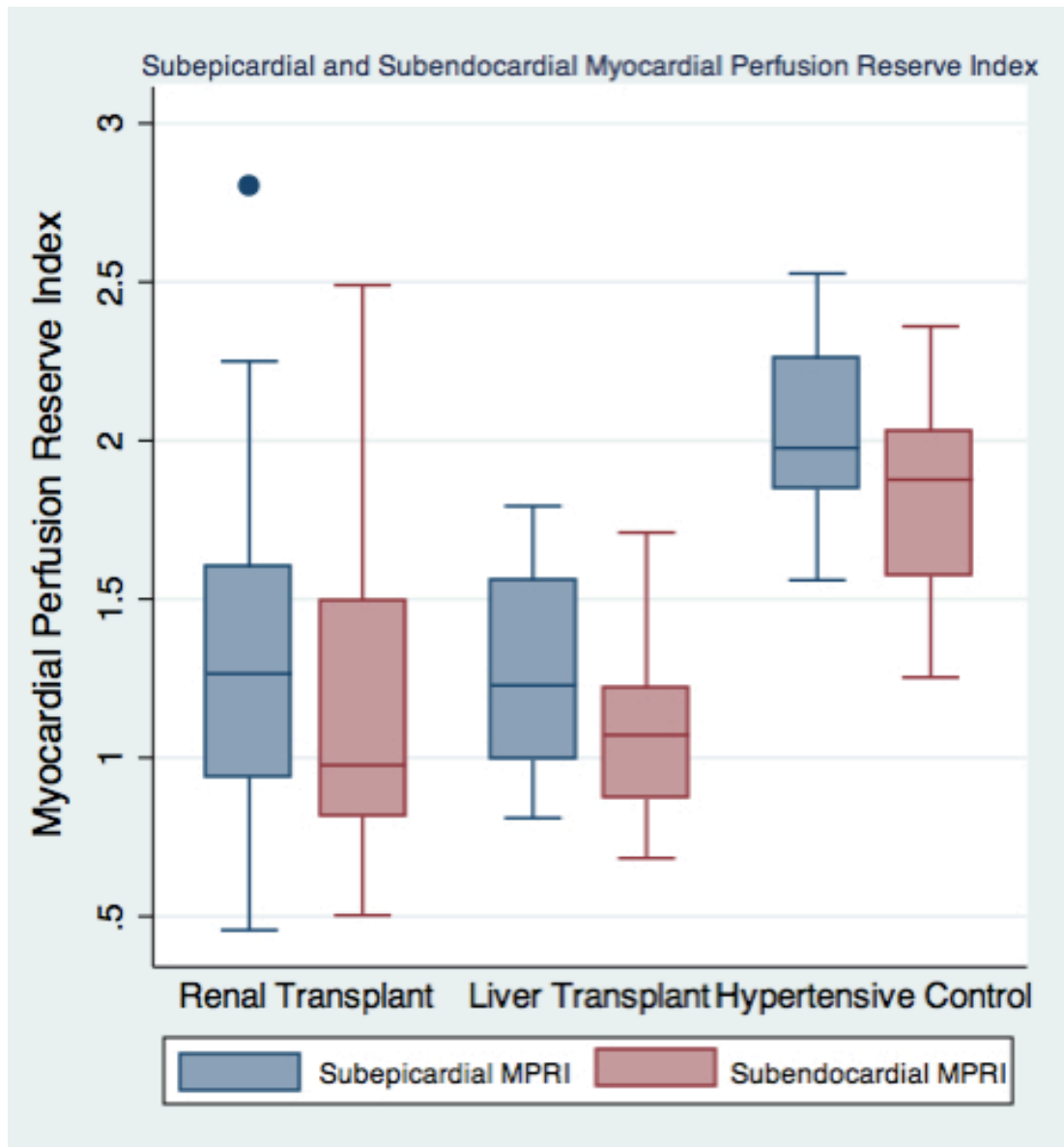


Figure 5.4 Subepicardial and Subendocardial Myocardial Perfusion Reserve Index (MPRI) of the Renal Transplant, Liver Transplant, and Hypertensive Controls (Subepicardial MPRI  $1.33 \pm 0.57$  in RT versus  $1.30 \pm 0.33$  in LT versus  $2.01 \pm 0.30$  in HT controls,  $p < 0.001$ ; Subendocardial MPRI  $1.19 \pm 0.54$  in RT versus  $1.11 \pm 0.31$  in LT versus  $1.85 \pm 0.34$  in HT controls,  $p < 0.0001$ ).

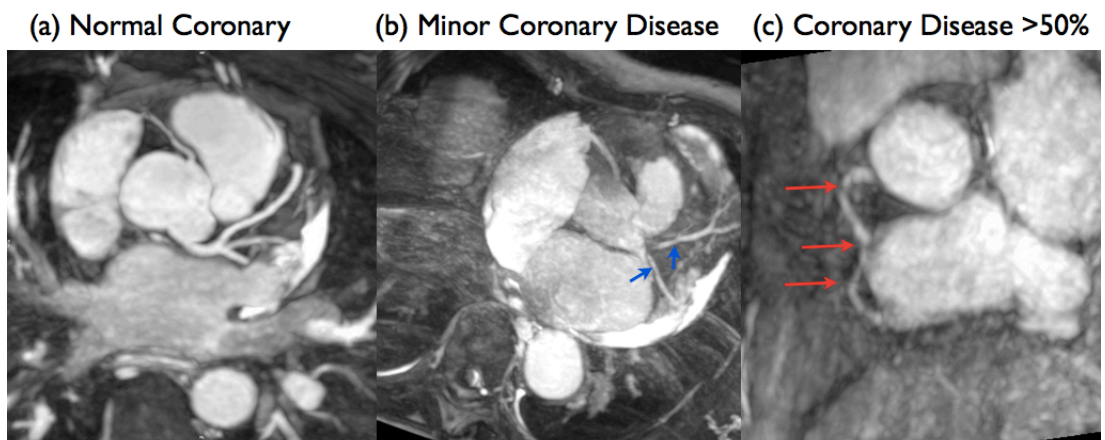


Figure 5.5 Reformatted whole-heart magnetic resonance angiography (MRCA) with navigator-gated 3D Steady-State Free Precession sequence in (a) transplant recipient with normal coronary arteries, (b) transplant recipient with minor coronary artery disease <50% with irregularities (arrows), and (c) transplant recipient with coronary artery disease >50% stenosis in RCA (arrows).

# **CHAPTER 6 - Relationship Between Myocardial Perfusion and Aortic Stiffness in Asymptomatic Renal Transplant Recipients**

## **6.1 Introduction**

Cardiovascular disease in chronic kidney disease and the post renal transplant population is attributable to atherosclerosis and arteriosclerosis [225, 226]. Our recent study [227] demonstrates a reduced myocardial perfusion reserve in the post renal transplant population which is not completely explained by the presence of epicardial coronary artery disease, and may reflect microvascular disease. Arteriosclerosis involves thickening and calcification of the medial arterial layer causing stiffening of large conduit arteries [225, 228], which disrupts pressure wave dampening resulting in increased wave reflection, pressure wave augmentation and increased central systolic and pulse pressures. Aortic pulse wave velocity (PWV) is considered the gold standard to measure aortic stiffness, and is now commonly assessed by cardiovascular magnetic resonance (CMR) imaging. The aim of this study was to assess central (aortic) vascular dysfunction in the post-renal transplant population using high-resolution CMR. We hypothesised that asymptomatic renal transplant recipients (without prior evidence of heart disease) would have increased aortic stiffness (defined by increased PWV), and that this might be associated with reduced myocardial perfusion.

## 6.2 Methods

### 6.2.1 Study Population

We conducted a prospective study of twenty renal transplant (RT) subjects and ten controls with a clinical history of hypertension (HT). All prospective study participants gave written informed consent as approved by the Southern Adelaide Health Service/Flinders University Human Research Ethics Committee.

### 6.2.2 CMR Protocol

CMR images were acquired to obtain measures of left ventricular (LV) mass, LV function, coronary perfusion both at rest and under stress and pulse wave velocity (PWV). The latter was assessed in the ascending aorta (between the ascending and proximal descending aorta), and in the descending aorta (between the proximal descending aorta and the abdominal aorta), through the main pulmonary artery [229]. For stress perfusion analysis, the basal, mid and apical segments at rest and during stress adenosine were divided into 6 segments according to American Heart Association criteria using the right ventricular insertion as the reference point. The Myocardial Perfusion Reserve Index (MPRI) was calculated as the ratio of perfusion during adenosine-induced hyperaemia to perfusion at rest. The aortic path lengths between the ascending and descending aorta were manually measured along the centre line of the CMR “scout image” of the oblique sagittal (“hockey stick”) view of the aorta (Figure 6.1). The quantification of flow was achieved by CMR<sup>42</sup> Version 4.1, Circle Cardiovascular Imaging Inc. processing of the through-plane coronary artery phase velocity map in the ascending and descending aorta. Pulse wave velocity (PWV) was calculated as [187, 188]:

$$\text{PWV (m/s)} = \Delta x / \Delta t,$$

where

$\Delta x$  is the aortic path length between the arrival of the systolic wave front at the site of the ascending and descending aorta

$\Delta t$  is the transit time of the flow wave.

### 6.3 Results

Twenty renal transplant (RT) subjects and ten controls with a clinical history of hypertension (HT) participated in the study. The clinical details are summarised in Table 6.1.

The CMR results were summarised in Table 6.2. A total of 840 myocardial segments (576 of RT and 264 of HT) were compared between the two groups using linear mixed models. Left ventricular mass index and septal wall diameter were similar in the two groups. The mean transmural MPRI across three coronary artery territories was significantly lower in the RT compared to HT ( $1.19 \pm 0.50$  in RT versus  $2.04 \pm 0.32$  in HT controls,  $p < 0.0001$ ) (Figure 6.2). The subendocardial MPRI was  $1.19 \pm 0.54$  in RT versus  $1.85 \pm 0.34$  in HT controls,  $p < 0.0001$  and the subepicardial MPRI was  $1.33 \pm 0.57$  in RT versus  $2.01 \pm 0.30$  in HT controls,  $p < 0.001$  (Figure 6.2). In the RT subgroup, the subendocardial MPRI was significantly lower than the subepicardial MPRI,  $1.19 \pm 0.54$  subendocardial versus  $1.33 \pm 0.57$  subepicardial,  $p = 0.01$ , but similar in the HT controls,  $1.85 \pm 0.34$  subendocardial versus  $2.01 \pm 0.30$  subepicardial,  $p = 0.12$ .

Pulse Wave Velocity (PWV) was not significantly different between RT and HT groups ( $4.26 \pm 1.77$  m/s versus  $4.65 \pm 2.45$  m/s respectively,  $p = 0.66$ ) (Figure 6.3). There was also no association between MPRI and PWV (m/s) ( $\beta = -0.06$ , 95% confidence interval -0.19 to 0.07,  $p = 0.35$ ).

Amongst both the RT and HT subjects, PWV was associated with left ventricular mass index ( $r^2 = 0.23$ , 95% confidence interval 0.01 to 0.16,  $p = 0.02$ ). Amongst RT

subjects alone, although MPRI was associated with estimated Glomerular Filtration Rate (eGFR) (mL/min/1.73 m<sup>2</sup>) ( $\beta$ = 0.014, 95%CI= 0.0023 to 0.026, p= 0.0019), PWV was not ( $\beta$ = -0.03, 95%CI= -0.063 to 0.005, p= 0.10).

## 6.4 Discussion

Our study is the first study to utilise high resolution CMR imaging to measure and compare aortic stiffness in post renal transplant patients to an age-matched hypertensive population with a similar degree of left ventricular hypertrophy. This allowed us to explore the relationship between aortic stiffness and the myocardial perfusion reserve index and its association with the renal failure and transplantation state. A strength of our study was the accurate assessment of central PWV which was achieved by obtaining image of the central thoracic aorta. Simultaneous assessment of stress and rest functional imaging as well as 3D left ventricular volumetric data in groups matched for left ventricular hypertrophy isolates the impact of the renal failure/transplant state on these cardiac parameters.

Central aortic stiffness measured by PWV was not increased in the renal transplant cohort compared to hypertensive controls and was not associated with changes in myocardial perfusion reserve index. In our renal transplant cohort, the subendocardial MPRI was lower than the subepicardial MPRI, which might indicate small distal vessel endothelial dysfunction rather than large vessel aortic dysfunction as a possible mechanism. In our cohort population one transplant recipient received cyclosporine, whereas the majority (16 out of 20) received tacrolimus. Both cyclosporine and tacrolimus may induce coronary vasoconstriction or spasm in similar way to vasoconstriction of the afferent and efferent glomerular arterioles [224], and it is tempting to speculate that this may explain, at least in part, our finding of reduced myocardial perfusion reserve, independent of changes in aortic stiffness. Our transplant and control group were well matched in terms of age, pulse pressure, and degree of left ventricular hypertrophy, although there was a trend for

higher body mass index in the hypertensive controls. The systemic inflammatory marker measured by high-sensitive C-reactive protein was similar between the groups, which could also partially explain the similarity of the central aortic PWV between the two groups.

CMR assessment of aortic PWV has been shown to have high reproducibility [187] and is higher in patients with hypertension compared to age-matched control subjects [230]. Aortic stiffness is elevated in chronic kidney disease population compared to hypertensive and normotensive population [231, 232]. Pan et al. found that there was no significant difference in aortic stiffness measured by carotid-femoral PWV in post-renal transplant and age-matched pre-renal transplant patients [233]. By contrast, Hotta et al. found that the aortic stiffness measured by PWV was significantly reduced post renal transplantation [234]. They found that PWV was associated with significant decreases in systolic and diastolic blood pressure post renal transplantation [234]. Several studies supported the hypothesis of significant hypertension as the mechanism of aortic stiffness in the post renal transplant population [226, 235]. These studies are consistent with our own observations that PWV was associated with left ventricular mass index and that post-transplant hypertension may arise due to increased aortic stiffness.

## **6.5 Conclusion**

We found no evidence of differences in aortic stiffness in post renal transplant patients compared to hypertensive patients with a similar degree of left ventricular hypertrophy. In addition, the impaired myocardial perfusion in post renal transplant population was independent of left ventricular hypertrophy and not related to aortic stiffness.

Table 6.1 Clinical characteristics

	Renal Transplant Subjects (n= 20)	Hypertensive Controls (n= 10)	p value <sup>4</sup>
Age, years (mean ± SD)	55 ± 11	55 ± 11	0.99
Male sex, n (%)	11 (55)	5 (50)	1.00
BMI <sup>1</sup> , kg/m <sup>2</sup> (mean ± SD)	29 ± 5	33 ± 3	0.065
eGFR <sup>2</sup> , mL/min/1.73 m <sup>2</sup> (mean±SD)	78 ± 19	108 ± 30	0.002
Pulse pressure (mmHg)	53 ± 15	60 ± 10	0.26
High-sensitive C-reactive protein (mg/L)	6.2 ± 9.0	2.9 ± 1.8	0.37
<b>Cardiovascular Risk Factors, n (%)</b>			
Hypertension	18 (90)	10 (100)	0.54
Diabetes Mellitus	3 (15)	2 (20)	0.73
Hypercholesterolemia	8 (32)	5 (50)	0.71
Smoking History	7 (35)	2 (20)	1.00
<b>Cardiac Medications, n (%)</b>			
Aspirin	1 (5)	2 (20)	0.25
Beta blocker	9 (45)	2 (20)	0.25
ACE <sup>3</sup> inhibitor	5 (25)	2 (20)	1.00
Angiotensin Receptor Blocker	3 (15)	5 (50)	0.08
Calcium channel blocker	5 (25)	5 (50)	0.23
Statin	7 (35)	2 (20)	0.68

Data are presented as n (%) or mean ± SD.

<sup>1</sup>BMI indicates body mass index; <sup>2</sup>eGFR, estimated Glomerular Filtration Rate;

<sup>3</sup>ACE, angiotensin-converting enzyme. <sup>4</sup> Assessed using t-test or Fisher's exact as appropriate.

Table 6.2 Left ventricular mass, septal and lateral wall thickness, ventricular volumes and ejection fractions

	<b>Renal Transplant Subjects (n= 20)</b>	<b>Hypertensive Controls (n= 10)</b>	<b>p value<sup>2</sup></b>
LV <sup>1</sup> Mass index, g/m <sup>2</sup>	64 ± 13	60 ± 10	0.42
LV Septal Wall diameter, cm	1.2 ± 0.3	1.1 ± 0.3	0.44
LV Lateral Wall diameter, cm	0.9 ± 0.3	0.9 ± 0.2	0.48
LV End Diastolic Volume index, ml/m <sup>2</sup>	68 ± 12	70 ± 13	0.88
LV End Systolic Volume index, ml/m <sup>2</sup>	18 ± 8	22 ± 9	0.33
LV Stroke Volume index, ml/m <sup>2</sup>	50 ± 12	46 ± 10	0.39
LV Ejection Fraction, %	74 ± 9	69 ± 8	0.23

All data are presented as mean ± SD.

<sup>1</sup>LV indicates LeftVentricle. <sup>2</sup> Assessed using t-test.

a



b

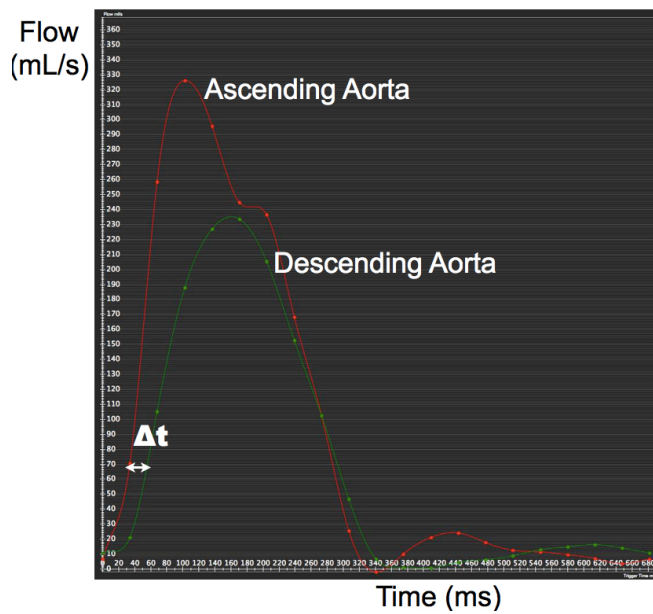


Figure 6.1 Analysis of Pulse Wave Velocity (PWV) with CMR.

- (a) The aortic path lengths between the ascending (1) and descending aorta (2) were manually measured along the centre line of the CMR “scout image” of the oblique sagittal (“hockey stick”) view of the aorta.
- (b) The flow curved in the ascending and descending aorta was achieved by CMR software. Transit time of the flow wave ( $\Delta t$ ) was the upstroke time difference of the velocity-time curve at the ascending and descending aorta.

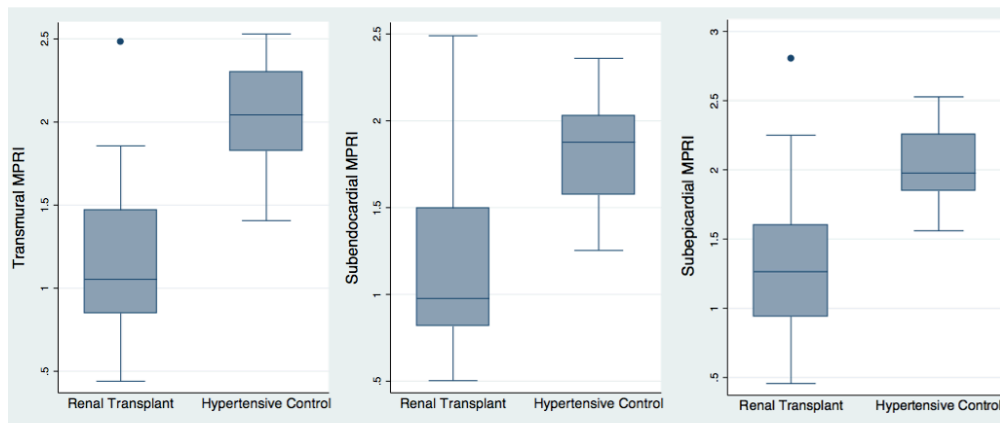


Figure 6.2 The transmural Myocardial Perfusion Reserve Index (MPRI) of the Renal Transplant (RT) was significantly lower than the Hypertensive (HT) Controls ( $1.19 \pm 0.50$  versus  $2.04 \pm 0.32$ ,  $p < 0.0001$ ). The subendocardial MPRI was  $1.19 \pm 0.54$  in RT versus  $1.85 \pm 0.34$  in HT Controls,  $p < 0.0001$ . The subepicardial MPRI  $1.33 \pm 0.57$  in RT versus  $2.01 \pm 0.30$  in HT Controls,  $p < 0.001$ .

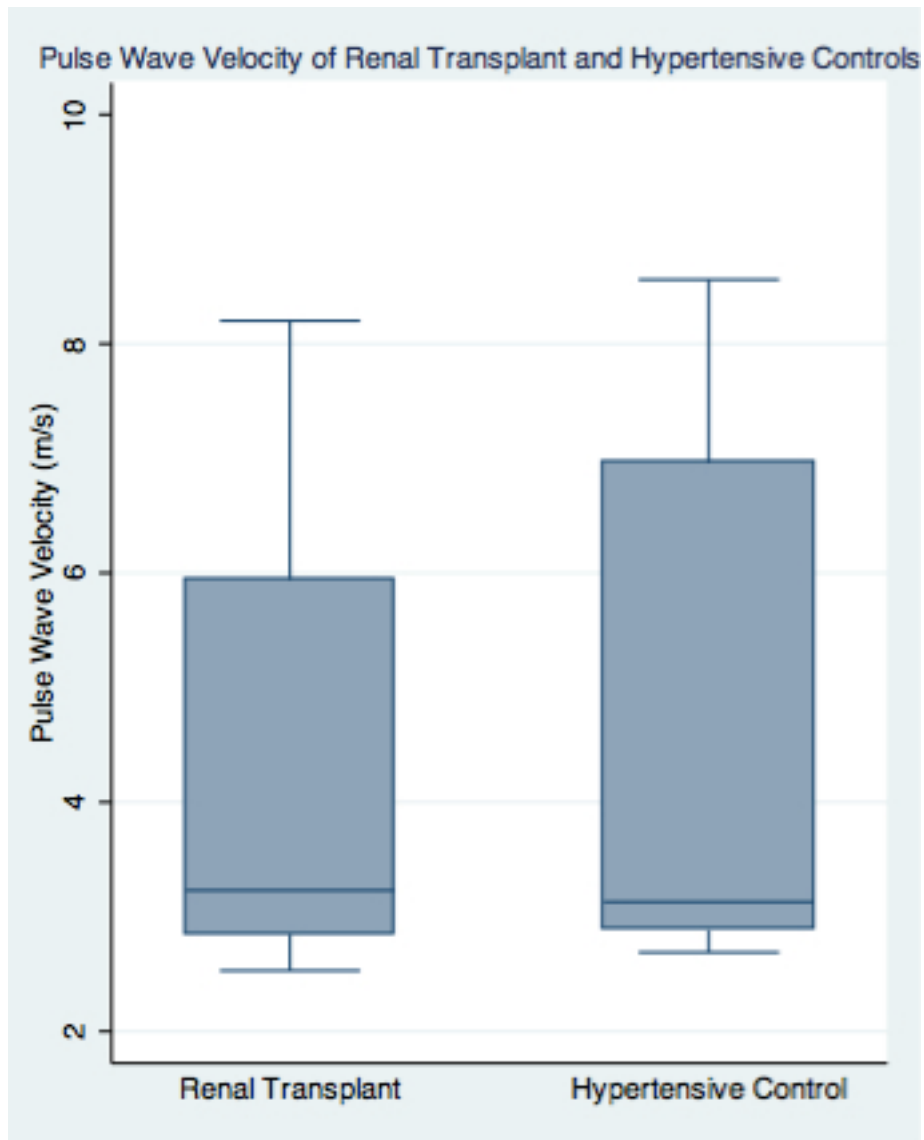


Figure 6.3 Aortic Pulse Wave Velocity (PWV) was not significantly different between the Renal Transplant and Hypertensive Control groups ( $4.26 \pm 1.77$  m/s versus  $4.65 \pm 2.45$  m/s,  $p = 0.66$ ).

# **CHAPTER 7 - Blood Oxygen Level Dependent (BOLD) Cardiovascular Magnetic Resonance (CMR) as Predictor of Cardiac Prognosis in Asymptomatic Chronic Kidney Disease Patients**

## **7.1 Introduction**

Cardiovascular disease (CVD) is the number one cause of death worldwide and is the leading cause of mortality and morbidity in people with chronic kidney disease (CKD) [3, 4], accounting for 50% of deaths [4-6]. Although renal transplantation significantly improves survival, CVD is still one of the most frequent causes of death and accounts for 35-50% of all-cause mortality [26].

Despite the high prevalence of CVD in CKD patients, the current functional cardiac investigations for ischaemia are not highly sensitive or specific for ischaemia for this population [60, 192]. Furthermore, current non-invasive cardiac investigations predict prognosis poorly, with negative test results still have adverse cardiac outcome [236]. CAD in the CKD population is complicated by the silent or asymptomatic presentation of myocardial ischaemia [14, 15].

Blood Oxygen Level Dependent (BOLD) Cardiovascular Magnetic Resonance (CMR) assesses myocardial tissue oxygenation, thus is potentially able to measure mismatches in myocardial oxygen demand and supply characteristic of myocardial ischaemia [193]. Our recent study utilising BOLD CMR demonstrates significant blunted myocardial oxygenation response to stress in the CKD patients [207]. We hypothesised that blunted myocardial oxygenation response to stress (defined by negative BOLD Signal Intensity (SI) Change value) could be an independent predictor for cardiovascular events in asymptomatic CKD patients.

## **7.2 Methods**

### **7.2.1 Study Population**

Thirty-nine subjects with pre-existing CKD with the following inclusion criteria: no symptoms of cardiac disease, no established CAD (no history of myocardial infarction, angina, coronary artery stent or bypass surgery or angiographically documented significant CAD>70%, and no significant inducible myocardial ischaemia on functional testing), and no previous systolic heart failure, were recruited into the study.

The exclusion criteria for each group were standard contraindications to CMR (e.g. severe claustrophobia, metallic implants) and contraindications to adenosine (second or third degree atrioventricular block, obstructive pulmonary disease and dipyridamole use).

All participants gave written informed consent, and the study was approved by Southern Adelaide Clinical Human Research Ethics Committee (SAC HREC).

### **7.2.2 CMR Protocol**

Subjects were instructed to refrain from caffeine 24 hours prior to the CMR examination at 3 Tesla. Cine imaging was acquired as previously described in Chapter 2 [179]. For BOLD imaging, a single mid-ventricular slice was acquired at mid-diastole using a T2-prepared ECG-gated SSFP sequence (TR 2.86 ms, TE 1.43 ms, T2 preparation time 40 ms, matrix 168 x 192, field of view 340 x 340 mm, slice thickness 8 mm, flip angle 44°), as previously described [92]. Shimming and centre frequency adjustments were performed as required before the oxygenation imaging to minimise off-resonance artifacts. A set of six BOLD images was acquired at rest during a single breath-hold over six heart beats. Six stress BOLD images comparable

to the ones acquired at rest were acquired at peak adenosine stress (140 µg/kg per minute) 90 seconds after initiation for at least 3 minutes [207].

CKD participants underwent additional non-contrast magnetic resonance coronary angiography (MRCA) imaging at 1.5 T on different day to investigate the presence of significant epicardial CAD, as described in Chapter 2.

### **7.2.3 CMR Image Analysis**

BOLD CMR analysis was performed with CMR<sup>42</sup> Version 4.1, Circle Cardiovascular Imaging Inc. (Calgary, Canada), as described in Chapter 2. Left and right ventricular functions were calculated using the 3D short axis stack and were indexed to body surface area. Each BOLD image was divided into six segments (anterior, anterolateral, inferolateral, inferior, inferoseptal, anteroseptal) according to the American Heart Association 17-segment model [182]. The mean myocardial Signal Intensity (SI) within each segment was obtained, both at rest and stress, and corrected to variations in heart rate with the equation previously described [92, 207]. MRCA analysis was performed as described in Chapter 2.

### **7.2.4 Follow-up**

Follow-up was determined from the hospital medical records, discharge summaries, and telephone interviews. We recorded all events: 1) death (cardiac death was defined as death from lethal arrhythmia, myocardial infarction, or cardiac failure, or sudden death without explanation); 2) non-fatal acute coronary syndrome (ischaemic symptoms with new ECG changes, and/or elevated troponin, and/or new segmental wall motion abnormalities on echocardiography); 3) heart failure (left and/or right ventricular systolic dysfunction, or symptoms of heart failure, i.e. dyspnoea caused by fluid overload requiring hospitalisation, or pulmonary congestion confirmed with

chest X-ray); 4) cardiac arrhythmia (sustained ventricular tachycardia, or ventricular fibrillation). The adjudication of events was not performed by an independent observer. The definition of major adverse cardiac events (MACE) included cardiovascular death, myocardial infarction, arrhythmia and pulmonary oedema.

### **7.2.5 Statistical Analysis**

Statistical analysis was performed with STATA version 13.0. Normally distributed data is expressed as mean  $\pm$  SD and compared using t tests. Fisher's exact test was used for comparison of categorical variables. BOLD SI evaluation of coronary artery level data was analysed using linear mixed modeling (LMM) with a random intercept used for each subject to account for the within-subject correlation present from measuring at three different artery sites. Cox regression hazard analysis was performed to detect risk factors of developing MACE. Cumulative event curves were compared by the Kaplan-Meier method using a log-rank test. Statistical tests were 2-tailed and a p-value  $<0.05$  was considered statistically significant.

## **7.3 Results**

### **7.3.1 Subject Characteristics**

Thirty-nine subjects with CKD participated in the study. The mean follow-up time was  $20.3 \pm 11.6$  months.

### **7.3.2 Outcomes**

There were a total of 28 cardiac events recorded in 13 of the 39 (33%) subjects with CKD. These events are described below, however only MACE events have been used in the calculation of outcomes. Six CKD patients had multiple cardiac events.

There were a total of seven myocardial infarction (one patient had two myocardial infarction). There were a total of five episodes of pulmonary oedema. There were three occurrences of newly diagnosed left ventricular systolic dysfunction. There was one each of newly diagnosed dilated left ventricle, new onset right heart failure, newly diagnosed rapidly progressive severe aortic stenosis, newly diagnosed moderate mitral regurgitation, ventricular tachycardia, new onset atrial fibrillation, and newly diagnosed inducible myocardial ischaemia on stress echocardiography. There were three episodes of syncope and two patients developed endocarditis. One patient had transiently unsteady gait, slurred speech and left sided weakness.

For analysis of MACE, when a patient experienced more than one event, death or the first myocardial infarction/heart failure was chosen. Ten patients (26%) had significant MACE ( $p= 0.01$ ). There were four (10%) deaths, three were cardiac and one unknown. There were four (10%) non-fatal myocardial infarctions. There were two (5%) heart failure, one had pulmonary oedema and one had ventricular dysfunction.

### **7.3.3 Comparison Between CKD Patients With and Without a Blunted Myocardial Oxygenation Response To Stress**

There were 20 out of 39 (51%) CKD subjects who had a negative BOLD SI Change values in any one coronary artery territory. The comparisons between the CKD group with and without negative BOLD Signal Intensity Change values are listed in Table 7.1. One CKD participant with MACE had stress BOLD images that were not analysable due to difficulty with breath holding. One participant had severe claustrophobia in the CMR machine, thus the scan was stopped. One participant could not continue with stress BOLD.

The CKD patients with negative BOLD SI Change value were older ( $63 \pm 13$  years versus  $55 \pm 9$  years). Cardiac risk factors were similar between the CKD patients

with and without negative BOLD SI Change value. The use of cardiac medications was similar between the CKD patients with and without negative BOLD SI Change value. Left and right ventricular ejection fractions between the CKD patients with and without negative BOLD SI Change value were similar. CKD patients with negative BOLD SI Change value had MACE significantly more often than the CKD patients without negative BOLD SI Change value [8 out of 20 (40%) in CKD patients with negative BOLD SI Change had MACE versus 1 out of 16 (6%) in CKD patients without negative BOLD SI Change had MACE,  $p= 0.026$ ].

Figure 7.1 shows examples of rest and stress BOLD images of CKD group with and without negative BOLD SI Change.

Twenty-seven CKD patients (15 with negative BOLD SI Change, 12 without negative BOLD SI Change) had follow-up investigation of coronary artery anatomy with MRCA. MRCA follow-up at different scanner 1.5T on different day was limited due to high cardiac events rate and comorbidities. One MRCA and one BOLD were not analysable. One patient died before MRCA. One patient had non-analysable stress BOLD and became claustrophobic, thus did not proceed with MRCA. One patient was unwell and declined. Two patients became claustrophobic. One patient had cancer. Four patients refused follow-up scan. There were 8 out of 15 (53%) CKD patients with negative BOLD SI Change value had  $CAD > 50\%$  compared to 6 out of 12 (50%) in those without,  $p= 1.00$ .

#### **7.3.4 Predictors of Major Adverse Cardiac Events**

The univariate predictors of major adverse cardiac events in the CKD group are listed in Table 7.2. Significant associations were found with the presence of diabetes mellitus, left ventricular mass indexed to body surface area, and negative BOLD SI Change value. On multivariate analysis (Table 7.3), the negative BOLD SI Change value was independently associated with adverse cardiac events (Hazard Ratio 19.48, 95% CI 1.28 - 295.44,  $p= 0.03$ ). The CKD group of patients with negative BOLD SI

Change value had significantly reduced MACE-free survival compared to the CKD patients with positive BOLD SI Change value ( $p = 0.03$ ) (Figure 7.2).

## 7.4 Discussion

Our study demonstrates that a blunted myocardial oxygenation response to stress as indicated by negative BOLD SI Change values in CKD patients is associated with a greater subsequent rate of major cardiac adverse events rate. To the best of our knowledge, this is the first study to assess BOLD CMR in predicting cardiac prognosis in the CKD population.

Coronary artery disease is highly prevalent in the CKD population [11], and is evident even in early renal disease [8, 12]. Epicardial and/or microvascular coronary disease is often present in the population [17] [18] and can cause silent or asymptomatic myocardial ischaemia [14, 15]. Wetmore, et al. demonstrated that painless myocardial ischaemia occurred more often in the CKD patients compared to individuals with normal renal function, and was associated with a higher mortality rate in CKD patients [206]. Both microvascular and epicardial coronary disease are associated with a higher major adverse cardiac event rate [15, 20].

Current diagnostic investigations of myocardial ischaemia in CKD patients lack sensitivity and specificity due to blunted chronotropic response, physical deconditioning, left ventricular hypertrophy obscuring wall motion abnormality, and false negative balanced ischaemia [192]. Stress perfusion CMR with adenosine and gadolinium contrast has not been utilised in the CKD population due to the risk of rare but serious side effect of nephrogenic systemic fibrosis, manifesting as hardening of the skin and internal organs, which is potentially irreversible and can be fatal. Dobutamine stress CMR without gadolinium potentially has a similar issue of lacking sensitivity in the CKD population with blunted chronotropic response.

BOLD CMR technique using adenosine has the capability of detecting ischaemia from both epicardial and microvascular coronary artery disease without the use of gadolinium contrast and without issues of blunted chronotropic response. It exploits the paramagnetic properties of deoxyhaemoglobin as an endogenous contrast agent, with increased deoxyhaemoglobin content leading to signal reduction on T2-weighted images [133]. BOLD CMR has moderate accuracy in detecting significant epicardial coronary artery disease [93, 132]. Chapter 3 demonstrated impaired myocardial oxygenation response to stress in CKD population without previously known epicardial CAD, irrespective of the degree of left ventricular hypertrophy and the presence of diabetes mellitus [207]. In this study we report the prognostic utility of BOLD CMR in this same group of patients with a medium term follow up. Furthermore, we are able to concurrently report on the presence of significant CAD measured by MRCA. Negative values of BOLD SI Change have been shown to be related to significant coronary artery stenoses by Luu et al. and Karamitsos et al. [196] [92], which may explain why CKD patients with negative BOLD SI Change value have a higher rate of major adverse cardiac events compared to those with positive value BOLD SI Change. Akinboboye et al. previously demonstrated myocardial ischaemia attributed to coronary steal in patients with multi-vessel CAD associated with significant reductions in blood flow to microvascular collateral-dependent myocardium [197]. Our study showed that negative and positive BOLD SI Change values in our CKD cohort had similar degree of epicardial CAD>50%, implying the involvement of severe microvascular disease contributing to blunted myocardial oxygenation response and poorer cardiac prognosis. Our study is consistent with previous studies demonstrating abnormal myocardial perfusion scintigraphy results in CKD patients associated with higher incidence of cardiac events and mortality [75-81].

Our study is limited by the relatively small sample size, whilst the hazard ratio for development of MACE is very high the confidence intervals are broad and, therefore, the findings need to be confirmed in a larger patient population. We applied strict inclusion and exclusion criteria to include patients with history of CKD who were asymptomatic, reasonably well and without previous coronary artery

disease, systolic heart failure, severe valvular disease, or significant conduction disorder. Nevertheless, in our cohort study there were ten significant MACE with a total of 28 events. Secondly, BOLD research techniques are evolving with new approaches with potentially less frequency artefacts. Our study may lead to better detection of asymptomatic ischaemia in CKD population to improve overall cardiac prognosis and survival. The question of whether medical management or intervention is indicated in such CKD patients with asymptomatic ischaemia, and whether it improves prognosis, needs to be answered by prospective randomised controlled studies.

## **7.5 Conclusion**

Our study suggests that CKD patients with blunted myocardial oxygenation response to stress have reduced event-free survival rate than those without. Non-contrast BOLD CMR is a promising technique to assess silent myocardial ischaemia in CKD patients, and may potentially offer a prognostic tool in this population.

Table 7.1 Comparison Between CKD Patients With and Without Negative BOLD SI Change

	<b>CKD With Negative BOLD SI Change (n= 20)</b>	<b>CKD Without Negative BOLD SI Change (n= 16)</b>	<b>p value<sup>8</sup></b>
Age, years (mean ± SD)	63 ± 13	55 ± 9	0.04
Male sex, n (%)	12 (60)	9 (56)	1.00
BMI <sup>1</sup> , kg/m <sup>2</sup> (mean ± SD)	26 ± 4	26 ± 5	0.91
eGFR <sup>2</sup> , mL/min/1.73 m <sup>2</sup> (mean ± SD)	23 ± 25	33 ± 30	0.28
Resting systolic blood pressure (mmHg)	138 ± 17	136 ± 21	0.86
Diabetes Mellitus	9 (45)	3 (19)	0.25
Total cholesterol (mmol/L)	4.3 ± 1.0	4.8 ± 1.3	0.23
Low-density lipoprotein (mmol/L)	2.2 ± 0.7	2.2 ± 1.1	0.96
Triglyceride (mmol/L)	1.9 ± 1.3	2.1 ± 1.2	0.59
Smoking History	8 (40)	6 (38)	1.00
Aspirin	2 (10)	0 (0)	0.49
Beta blocker	6 (30)	6 (38)	0.73
ACE <sup>3</sup> inhibitor	5 (25)	3 (19)	0.71
Angiotensin Receptor Blocker	1 (5)	3 (19)	0.30
Calcium channel blocker	5 (25)	6 (38)	0.48
Statin	5 (25)	4 (25)	1.00
LV <sup>4</sup> Ejection Fraction, %	69 ± 10	68 ± 12	0.79
RV <sup>5</sup> Ejection Fraction, %	62 ± 9	62 ± 12	0.93
MACE, n (%)	8 (40)	1 (6)	0.026

Data are presented as n (%) or mean ± SD.

<sup>1</sup>BMI indicates body mass index; <sup>2</sup>eGFR, estimated Glomerular Filtration Rate;

<sup>3</sup>ACE, angiotensin-converting enzyme; <sup>4</sup>LV, Left Ventricle; <sup>5</sup>RV, Right Ventricle;

<sup>6</sup>BOLD SI, Blood Oxygen Level Dependent Signal Intensity; <sup>7</sup>MACE, Major Adverse Cardiac Events; <sup>8</sup> Assessed using t-test or Fisher's exact as appropriate, BOLD SI Change was analysed with linear mixed modeling.

Table 7.2 Univariate Analysis of Predictor of MACE in the CKD Patients

	Hazard Ratio	95% CI	p value <sup>6</sup>
Age, years	1.05	0.99 - 1.10	0.08
Male sex	0.75	0.23 - 2.47	0.64
eGFR <sup>1</sup> , mL/min/1.73 m <sup>2</sup>	0.98	0.94 - 1.01	0.10
Diabetes Mellitus	2.52	1.30 - 4.89	0.006
BMI <sup>2</sup> , kg/m <sup>2</sup>	0.95	0.82 - 1.09	0.45
Low-density lipoprotein (mmol/L)	0.87	0.31 - 2.43	0.79
Triglyceride (mmol/L)	1.01	0.76 - 1.34	0.95
LV <sup>3</sup> Mass index, g/m <sup>2</sup>	1.04	1.01 - 1.08	0.02
LV Ejection Fraction, %	0.96	0.90 - 1.02	0.16
RV <sup>4</sup> Ejection Fraction, %	0.98	0.92 - 1.03	0.39
Negative Value BOLD SI <sup>5</sup> Change	4.72	1.00 - 22.39	0.027

All data are presented as mean  $\pm$  SD.

<sup>1</sup> eGFR indicates estimated Glomerular Filtration Rate; <sup>2</sup> BMI, body mass index; <sup>3</sup> LV, Left Ventricle; <sup>4</sup> RV, Right Ventricle; <sup>5</sup> BOLD SI, Blood Oxygen Level Dependent Signal Intensity; <sup>6</sup> Assessed using Cox regression analysis.

Table 7.3 Multivariate Analysis of Predictors of MACE in the CKD Patients

	Hazard Ratio	95% CI	p value <sup>6</sup>
Age, years	1.05	0.98 - 1.12	0.13
LV <sup>1</sup> Mass index, g/m <sup>2</sup>	1.04	0.98 - 1.11	0.15
LV Ejection Fraction, %	0.82	0.68 - 0.99	0.04
RV <sup>2</sup> Ejection Fraction, %	1.10	0.96 - 1.27	0.17
eGFR <sup>3</sup> , mL/min/1.73 m <sup>2</sup> (median) (range)	1.02	0.98 - 1.10	0.17
Diabetes Mellitus	2.14	0.77 - 5.93	0.15
BMI <sup>4</sup> , kg/m <sup>2</sup> (mean ± SD)	0.82	0.61 - 1.09	0.18
Negative Value BOLD SI <sup>5</sup> Change	19.48	1.28 - 295.44	0.03

All data are presented as mean ± SD.

<sup>1</sup>LV indicates Left Ventricle; <sup>2</sup>RV, Right Ventricle; <sup>3</sup>eGFR, estimated Glomerular Filtration Rate; <sup>4</sup>BMI, body mass index; <sup>5</sup>BOLD SI, Blood Oxygen Level Dependent Signal Intensity; <sup>6</sup>Assessed using Cox regression analysis.

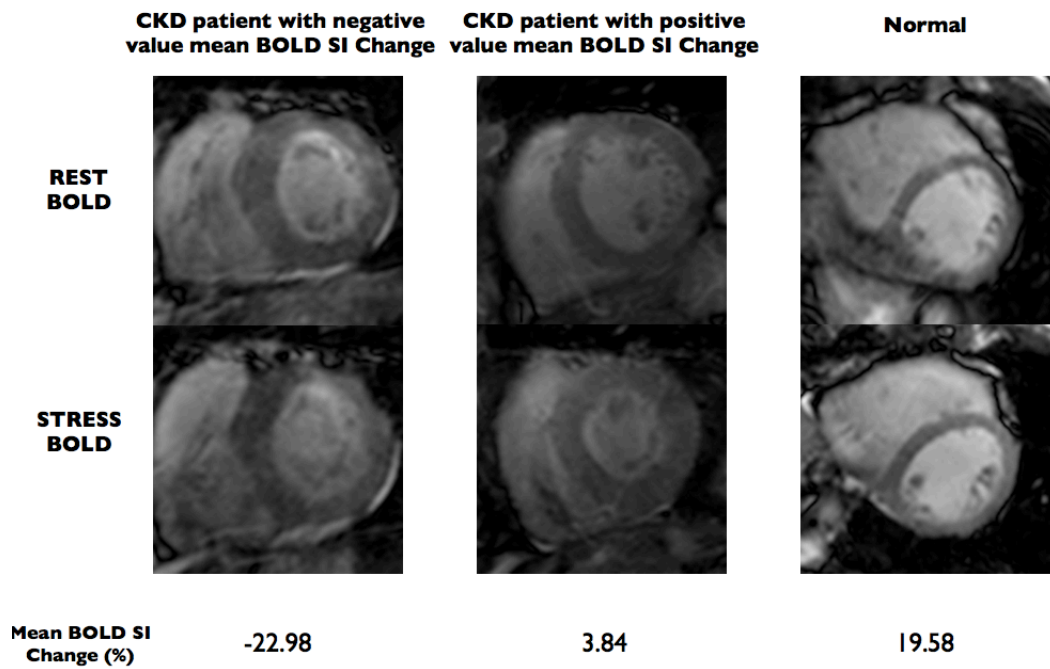


Figure 7.1 Examples of BOLD images at rest and during stress of a CKD patient with negative BOLD Signal Intensity (SI) Change value who had significant adverse cardiac event (left), a CKD patient with positive BOLD SI Change (middle), and a normal volunteer without history of kidney disease (right).

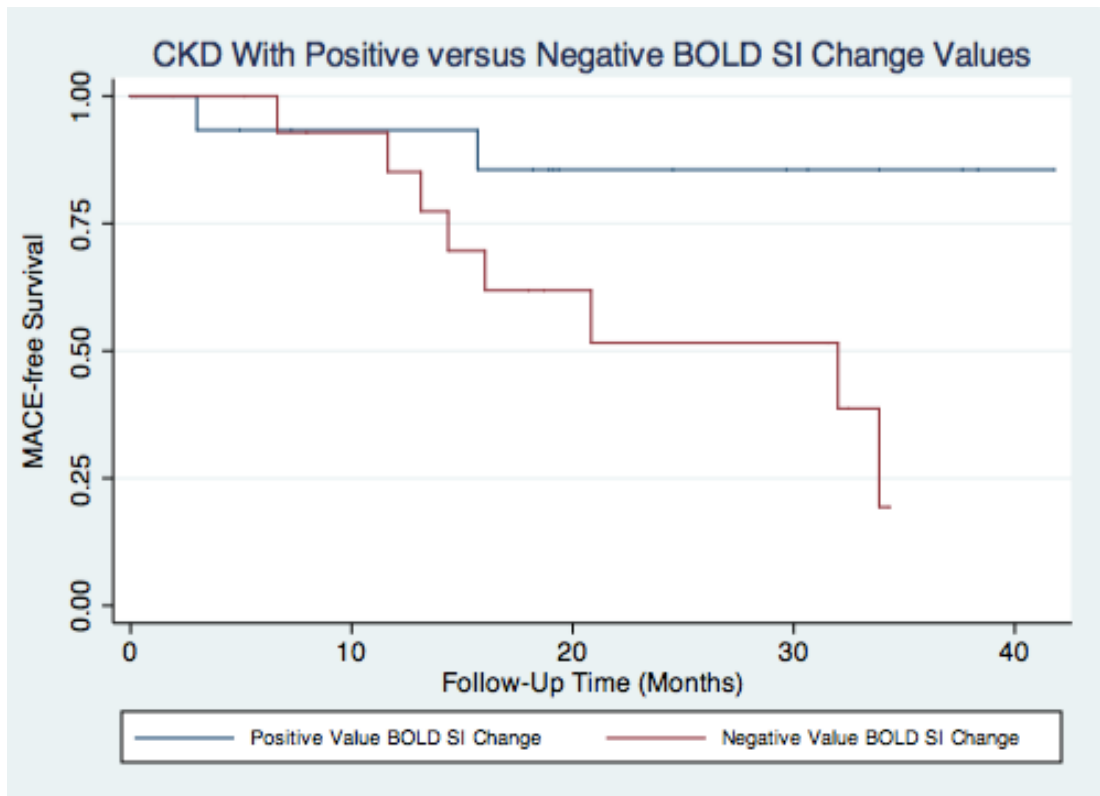


Figure 7.2 Kaplan-Meier survival graph showing CKD with negative BOLD Signal Intensity (SI) Change Values had significantly higher major adverse cardiac events (MACE) rate compared to CKD with positive BOLD Signal Intensity (SI) Change Values (p= 0.03).

## **CHAPTER 8 - Conclusion**

This thesis study provided a better understanding of the cardiac phenotype of the CKD and post-renal transplant patients, which previously were not well-defined. The thesis proposed a non-invasive diagnostic imaging that is safe and potentially can predict prognosis. Furthermore, this thesis demonstrates there is probably a complex interplay of post-transplant factors and/or immunosuppressants causing microvascular ischaemia. Although asymptomatic, myocardial ischaemia and microvascular coronary disease are very important in the CKD and renal transplant patients and may explain their poor cardiac prognosis.

### **8.1 Myocardial Oxygenation Response to Stress in Chronic Kidney Disease Patients**

Although cardiovascular disease is a major cause of mortality in the CKD population, the current cardiac stress investigations are not sensitive and have high false negative rates. Chapter 3 aimed to utilise non-contrast BOLD CMR to assess myocardial oxygenation response to stress as a measure of ischaemia in CKD patients asymptomatic of cardiac disease and without previously known cardiac disease. Our study was the first to demonstrate impaired myocardial oxygenation response to stress in CKD and renal transplant patients irrespective of the degree of LVH, myocardial fibrosis and the presence of diabetes mellitus. We found that the BOLD Signal Intensity Change correlated with the degree of renal impairment, but not with the degree of anaemia.

Chapter 4 evaluated the coronary artery anatomy of the CKD and renal transplant patients using non-contrast whole-heart MRCA. We found that there was a dissociation between myocardial oxygenation and coronary stenosis.

Blunted myocardial oxygenation response to stress with negative BOLD Signal Intensity values has previously been shown to correlate with a severe degree of coronary stenosis. Our study in Chapter 7 indicates that negative value BOLD Signal Intensity may relate to poorer prognosis. Although there are limitations with the current BOLD sequences, the BOLD literature does not stop and the techniques are evolving.

## **8.2 Myocardial Perfusion in Renal Transplant Recipients**

Although renal transplantation significantly improved mortality in end-stage renal disease patients, cardiovascular disease is still a major cause of mortality post transplant. Cardiac phenotypes of renal transplant recipients are not well-defined. Chapter 5 examined the utility of stress perfusion CMR and MRCA in the post renal transplant recipients, asymptomatic of cardiac disease, with no known cardiac disease and no significant epicardial CAD pre-transplant. We compared the renal transplant recipients with hypertensive controls to control for the degree of LVH and with liver transplant recipients with no prior history of CKD to investigate whether this was post transplant or previous CKD effect. We demonstrated that renal transplant recipients had impaired myocardial perfusion reserve independent of the degree of left ventricular hypertrophy or the presence of diabetes mellitus. We further evaluated the degree of epicardial CAD with MRCA, and did not find significant association between myocardial perfusion and epicardial CAD in the post-transplant recipients, thus likely due to underlying microvascular disease. We showed that the liver transplant recipients without prior history of CKD had a similar degree of impaired myocardial perfusion and coronary disease to the renal transplant recipients, despite the relatively low prevalence of CAD in pre-transplant chronic liver disease compared to CKD patients. The reasons are unclear, perhaps a complex interplay of transplant milieu factors and/or immunosuppressants, and requiring further research in liver transplant patients.

Chapter 6 showed no association between myocardial perfusion reserve and central aortic stiffness examined by aortic pulse wave velocity in the renal transplant recipients as compared to controls with similar degree of hypertension. In our renal transplant cohort, the subendocardial MPRI was lower than the subepicardial MPRI, which might indicate small distal vessel endothelial dysfunction rather than large vessel aortic dysfunction as a possible mechanism. Both cyclosporine and tacrolimus may induce coronary vasoconstriction or spasm in a similar way to vasoconstriction of the afferent and efferent glomerular arterioles, and it may explain our finding of reduced myocardial perfusion reserve, independent of changes in aortic stiffness.

## **CHAPTER 9 - Future Directions**

Utility of stress CMR in the CKD and post renal transplant population detects inducible myocardial ischaemia from epicardial and microvascular coronary artery disease, which both reduce survival. Non-contrast BOLD CMR is promising to detect future events in patients with underlying CKD. Our pilot study may assist in primary prevention and management of silent ischaemia from microvascular disease. Recently, myocardial oxygenation response to breathing manoeuvres [203] and controlled vasodilatory carbon dioxide delivery through hypercapnia [204] have been described, and may be able to offer more comfortable option of BOLD CMR in CKD patients, however, further research is indicated. BOLD techniques are constantly evolving. The new approach of cardiac phase-resolved BOLD (CP-BOLD) potentially may enable assessment of myocardial ischaemia completely at rest [205].

Our pilot study needs to be confirmed in larger, multi-centre studies. Non-contrast T1 mapping studies may assist in detecting diffuse fibrosis in the CKD population, however this technique needs to be well-validated in multi-centre trials and multi-software applications. BOLD CMR technique needs to be improved to minimise frequency artifacts. Larger studies examining individual immunosuppressants

potentially can be challenging given most transplant recipients are taking more than one immunosuppressive therapy. Multi-centre randomised controlled trials are needed to examine the short-term and long-term outcome of medical versus revascularisation therapy in the renal population with silent myocardial ischaemia.

## References

1. *Cardiovascular disease: Australia facts 2011*, 2011, AIHW.
2. *ANZDATA Annual Report 2013*.
3. Tonelli, M., et al., *Chronic kidney disease and mortality risk: a systematic review*. *J Am Soc Nephrol*, 2006. **17**(7): p. 2034-47.
4. Sarnak, M.J., et al., *Kidney disease as a risk factor for development of cardiovascular disease: a statement from the American Heart Association Councils on Kidney in Cardiovascular Disease, High Blood Pressure Research, Clinical Cardiology, and Epidemiology and Prevention*. *Circulation*, 2003. **108**(17): p. 2154-69.
5. Gansevoort, R.T., et al., *Chronic kidney disease and cardiovascular risk: epidemiology, mechanisms, and prevention*. *Lancet*, 2013. **382**(9889): p. 339-52.
6. *K/DOQI clinical practice guidelines for chronic kidney disease: evaluation, classification, and stratification*. *Am J Kidney Dis*, 2002. **39**(2 Suppl 1): p. S1-266.
7. Sharples, E.J., et al., *Coronary artery calcification measured with electron-beam computerized tomography correlates poorly with coronary artery angiography in dialysis patients*. *Am J Kidney Dis*, 2004. **43**(2): p. 313-9.
8. Joosen, I.A., et al., *Relation between Mild to Moderate Chronic Kidney Disease and Coronary Artery Disease Determined with Coronary CT Angiography*. *PLoS One*, 2012. **7**(10): p. e47267.
9. Matsushita, K., et al., *Association of estimated glomerular filtration rate and albuminuria with all-cause and cardiovascular mortality in general population cohorts: a collaborative meta-analysis*. *Lancet*, 2010. **375**(9731): p. 2073-81.
10. Manjunath, G., et al., *Level of kidney function as a risk factor for atherosclerotic cardiovascular outcomes in the community*. *J Am Coll Cardiol*, 2003. **41**(1): p. 47-55.

11. Stack, A.G. and W.E. Bloembergen, *Prevalence and clinical correlates of coronary artery disease among new dialysis patients in the United States: a cross-sectional study*. J Am Soc Nephrol, 2001. **12**(7): p. 1516-23.
12. Henry, R.M., et al., *Mild renal insufficiency is associated with increased cardiovascular mortality: The Hoorn Study*. Kidney Int, 2002. **62**(4): p. 1402-7.
13. Goodman, W.G., et al., *Coronary-artery calcification in young adults with end-stage renal disease who are undergoing dialysis*. N Engl J Med, 2000. **342**(20): p. 1478-83.
14. Ohtake, T., et al., *High prevalence of occult coronary artery stenosis in patients with chronic kidney disease at the initiation of renal replacement therapy: an angiographic examination*. J Am Soc Nephrol, 2005. **16**(4): p. 1141-8.
15. Hase, H., et al., *Risk factors for de novo acute cardiac events in patients initiating hemodialysis with no previous cardiac symptom*. Kidney Int, 2006. **70**(6): p. 1142-8.
16. Cho, I., et al., *Coronary atherosclerosis detected by coronary CT angiography in asymptomatic subjects with early chronic kidney disease*. Atherosclerosis, 2010. **208**(2): p. 406-11.
17. Kawai, H., et al., *Coronary plaque characteristics in patients with mild chronic kidney disease. Analysis by 320-row area detector computed tomography*. Circ J, 2012. **76**(6): p. 1436-41.
18. Charytan, D.M., H.R. Shelbert, and M.F. Di Carli, *Coronary microvascular function in early chronic kidney disease*. Circ Cardiovasc Imaging, 2010. **3**(6): p. 663-71.
19. Chade, A.R., et al., *Mild renal insufficiency is associated with reduced coronary flow in patients with non-obstructive coronary artery disease*. Kidney Int, 2006. **69**(2): p. 266-71.
20. Lin, T., et al., *Reduced survival in patients with "coronary microvascular disease"*. Int J Angiol, 2012. **21**(2): p. 89-94.

21. Foley, R.N., P.S. Parfrey, and M.J. Sarnak, *Epidemiology of cardiovascular disease in chronic renal disease*. J Am Soc Nephrol, 1998. **9**(12 Suppl): p. S16-23.
22. Levin, A., et al., *Prevalent left ventricular hypertrophy in the predialysis population: identifying opportunities for intervention*. Am J Kidney Dis, 1996. **27**(3): p. 347-54.
23. Zoccali, C., et al., *Prognostic impact of the indexation of left ventricular mass in patients undergoing dialysis*. J Am Soc Nephrol, 2001. **12**(12): p. 2768-74.
24. Kahwaji, J., et al., *Cause of death with graft function among renal transplant recipients in an integrated healthcare system*. Transplantation, 2011. **91**(2): p. 225-30.
25. Ojo, A.O., *Cardiovascular complications after renal transplantation and their prevention*. Transplantation, 2006. **82**(5): p. 603-11.
26. Dimeny, E.M., *Cardiovascular disease after renal transplantation*. Kidney Int Suppl, 2002(80): p. 78-84.
27. *ANZDATA Annual Report 2011*. Available from: [www.anzdata.org.au](http://www.anzdata.org.au).
28. Nanmoku, K., et al., *Clinical characteristics and outcomes of renal transplantation in elderly recipients*. Transplant Proc, 2012. **44**(1): p. 281-3.
29. Rigatto, C., et al., *Congestive heart failure in renal transplant recipients: risk factors, outcomes, and relationship with ischemic heart disease*. J Am Soc Nephrol, 2002. **13**(4): p. 1084-90.
30. Marcassi, A.P., et al., *Ventricular arrhythmia in incident kidney transplant recipients: prevalence and associated factors*. Transpl Int, 2011. **24**(1): p. 67-72.
31. Boots, J.M., M.H. Christiaans, and J.P. van Hooff, *Effect of immunosuppressive agents on long-term survival of renal transplant recipients: focus on the cardiovascular risk*. Drugs, 2004. **64**(18): p. 2047-73.
32. Lang, P., A. Pardon, and V. Audard, *Long-term benefit of mycophenolate mofetil in renal transplantation*. Transplantation, 2005. **79**(3 Suppl): p. S47-8.
33. Borrows, R., et al., *Anaemia and congestive heart failure early post-renal transplantation*. Nephrol Dial Transplant, 2008. **23**(5): p. 1728-34.

34. Chueh, S.C. and B.D. Kahan, *Dyslipidemia in renal transplant recipients treated with a sirolimus and cyclosporine-based immunosuppressive regimen: incidence, risk factors, progression, and prognosis*. *Transplantation*, 2003. **76**(2): p. 375-82.
35. First, M.R., et al., *Hypertension after renal transplantation*. *J Am Soc Nephrol*, 1994. **4**(8 Suppl): p. S30-6.
36. Burdmann, E.A., et al., *Cyclosporine nephrotoxicity*. *Semin Nephrol*, 2003. **23**(5): p. 465-76.
37. Ruggenenti, P., et al., *Calcium channel blockers protect transplant patients from cyclosporine-induced daily renal hypoperfusion*. *Kidney Int*, 1993. **43**(3): p. 706-11.
38. Lipkin, G.W., et al., *Ambulatory blood pressure and left ventricular mass in cyclosporin- and non-cyclosporin-treated renal transplant recipients*. *J Hypertens*, 1993. **11**(4): p. 439-42.
39. Pirsch, J.D., et al., *A comparison of tacrolimus (FK506) and cyclosporine for immunosuppression after cadaveric renal transplantation*. *FK506 Kidney Transplant Study Group*. *Transplantation*, 1997. **63**(7): p. 977-83.
40. Ekberg, H., et al., *Reduced exposure to calcineurin inhibitors in renal transplantation*. *N Engl J Med*, 2007. **357**(25): p. 2562-75.
41. Margreiter, R., *Efficacy and safety of tacrolimus compared with ciclosporin microemulsion in renal transplantation: a randomised multicentre study*. *Lancet*, 2002. **359**(9308): p. 741-6.
42. Ahsan, N., et al., *Randomized trial of tacrolimus plus mycophenolate mofetil or azathioprine versus cyclosporine oral solution (modified) plus mycophenolate mofetil after cadaveric kidney transplantation: results at 2 years*. *Transplantation*, 2001. **72**(2): p. 245-50.
43. Johnson, C., et al., *Randomized trial of tacrolimus (Prograf) in combination with azathioprine or mycophenolate mofetil versus cyclosporine (Neoral) with mycophenolate mofetil after cadaveric kidney transplantation*. *Transplantation*, 2000. **69**(5): p. 834-41.
44. Tory, R., et al., *Tacrolimus-induced elevation in plasma triglyceride concentrations after administration to renal transplant patients is partially*

- due to a decrease in lipoprotein lipase activity and plasma concentrations.* Transplantation, 2009. **88**(1): p. 62-8.
45. Chang, R.K., et al., *Marked left ventricular hypertrophy in children on tacrolimus (FK506) after orthotopic liver transplantation.* Am J Cardiol, 1998. **81**(10): p. 1277-80.
  46. Euvrard, S., et al., *Sirolimus and secondary skin-cancer prevention in kidney transplantation.* N Engl J Med, 2012. **367**(4): p. 329-39.
  47. Morice, M.C., et al., *A randomized comparison of a sirolimus-eluting stent with a standard stent for coronary revascularization.* N Engl J Med, 2002. **346**(23): p. 1773-80.
  48. Serruys, P.W., et al., *Intravascular ultrasound findings in the multicenter, randomized, double-blind RAVEL (RAnomized study with the sirolimus-eluting VElocity balloon-expandable stent in the treatment of patients with de novo native coronary artery Lesions) trial.* Circulation, 2002. **106**(7): p. 798-803.
  49. Webster, A.C., et al., *Target of rapamycin inhibitors (TOR-I; sirolimus and everolimus) for primary immunosuppression in kidney transplant recipients.* Cochrane Database Syst Rev, 2006(2): p. CD004290.
  50. Levy, G., et al., *Safety, tolerability, and efficacy of everolimus in de novo liver transplant recipients: 12- and 36-month results.* Liver Transpl, 2006. **12**(11): p. 1640-8.
  51. Gurk-Turner, C., W. Manitpisitkul, and M. Cooper, *A comprehensive review of everolimus clinical reports: a new mammalian target of rapamycin inhibitor.* Transplantation, 2012. **94**(7): p. 659-68.
  52. Gianrossi, R., et al., *Exercise-induced ST depression in the diagnosis of coronary artery disease. A meta-analysis.* Circulation, 1989. **80**(1): p. 87-98.
  53. Sharma, R., et al., *Dobutamine stress echocardiography and the resting but not exercise electrocardiograph predict severe coronary artery disease in renal transplant candidates.* Nephrol Dial Transplant, 2005. **20**(10): p. 2207-14.

54. Schmidt, A., et al., *Informational contribution of noninvasive screening tests for coronary artery disease in patients on chronic renal replacement therapy*. Am J Kidney Dis, 2001. **37**(1): p. 56-63.
55. Howden, E.J., et al., *Cardiorespiratory fitness and cardiovascular burden in chronic kidney disease*. J Sci Med Sport, 2014.
56. Banerjee, A., et al., *Diagnostic accuracy of exercise stress testing for coronary artery disease: a systematic review and meta-analysis of prospective studies*. Int J Clin Pract, 2012. **66**(5): p. 477-92.
57. Armstrong, W.F. and W.A. Zoghbi, *Stress echocardiography: current methodology and clinical applications*. J Am Coll Cardiol, 2005. **45**(11): p. 1739-47.
58. Nakanishi, K., et al., *Prognostic value of coronary flow reserve on long-term cardiovascular outcomes in patients with chronic kidney disease*. Am J Cardiol, 2013. **112**(7): p. 928-32.
59. Picano, E., S. Molinaro, and E. Pasanisi, *The diagnostic accuracy of pharmacological stress echocardiography for the assessment of coronary artery disease: a meta-analysis*. Cardiovasc Ultrasound, 2008. **6**: p. 30.
60. Wang, L.W., et al., *Cardiac testing for coronary artery disease in potential kidney transplant recipients: a systematic review of test accuracy studies*. Am J Kidney Dis, 2011. **57**(3): p. 476-87.
61. Tita, C., et al., *Stress echocardiography for risk stratification in patients with end-stage renal disease undergoing renal transplantation*. J Am Soc Echocardiogr, 2008. **21**(4): p. 321-6.
62. Bergeron, S., et al., *Prognostic value of dobutamine stress echocardiography in patients with chronic kidney disease*. Am Heart J, 2007. **153**(3): p. 385-91.
63. Herzog, C.A., et al., *Dobutamine stress echocardiography for the detection of significant coronary artery disease in renal transplant candidates*. Am J Kidney Dis, 1999. **33**(6): p. 1080-90.
64. Marwick, T.H., et al., *Use of dobutamine echocardiography for cardiac risk stratification of patients with chronic renal failure*. J Intern Med, 1998. **244**(2): p. 155-61.

65. Makani, H., et al., *Cardiac outcomes with submaximal normal stress echocardiography: a meta-analysis*. J Am Coll Cardiol, 2012. **60**(15): p. 1393-401.
66. Salerno, M. and G.A. Beller, *Noninvasive assessment of myocardial perfusion*. Circ Cardiovasc Imaging, 2009. **2**(5): p. 412-24.
67. De Vriese, A.S., et al., *Should we screen for coronary artery disease in asymptomatic chronic dialysis patients?* Kidney Int, 2012. **81**(2): p. 143-51.
68. Bourque, J.M. and G.A. Beller, *Stress myocardial perfusion imaging for assessing prognosis: an update*. JACC Cardiovasc Imaging, 2011. **4**(12): p. 1305-19.
69. Lima, R.S., et al., *Incremental value of combined perfusion and function over perfusion alone by gated SPECT myocardial perfusion imaging for detection of severe three-vessel coronary artery disease*. J Am Coll Cardiol, 2003. **42**(1): p. 64-70.
70. Furuhashi, T., et al., *Prediction of cardiovascular events in pre-dialysis chronic kidney disease patients with normal SPECT myocardial perfusion imaging*. J Cardiol, 2014. **63**(2): p. 154-8.
71. Hakeem, A., et al., *Predictive value of myocardial perfusion single-photon emission computed tomography and the impact of renal function on cardiac death*. Circulation, 2008. **118**(24): p. 2540-9.
72. Wang, L.W., et al., *Prognostic Value of Cardiac Tests in Potential Kidney Transplant Recipients: A Systematic Review*. Transplantation, 2015. **99**(4): p. 731-745.
73. Fukushima, K., et al., *Impaired global myocardial flow dynamics despite normal left ventricular function and regional perfusion in chronic kidney disease: a quantitative analysis of clinical <sup>82</sup>Rb PET/CT studies*. J Nucl Med, 2012. **53**(6): p. 887-93.
74. Koivuviita, N., et al., *Increased basal myocardial perfusion in patients with chronic kidney disease without symptomatic coronary artery disease*. Nephrol Dial Transplant, 2009. **24**(9): p. 2773-9.
75. Joki, N., et al., *Myocardial perfusion imaging for predicting cardiac events in Japanese patients with advanced chronic kidney disease: 1-year interim*

- report of the J-ACCESS 3 investigation. Eur J Nucl Med Mol Imaging, 2014. 41(9): p. 1701-9.*
76. Bhatti, S., et al., *Prognostic value of regadenoson myocardial single-photon emission computed tomography in patients with different degrees of renal dysfunction. Eur Heart J Cardiovasc Imaging, 2014. 15(8): p. 933-40.*
  77. Yoda, S., et al., *Risk stratification of cardiovascular events in patients at all stages of chronic kidney disease using myocardial perfusion SPECT. J Cardiol, 2012. 60(5): p. 377-82.*
  78. Okuyama, C., et al., *Incremental prognostic value of myocardial perfusion single photon emission computed tomography for patients with diabetes and chronic kidney disease. Nucl Med Commun, 2011. 32(10): p. 913-9.*
  79. Al-Mallah, M.H., et al., *Incremental prognostic value of myocardial perfusion imaging in patients referred to stress single-photon emission computed tomography with renal dysfunction. Circ Cardiovasc Imaging, 2009. 2(6): p. 429-36.*
  80. Hatta, T., S. Nishimura, and T. Nishimura, *Prognostic risk stratification of myocardial ischaemia evaluated by gated myocardial perfusion SPECT in patients with chronic kidney disease. Eur J Nucl Med Mol Imaging, 2009. 36(11): p. 1835-41.*
  81. Momose, M., et al., *Prognostic significance of stress myocardial ECG-gated perfusion imaging in asymptomatic patients with diabetic chronic kidney disease on initiation of haemodialysis. Eur J Nucl Med Mol Imaging, 2009. 36(8): p. 1315-21.*
  82. Rabbat, C.G., et al., *Prognostic value of myocardial perfusion studies in patients with end-stage renal disease assessed for kidney or kidney-pancreas transplantation: a meta-analysis. J Am Soc Nephrol, 2003. 14(2): p. 431-9.*
  83. Hage, F.G., et al., *The prognostic value of the heart rate response to adenosine in relation to diabetes mellitus and chronic kidney disease. Am Heart J, 2011. 162(2): p. 356-62.*
  84. Hage, F.G., et al., *A blunted heart rate response to regadenoson is an independent prognostic indicator in patients undergoing myocardial perfusion imaging. J Nucl Cardiol, 2011. 18(6): p. 1086-94.*

85. Venkataraman, R., et al., *Relation between heart rate response to adenosine and mortality in patients with end-stage renal disease*. Am J Cardiol, 2009. **103**(8): p. 1159-64.
86. Saxena, S.K., et al., *Nephrogenic systemic fibrosis: an emerging entity*. Int Urol Nephrol, 2008. **40**(3): p. 715-24.
87. Rydahl, C., H.S. Thomsen, and P. Marckmann, *High prevalence of nephrogenic systemic fibrosis in chronic renal failure patients exposed to gadodiamide, a gadolinium-containing magnetic resonance contrast agent*. Invest Radiol, 2008. **43**(2): p. 141-4.
88. Othersen, J.B., et al., *Nephrogenic systemic fibrosis after exposure to gadolinium in patients with renal failure*. Nephrol Dial Transplant, 2007. **22**(11): p. 3179-85.
89. Malatesta-Muncher, R., et al., *Early cardiac dysfunction in pediatric patients on maintenance dialysis and post kidney transplant*. Pediatr Nephrol, 2012. **27**(7): p. 1157-64.
90. Ripley, D.P., et al., *Safety and feasibility of dobutamine stress cardiac magnetic resonance for cardiovascular assessment prior to renal transplantation*. J Cardiovasc Med (Hagerstown), 2014. **15**(4): p. 288-94.
91. Karamitsos, T.D., et al., *Patients with syndrome X have normal transmural myocardial perfusion and oxygenation: a 3-T cardiovascular magnetic resonance imaging study*. Circ Cardiovasc Imaging, 2012. **5**(2): p. 194-200.
92. Karamitsos, T.D., et al., *Relationship between regional myocardial oxygenation and perfusion in patients with coronary artery disease: insights from cardiovascular magnetic resonance and positron emission tomography*. Circ Cardiovasc Imaging, 2010. **3**(1): p. 32-40.
93. Wacker, C.M., et al., *Susceptibility-sensitive magnetic resonance imaging detects human myocardium supplied by a stenotic coronary artery without a contrast agent*. J Am Coll Cardiol, 2003. **41**(5): p. 834-40.
94. Friedrich, M.G., et al., *Blood oxygen level-dependent magnetic resonance imaging in patients with stress-induced angina*. Circulation, 2003. **108**(18): p. 2219-23.

95. Beache, G.M., et al., *Attenuated myocardial vasodilator response in patients with hypertensive hypertrophy revealed by oxygenation-dependent magnetic resonance imaging*. *Circulation*, 2001. **104**(11): p. 1214-7.
96. Karamitsos, T.D., et al., *Blunted myocardial oxygenation response during vasodilator stress in patients with hypertrophic cardiomyopathy*. *J Am Coll Cardiol*, 2013. **61**(11): p. 1169-76.
97. Mahmood, M., et al., *Myocardial perfusion and oxygenation are impaired during stress in severe aortic stenosis and correlate with impaired energetics and subclinical left ventricular dysfunction*. *J Cardiovasc Magn Reson*, 2014. **16**: p. 29.
98. Wilson, R.F., et al., *Effects of adenosine on human coronary arterial circulation*. *Circulation*, 1990. **82**(5): p. 1595-606.
99. Karamitsos, T.D., et al., *Ischemic heart disease: comprehensive evaluation by cardiovascular magnetic resonance*. *Am Heart J*, 2011. **162**(1): p. 16-30.
100. Gerber, B.L., et al., *Myocardial first-pass perfusion cardiovascular magnetic resonance: history, theory, and current state of the art*. *J Cardiovasc Magn Reson*, 2008. **10**: p. 18.
101. Hamon, M., et al., *Meta-analysis of the diagnostic performance of stress perfusion cardiovascular magnetic resonance for detection of coronary artery disease*. *J Cardiovasc Magn Reson*, 2010. **12**(1): p. 29.
102. Nandalur, K.R., et al., *Diagnostic performance of stress cardiac magnetic resonance imaging in the detection of coronary artery disease: a meta-analysis*. *J Am Coll Cardiol*, 2007. **50**(14): p. 1343-53.
103. Greenwood, J.P., et al., *Cardiovascular magnetic resonance and single-photon emission computed tomography for diagnosis of coronary heart disease (CE-MARC): a prospective trial*. *Lancet*, 2012. **379**(9814): p. 453-60.
104. Schwitter, J., et al., *MR-IMPACT II: Magnetic Resonance Imaging for Myocardial Perfusion Assessment in Coronary artery disease Trial: perfusion-cardiac magnetic resonance vs. single-photon emission computed tomography for the detection of coronary artery disease: a comparative multicentre, multivendor trial*. *Eur Heart J*, 2012.

105. Desai, R.R. and S. Jha, *Diagnostic performance of cardiac stress perfusion MRI in the detection of coronary artery disease using fractional flow reserve as the reference standard: a meta-analysis*. AJR Am J Roentgenol, 2013. **201**(2): p. W245-52.
106. Lockie, T., et al., *High-resolution magnetic resonance myocardial perfusion imaging at 3.0-Tesla to detect hemodynamically significant coronary stenoses as determined by fractional flow reserve*. J Am Coll Cardiol, 2011. **57**(1): p. 70-5.
107. Costa, M.A., et al., *Quantitative magnetic resonance perfusion imaging detects anatomic and physiologic coronary artery disease as measured by coronary angiography and fractional flow reserve*. J Am Coll Cardiol, 2007. **50**(6): p. 514-22.
108. Panting, J.R., et al., *Abnormal subendocardial perfusion in cardiac syndrome X detected by cardiovascular magnetic resonance imaging*. N Engl J Med, 2002. **346**(25): p. 1948-53.
109. Chung, S.Y., et al., *Comparison of stress perfusion MRI and SPECT for detection of myocardial ischemia in patients with angiographically proven three-vessel coronary artery disease*. AJR Am J Roentgenol, 2010. **195**(2): p. 356-62.
110. Chih, S., et al., *Reproducibility of adenosine stress cardiovascular magnetic resonance in multi-vessel symptomatic coronary artery disease*. J Cardiovasc Magn Reson, 2010. **12**: p. 42.
111. Lo, K.Y., et al., *Prognostic value of adenosine stress myocardial perfusion by cardiac magnetic resonance imaging in patients with known or suspected coronary artery disease*. QJM, 2011. **104**(5): p. 425-32.
112. Korosoglou, G., et al., *Prognostic value of high-dose dobutamine stress magnetic resonance imaging in 1,493 consecutive patients: assessment of myocardial wall motion and perfusion*. J Am Coll Cardiol, 2010. **56**(15): p. 1225-34.
113. Bodi, V., et al., *Prognostic and therapeutic implications of dipyridamole stress cardiovascular magnetic resonance on the basis of the ischaemic cascade*. Heart, 2009. **95**(1): p. 49-55.

114. Jahnke, C., et al., *Prognostic value of cardiac magnetic resonance stress tests: adenosine stress perfusion and dobutamine stress wall motion imaging*. *Circulation*, 2007. **115**(13): p. 1769-76.
115. Pilz, G., et al., *Negative predictive value of normal adenosine-stress cardiac MRI in the assessment of coronary artery disease and correlation with semiquantitative perfusion analysis*. *J Magn Reson Imaging*, 2010. **32**(3): p. 615-21.
116. Lubbers, D.D., et al., *Performance of adenosine "stress-only" perfusion MRI in patients without a history of myocardial infarction: a clinical outcome study*. *Int J Cardiovasc Imaging*, 2012. **28**(1): p. 109-15.
117. Karamitsos, T.D., et al., *Tolerance and safety of adenosine stress perfusion cardiovascular magnetic resonance imaging in patients with severe coronary artery disease*. *Int J Cardiovasc Imaging*, 2009. **25**(3): p. 277-83.
118. Patel, A.R., et al., *Assessment of advanced coronary artery disease: advantages of quantitative cardiac magnetic resonance perfusion analysis*. *J Am Coll Cardiol*, 2010. **56**(7): p. 561-9.
119. Huber, A., et al., *Magnetic resonance perfusion of the myocardium: semiquantitative and quantitative evaluation in comparison with coronary angiography and fractional flow reserve*. *Invest Radiol*, 2012. **47**(6): p. 332-8.
120. Heer, T., et al., *Diagnostic performance of non-contrast-enhanced whole-heart magnetic resonance coronary angiography in combination with adenosine stress perfusion cardiac magnetic resonance imaging*. *Am Heart J*, 2013. **166**(6): p. 999-1009.
121. Bettencourt, N., et al., *Additive value of magnetic resonance coronary angiography in a comprehensive cardiac magnetic resonance stress-rest protocol for detection of functionally significant coronary artery disease: a pilot study*. *Circ Cardiovasc Imaging*, 2013. **6**(5): p. 730-8.
122. Anderson, L.J., et al., *Cardiovascular T2-star (T2\*) magnetic resonance for the early diagnosis of myocardial iron overload*. *Eur Heart J*, 2001. **22**(23): p. 2171-9.

123. Zheng, J., et al., *Dynamic estimation of the myocardial oxygen extraction ratio during dipyridamole stress by MRI: a preliminary study in canines*. Magn Reson Med, 2004. **51**(4): p. 718-26.
124. Vohringer, M., et al., *Oxygenation-sensitive CMR for assessing vasodilator-induced changes of myocardial oxygenation*. J Cardiovasc Magn Reson, 2010. **12**: p. 20.
125. McCommis, K.S., et al., *Myocardial blood volume is associated with myocardial oxygen consumption: an experimental study with cardiac magnetic resonance in a canine model*. JACC Cardiovasc Imaging, 2009. **2**(11): p. 1313-20.
126. McCommis, K.S., et al., *Quantification of regional myocardial oxygenation by magnetic resonance imaging: validation with positron emission tomography*. Circ Cardiovasc Imaging, 2010. **3**(1): p. 41-6.
127. Reeder, S.B., et al., *Simultaneous noninvasive determination of regional myocardial perfusion and oxygen content in rabbits: toward direct measurement of myocardial oxygen consumption at MR imaging*. Radiology, 1999. **212**(3): p. 739-47.
128. Shea, S.M., et al., *T2-prepared steady-state free precession blood oxygen level-dependent MR imaging of myocardial perfusion in a dog stenosis model*. Radiology, 2005. **236**(2): p. 503-9.
129. Foltz, W.D., et al., *Vasodilator response assessment in porcine myocardium with magnetic resonance relaxometry*. Circulation, 2002. **106**(21): p. 2714-9.
130. Fieno, D.S., et al., *Myocardial perfusion imaging based on the blood oxygen level-dependent effect using T2-prepared steady-state free-precession magnetic resonance imaging*. Circulation, 2004. **110**(10): p. 1284-90.
131. Dharmakumar, R., et al., *Assessment of regional myocardial oxygenation changes in the presence of coronary artery stenosis with balanced SSFP imaging at 3.0 T: theory and experimental evaluation in canines*. J Magn Reson Imaging, 2008. **27**(5): p. 1037-45.
132. Wacker, C.M., et al., *BOLD-MRI in ten patients with coronary artery disease: evidence for imaging of capillary recruitment in myocardium supplied by the stenotic artery*. MAGMA, 1999. **8**(1): p. 48-54.

133. Manka, R., et al., *BOLD cardiovascular magnetic resonance at 3.0 tesla in myocardial ischemia*. J Cardiovasc Magn Reson, 2010. **12**: p. 54.
134. Arnold, J.R., et al., *Myocardial oxygenation in coronary artery disease: insights from blood oxygen level-dependent magnetic resonance imaging at 3 tesla*. J Am Coll Cardiol, 2012. **59**(22): p. 1954-64.
135. Walcher, T., et al., *Myocardial perfusion reserve assessed by T2-prepared steady-state free precession blood oxygen level-dependent magnetic resonance imaging in comparison to fractional flow reserve*. Circ Cardiovasc Imaging, 2012. **5**(5): p. 580-6.
136. Mandapaka, S., R. D'Agostino, Jr., and W.G. Hundley, *Does late gadolinium enhancement predict cardiac events in patients with ischemic cardiomyopathy?* Circulation, 2006. **113**(23): p. 2676-8.
137. Vogel-Claussen, J., et al., *Delayed enhancement MR imaging: utility in myocardial assessment*. Radiographics, 2006. **26**(3): p. 795-810.
138. Saeed, M., et al., *Occlusive and reperfused myocardial infarcts: differentiation with Mn-DPDP--enhanced MR imaging*. Radiology, 1989. **172**(1): p. 59-64.
139. Sueyoshi, E., I. Sakamoto, and M. Uetani, *Myocardial delayed contrast-enhanced MRI: relationships between various enhancing patterns and myocardial diseases*. Br J Radiol, 2009. **82**(980): p. 691-7.
140. Wagner, A., et al., *Contrast-enhanced MRI and routine single photon emission computed tomography (SPECT) perfusion imaging for detection of subendocardial myocardial infarcts: an imaging study*. Lancet, 2003. **361**(9355): p. 374-9.
141. Dewey, M., et al., *Assessment of myocardial infarction in pigs using a rapid clearance blood pool contrast medium*. Magn Reson Med, 2004. **51**(4): p. 703-9.
142. Duan, X., et al., *Prognostic value of late gadolinium enhancement in dilated cardiomyopathy patients: a meta-analysis*. Clin Radiol, 2015. **70**(9): p. 999-1008.

143. Briasoulis, A., et al., *Myocardial fibrosis on cardiac magnetic resonance and cardiac outcomes in hypertrophic cardiomyopathy: a meta-analysis*. Heart, 2015. **101**(17): p. 1406-11.
144. Kwon, D.H., et al., *Extent of left ventricular scar predicts outcomes in ischemic cardiomyopathy patients with significantly reduced systolic function: a delayed hyperenhancement cardiac magnetic resonance study*. JACC Cardiovasc Imaging, 2009. **2**(1): p. 34-44.
145. Marcu, C.B., A.M. Beek, and A.C. Van Rossum, *Cardiovascular magnetic resonance imaging for the assessment of right heart involvement in cardiac and pulmonary disease*. Heart Lung Circ, 2006. **15**(6): p. 362-70.
146. Prince, M.R., et al., *Incidence of nephrogenic systemic fibrosis at two large medical centers*. Radiology, 2008. **248**(3): p. 807-16.
147. Golding, L.P. and J.M. Provenzale, *Nephrogenic systemic fibrosis: possible association with a predisposing infection*. AJR Am J Roentgenol, 2008. **190**(4): p. 1069-75.
148. *American College of Radiology - ACR Manual on Contrast Media*. 2015. **Version 10.1**.
149. Bose, C., et al., *Evidence Suggesting a Role of Iron in a Mouse Model of Nephrogenic Systemic Fibrosis*. PLoS One, 2015. **10**(8): p. e0136563.
150. Ferreira, V.M., et al., *Native T1-mapping detects the location, extent and patterns of acute myocarditis without the need for gadolinium contrast agents*. J Cardiovasc Magn Reson, 2014. **16**: p. 36.
151. Sakuma, H., et al., *Assessment of coronary arteries with total study time of less than 30 minutes by using whole-heart coronary MR angiography*. Radiology, 2005. **237**(1): p. 316-21.
152. Wittlinger, T., et al., *Assessment of coronary artery bypass grafts patency with different magnetic resonance technologies*. Eur J Cardiothorac Surg, 2006. **30**(3): p. 436-42.
153. Kato, S., et al., *Assessment of coronary artery disease using magnetic resonance coronary angiography: a national multicenter trial*. J Am Coll Cardiol, 2010. **56**(12): p. 983-91.

154. Flacke, S., et al., *Coronary aneurysms in Kawasaki's disease detected by magnetic resonance coronary angiography*. *Circulation*, 2000. **101**(14): p. E156-7.
155. Gharib, A.M., et al., *Coronary artery anomalies and variants: technical feasibility of assessment with coronary MR angiography at 3 T*. *Radiology*, 2008. **247**(1): p. 220-7.
156. Nunoda, S., et al., *Evaluation of cardiac allograft vasculopathy by multidetector computed tomography and whole-heart magnetic resonance coronary angiography*. *Circ J*, 2010. **74**(5): p. 946-53.
157. Uribe, S., et al., *Congenital heart disease in children: coronary MR angiography during systole and diastole with dual cardiac phase whole-heart imaging*. *Radiology*, 2011. **260**(1): p. 232-40.
158. Suzuki, A., et al., *Magnetic resonance coronary angiography to evaluate coronary arterial lesions in patients with Kawasaki disease*. *Cardiol Young*, 2006. **16**(6): p. 563-71.
159. Manning, W.J., et al., *Fat-suppressed breath-hold magnetic resonance coronary angiography*. *Circulation*, 1993. **87**(1): p. 94-104.
160. Botnar, R.M., et al., *Improved coronary artery definition with T2-weighted, free-breathing, three-dimensional coronary MRA*. *Circulation*, 1999. **99**(24): p. 3139-48.
161. Hofman, M.B., et al., *Blood pool agent strongly improves 3D magnetic resonance coronary angiography using an inversion pre-pulse*. *Magn Reson Med*, 1999. **41**(2): p. 360-7.
162. Deshpande, V.S., et al., *Comparison of gradient-echo and steady-state free precession for coronary artery magnetic resonance angiography using a gadolinium-based intravascular contrast agent*. *Invest Radiol*, 2006. **41**(3): p. 292-8.
163. Taylor, A.M., et al., *A comparison between segmented k-space FLASH and interleaved spiral MR coronary angiography sequences*. *J Magn Reson Imaging*, 2000. **11**(4): p. 394-400.

164. Barkhausen, J., et al., [*Comparison of gradient-echo and steady state free precession sequences for 3D-navigator MR angiography of coronary arteries*]. *Rofo*, 2002. **174**(6): p. 725-30.
165. Lai, P., et al., *A respiratory self-gating technique with 3D-translation compensation for free-breathing whole-heart coronary MRA*. *Magn Reson Med*, 2009. **62**(3): p. 731-8.
166. Roes, S.D., et al., *Correction for heart rate variability during 3D whole heart MR coronary angiography*. *J Magn Reson Imaging*, 2008. **27**(5): p. 1046-53.
167. Jin, H., et al., *3D coronary MR angiography at 1.5 T: Volume-targeted versus whole-heart acquisition*. *J Magn Reson Imaging*, 2013. **38**(3): p. 594-602.
168. Chang, S., et al., *3-T navigator parallel-imaging coronary MR angiography: targeted-volume versus whole-heart acquisition*. *AJR Am J Roentgenol*, 2008. **191**(1): p. 38-42.
169. Yang, Q., et al., *Contrast-enhanced whole-heart coronary magnetic resonance angiography at 3.0-T: a comparative study with X-ray angiography in a single center*. *J Am Coll Cardiol*, 2009. **54**(1): p. 69-76.
170. Nagata, M., et al., *Diagnostic accuracy of 1.5-T unenhanced whole-heart coronary MR angiography performed with 32-channel cardiac coils: initial single-center experience*. *Radiology*, 2011. **259**(2): p. 384-92.
171. Takemura, A., et al., [*The utility of coronary magnetic resonance angiography in children under six years of age with Kawasaki disease*]. *Nihon Hoshasen Gijutsu Gakkai Zasshi*, 2008. **64**(7): p. 874-6.
172. Casolo, G., et al., *Detection and assessment of coronary artery anomalies by three-dimensional magnetic resonance coronary angiography*. *Int J Cardiol*, 2005. **103**(3): p. 317-22.
173. Schuetz, G.M., et al., *Meta-analysis: noninvasive coronary angiography using computed tomography versus magnetic resonance imaging*. *Ann Intern Med*, 2010. **152**(3): p. 167-77.
174. Schuijff, J.D., et al., *Meta-analysis of comparative diagnostic performance of magnetic resonance imaging and multislice computed tomography for noninvasive coronary angiography*. *Am Heart J*, 2006. **151**(2): p. 404-11.

175. Kim, W.Y., et al., *Coronary magnetic resonance angiography for the detection of coronary stenoses*. N Engl J Med, 2001. **345**(26): p. 1863-9.
176. Greil, G.F., et al., *Reproducibility of free-breathing cardiovascular magnetic resonance coronary angiography*. J Cardiovasc Magn Reson, 2007. **9**(1): p. 49-56.
177. Yoon, Y.E., et al., *Prognostic value of coronary magnetic resonance angiography for prediction of cardiac events in patients with suspected coronary artery disease*. J Am Coll Cardiol, 2012. **60**(22): p. 2316-22.
178. Grover, S., D.P. Leong, and J.B. Selvanayagam, *Evaluation of left ventricular function using cardiac magnetic resonance imaging*. J Nucl Cardiol, 2011. **18**(2): p. 351-65.
179. Karamitsos, T.D., et al., *Operator induced variability in left ventricular measurements with cardiovascular magnetic resonance is improved after training*. J Cardiovasc Magn Reson, 2007. **9**(5): p. 777-83.
180. Selvanayagam, J.B., et al., *Resting myocardial blood flow is impaired in hibernating myocardium: a magnetic resonance study of quantitative perfusion assessment*. Circulation, 2005. **112**(21): p. 3289-96.
181. Cheng, A.S., et al., *Irreversible myocardial injury: assessment with cardiovascular delayed-enhancement MR imaging and comparison of 1.5 and 3.0 T--initial experience*. Radiology, 2007. **242**(3): p. 735-42.
182. Cerqueira, M.D., et al., *Standardized myocardial segmentation and nomenclature for tomographic imaging of the heart. A statement for healthcare professionals from the Cardiac Imaging Committee of the Council on Clinical Cardiology of the American Heart Association*. Int J Cardiovasc Imaging, 2002. **18**(1): p. 539-42.
183. Cerqueira, M.D., et al., *Standardized myocardial segmentation and nomenclature for tomographic imaging of the heart: a statement for healthcare professionals from the Cardiac Imaging Committee of the Council on Clinical Cardiology of the American Heart Association*. Circulation, 2002. **105**(4): p. 539-42.
184. Czernin, J., et al., *Influence of age and hemodynamics on myocardial blood flow and flow reserve*. Circulation, 1993. **88**(1): p. 62-9.

185. Nagel, E., et al., *Magnetic resonance perfusion measurements for the noninvasive detection of coronary artery disease*. *Circulation*, 2003. **108**(4): p. 432-7.
186. Yan, A.T., et al., *Characterization of the peri-infarct zone by contrast-enhanced cardiac magnetic resonance imaging is a powerful predictor of post-myocardial infarction mortality*. *Circulation*, 2006. **114**(1): p. 32-9.
187. Grotenhuis, H.B., et al., *Validation and reproducibility of aortic pulse wave velocity as assessed with velocity-encoded MRI*. *J Magn Reson Imaging*, 2009. **30**(3): p. 521-6.
188. Chaosuwannakit, N., et al., *Aortic stiffness increases upon receipt of anthracycline chemotherapy*. *J Clin Oncol*, 2010. **28**(1): p. 166-72.
189. Foley, R.N., et al., *Chronic kidney disease and the risk for cardiovascular disease, renal replacement, and death in the United States Medicare population, 1998 to 1999*. *J Am Soc Nephrol*, 2005. **16**(2): p. 489-95.
190. Meier-Kriesche, H.U., R. Baliga, and B. Kaplan, *Decreased renal function is a strong risk factor for cardiovascular death after renal transplantation*. *Transplantation*, 2003. **75**(8): p. 1291-5.
191. Charytan, D., et al., *Distribution of coronary artery disease and relation to mortality in asymptomatic hemodialysis patients*. *Am J Kidney Dis*, 2007. **49**(3): p. 409-16.
192. Parnham, S., Gleadle, J., De Pasquale, C., Selvanayagam, J., *Myocardial Ischemia Assessment in Chronic Kidney Disease: Challenges and Pitfalls*. *Frontiers in Cardiovascular Medicine*, 2014. **1**(13).
193. Parnham, S., Selvanayagam, J., *Myocardial Blood Oxygenation Assessment: Ready for Clinical Prime Time?* *Curr Cardiovasc Imaging Rep*, 2013(September 2013): p. 1-3.
194. Matsushita, K., et al., *Comparison of risk prediction using the CKD-EPI equation and the MDRD study equation for estimated glomerular filtration rate*. *JAMA*, 2012. **307**(18): p. 1941-51.
195. Friedrich, M.G. and T.D. Karamitsos, *Oxygenation-sensitive cardiovascular magnetic resonance*. *J Cardiovasc Magn Reson*, 2013. **15**: p. 43.

196. Luu, J.M., et al., *Relationship of vasodilator-induced changes in myocardial oxygenation with the severity of coronary artery stenosis: a study using oxygenation-sensitive cardiovascular magnetic resonance*. Eur Heart J Cardiovasc Imaging, 2014. **15**(12): p. 1358-67.
197. Akinboboye, O.O., et al., *Absolute quantitation of coronary steal induced by intravenous dipyridamole*. J Am Coll Cardiol, 2001. **37**(1): p. 109-16.
198. Marcus, M.L., et al., *Alterations in the coronary circulation in hypertrophied ventricles*. Circulation, 1987. **75**(1 Pt 2): p. 119-25.
199. Egred, M., et al., *Detection of scarred and viable myocardium using a new magnetic resonance imaging technique: blood oxygen level dependent (BOLD) MRI*. Heart, 2003. **89**(7): p. 738-44.
200. Dattilo, G., et al., *2-Dimensional strain echocardiography and early detection of myocardial ischemia*. Int J Cardiol, 2010. **145**(1): p. e6-8.
201. Gjesdal, O., et al., *Global longitudinal strain measured by two-dimensional speckle tracking echocardiography is closely related to myocardial infarct size in chronic ischaemic heart disease*. Clin Sci (Lond), 2007. **113**(6): p. 287-96.
202. Bello, A.K., et al., *Associations among estimated glomerular filtration rate, proteinuria, and adverse cardiovascular outcomes*. Clin J Am Soc Nephrol, 2011. **6**(6): p. 1418-26.
203. Fischer, K., D.P. Guensch, and M.G. Friedrich, *Response of myocardial oxygenation to breathing manoeuvres and adenosine infusion*. Eur Heart J Cardiovasc Imaging, 2015. **16**(4): p. 395-401.
204. Guensch, D.P., et al., *Impact of intermittent apnea on myocardial tissue oxygenation--a study using oxygenation-sensitive cardiovascular magnetic resonance*. PLoS One, 2013. **8**(1): p. e53282.
205. Rusu, C., et al., *Synthetic generation of myocardial blood-oxygen-level-dependent MRI time series via structural sparse decomposition modeling*. IEEE Trans Med Imaging, 2014. **33**(7): p. 1422-33.
206. Wetmore, J.B., et al., *Painless myocardial ischemia is associated with mortality in patients with chronic kidney disease*. Nephron Clin Pract, 2012. **122**(1-2): p. 9-16.

207. Parnham, S., et al., *Impaired Myocardial Oxygenation Response to Stress in Patients With Chronic Kidney Disease*. J Am Heart Assoc, 2015. **4**(8): p. 1-11.
208. Kuettner, A., et al., *Diagnostic accuracy of multidetector computed tomography coronary angiography in patients with angiographically proven coronary artery disease*. J Am Coll Cardiol, 2004. **43**(5): p. 831-9.
209. Li, D., et al., *Myocardial signal response to dipyridamole and dobutamine: demonstration of the BOLD effect using a double-echo gradient-echo sequence*. Magn Reson Med, 1996. **36**(1): p. 16-20.
210. Bozbas, H., et al., *Evaluation of coronary microvascular function in patients with end-stage renal disease, and renal allograft recipients*. Atherosclerosis, 2009. **202**(2): p. 498-504.
211. Wadei, H.M. and S.C. Textor, *Hypertension in the kidney transplant recipient*. Transplant Rev (Orlando), 2010. **24**(3): p. 105-20.
212. Patel, R.K., et al., *Renal transplantation is not associated with regression of left ventricular hypertrophy: a magnetic resonance study*. Clin J Am Soc Nephrol, 2008. **3**(6): p. 1807-11.
213. Lentine, K.L., et al., *Cardiac disease evaluation and management among kidney and liver transplantation candidates: a scientific statement from the American Heart Association and the American College of Cardiology Foundation*. J Am Coll Cardiol, 2012. **60**(5): p. 434-80.
214. Selvanayagam, J.B., et al., *Troponin elevation after percutaneous coronary intervention directly represents the extent of irreversible myocardial injury: insights from cardiovascular magnetic resonance imaging*. Circulation, 2005. **111**(8): p. 1027-32.
215. Flett, A.S., et al., *Evaluation of techniques for the quantification of myocardial scar of differing etiology using cardiac magnetic resonance*. JACC Cardiovasc Imaging, 2011. **4**(2): p. 150-6.
216. Watkins, S., et al., *Validation of magnetic resonance myocardial perfusion imaging with fractional flow reserve for the detection of significant coronary heart disease*. Circulation, 2009. **120**(22): p. 2207-13.

217. Caliskan, Y., et al., *Coronary flow reserve dysfunction in hemodialysis and kidney transplant patients*. Clin Transplant, 2008. **22**(6): p. 785-93.
218. Turiel, M., et al., *Subclinical impairment of coronary flow velocity reserve assessed by transthoracic echocardiography in young renal transplant recipients*. Atherosclerosis, 2009. **204**(2): p. 435-9.
219. Vigano, S.M., et al., *Reduced coronary flow reserve in young adults with renal transplant*. Nephrol Dial Transplant, 2007. **22**(8): p. 2328-33.
220. Nakajima, H., et al., *Hypertension impairs myocardial blood perfusion reserve in subjects without regional myocardial ischemia*. Hypertens Res, 2010. **33**(11): p. 1144-9.
221. An, J., et al., *Prevalence and prediction of coronary artery disease in patients with liver cirrhosis: a registry-based matched case-control study*. Circulation, 2014. **130**(16): p. 1353-62.
222. Pruthi, J., et al., *Analysis of causes of death in liver transplant recipients who survived more than 3 years*. Liver Transpl, 2001. **7**(9): p. 811-5.
223. Fussner, L.A., et al., *Cardiovascular Disease After Liver Transplantation. When, what and who is at risk*. Liver Transpl, 2015.
224. Lanese, D.M. and J.D. Conger, *Effects of endothelin receptor antagonist on cyclosporine-induced vasoconstriction in isolated rat renal arterioles*. J Clin Invest, 1993. **91**(5): p. 2144-9.
225. Edwards, N.C., et al., *The treatment of coronary artery disease in patients with chronic kidney disease*. QJM, 2006. **99**(11): p. 723-36.
226. Joannides, R., et al., *Comparative effects of sirolimus and cyclosporin on conduit arteries endothelial function in kidney recipients*. Transpl Int, 2010. **23**(11): p. 1135-43.
227. Parnham, S., et al., *Myocardial perfusion is impaired in asymptomatic renal and liver transplant recipients: a cardiovascular magnetic resonance study*. J Cardiovasc Magn Reson, 2015. **17**: p. 56.
228. Moody, W.E., et al., *Arterial disease in chronic kidney disease*. Heart, 2013. **99**(6): p. 365-72.
229. Grover, S., et al., *Early and late changes in markers of aortic stiffness with breast cancer therapy*. Intern Med J, 2015. **45**(2): p. 140-7.

230. Wallace, S.M., et al., *Isolated systolic hypertension is characterized by increased aortic stiffness and endothelial dysfunction*. Hypertension, 2007. **50**(1): p. 228-33.
231. Briet, M., et al., *Arterial stiffness and enlargement in mild-to-moderate chronic kidney disease*. Kidney Int, 2006. **69**(2): p. 350-7.
232. Tholen, S., et al., *Progression of aortic pulse wave velocity in patients with chronic kidney disease*. J Clin Hypertens (Greenwich), 2013. **15**(11): p. 833-8.
233. Pan, C.R., et al., *Comparing aortic stiffness in kidney transplant recipients, hemodialysis patients, and patients with chronic renal failure*. Clin Transplant, 2011. **25**(4): p. E463-8.
234. Hotta, K., et al., *Successful kidney transplantation ameliorates arterial stiffness in end-stage renal disease patients*. Transplant Proc, 2012. **44**(3): p. 684-6.
235. Locsey, L., et al., *Arterial stiffness in chronic renal failure and after renal transplantation*. Transplant Proc, 2010. **42**(6): p. 2299-303.
236. Wang, L.W., et al., *Prognostic value of cardiac tests in potential kidney transplant recipients: a systematic review*. Transplantation, 2015. **99**(4): p. 731-45.